UNIVERSITÀ
DEGLI STUDI
DI PADOVA

Sede Amministrativa: Università degli Studi di Padova

Dipartimento di Biologia

CORSO DI DOTTORATO DI RICERCA IN: BIOSCIENZE E BIOTECNOLOGIA

CURRICOLUM: NEUROBIOLOGIA

CICLO XXIX

Transcription Factor EB controls metabolic flexibility during exercise

Tesi redatta con il contributo finanziario del Fondazione CaRiPaRo

Coordinatore: Ch.mo Prof. Paolo Bernardi

Supervisore: Ch.mo Prof. Marco Sandri

Dottorando : Andrea Armani

Index

Abstract

Skeletal muscle is the most abundant tissue in the whole organism representing more than 40% of the total body mass. This organ is responsible for the 30% of metabolic rate in basal condition, suggesting its great relevance not only for locomotor activity, but also for the control of whole body metabolism. Indeed skeletal muscle is a highly dynamic tissue that modulates its metabolism and mass as a consequence of different physiopathological conditions. One stimulus that triggers major adaptations is exercise, which is also well known to activate autophagy (Grumati, Coletto, Schiavinato, et al., 2011). Physical exercise elicits several beneficial effects acting on mitochondrial content/function, fatty acid oxidation and glucose uptake; however it is considered a disruptive trigger for myofiber homeostasis that needs to be counterbalanced through the activation of transcriptionally regulated pathways ready to contrast mechanical and metabolic stresses produced during contraction. The role of FoxOs transcription factors and TFEB in regulating protein breakdown and autophagy is known (Milan et al., 2015; Settembre et al., 2011). However the role of TFEB in skeletal muscle and its possible effects in controlling exercise-dependent adaptations in this tissue were not proved.

TFEB has been proposed as the key factor that coordinates autophagy to lysosomal biogenesis in cell culture, with different evidences showing the regulation of its activity. In particular it is known that an mTORC1 phosphorylation is able to prevent TFEB function by retaining it in the cytoplasm. However, there were no evidences concerning the possible phosphatases involved in TFEB activation.

Using a cellular high content screening able to monitor TFEB nuclear translocation during starvation, we identified PPP3CB, the catalytic subunit of calcineurin, as one of the highest hit for TFEB nuclear relocalization. We demonstrated that calcineurin activity is necessary and sufficient to push TFEB in the nucleus, where it can complete its function. Nevertheless, calcineurin is known to be active in skeletal muscle during contraction as a consequence of calcium oscillations. For this reason we wondered whether calcineurin activity could affect TFEB translocation also in adult skeletal muscle during exercise.

Using muscles transfected with a TFEB-GFP reporter, we demonstrated that calcineurin activity is necessary and sufficient to promote TFEB nuclear translocation even in adult skeletal muscle during coxntraction.

However, the physiological meaning of this nuclear translocation in skeletal muscle remained to be addressed.

To answer this question we used gain and loss of function approaches, by mean of viral infection of TFEB overesxpressing vectors, muscle specific TFEB knockout animals and tamoxifen inducible muscle specific TFEB transgenic animals.

From microarray analysis of muscles overexpressing and lacking TFEB, we realized that the major pathways affected by genetic manipulation are related to mitochondrial biogenesis and function, lipid utilization and glucose homeostasis. Thus we started to dissect the function of TFEB in skeletal muscle proving that its activation is required for mitochondrial biogenesis that is indeed increased in transgenic muscle. We also found an augmented mitochondrial number and size in transgenic muscle, with only a small percentage of dysfunctional mitochondria in KO animals.

These changes were paralleled by a TFEB signature in gene expression of genes involved in mitochondrial biogenesis and functionality. Moreover, these morphometric and gene expression evidences correlate with increased mitochondrial respiration and higher activity of respiratory chain complexes. For this reason transgenic muscles produce more ATP than normal mice, while KO muscles have a lower ATP synthesis because mitochondria present a leak in mitochondrial membrane that dissipate membrane potential.

Nevertheless, in order to understand if TFEB is able to promote this mitochondrial program independently from PGC1α, we checked the expression of NRF1/2, TFAM and other genes involved in mitochondrial biogenesis in a model of PGC1α ablation during TFEB overexpression. These data, and complexes activity measurements, demonstrate that TFEB is able per se to activate the transcriptional program directly binding to NRF1 and NRF2 genes promoters without the need of the transcriptional co-activator.

At this point, we challenged mice with exercise finding that transgenic mice are more resistant to exhaustive contraction than control; conversely muscle specific TFEB-KO animals display pronounced exercise intolerance due to their lack in ATP production.

In order to better explain this latter finding, thanks to metabolic measurements we realized that KO muscles rely more on glucose oxidation both in basal condition and during the first phases of exercise thus explaining the observed exercise intolerance triggered by glycogen storage depletion. Furthermore lactate quantification in serum before and after exercise suggests that KO animal depend more on anaerobic glycolysis with respect to control and transgenic counterpart. To deeply investigate the role of glucose oxidation that seems the cause of exercise intolerance, we monitored glycogen levels in muscle of KO animals in resting condition, revealing a reduction of glycogen storage. For this reason after the early stages of exercise TFEB-KO animals need to rapidly shift their metabolism to fatty acid oxidation that however cannot support energy demand because of the presence of dysfunctional mitochondria.

Altogether these findings indicate that TFEB is impinging more on metabolism rather than autophagy, that indeed is not affected by TFEB genetic modulation; more in detail TFEB seems to significantly modulate muscular glucose homeostasis that is altered in KO animals. Reduced glucose uptake and glycogen synthesis during EU clamps explains why glycogen storages are depleted in KO animals, while the transgenic counterpart present more glycogen accumulation. This phenotypic effect is paralleled by a change in glucose related genes expression, with higher levels of glucose transporters and glycogen synthesis regulator in transgenic muscles, even in the absence of PGC1α. Nevertheless TFEB overexpression is also able to drive factors such as nNOS and AMPK activity, thus modulating not only the expression but also the signalling pathways related to glucose homeostasis.

In conclusion all these findings strongly support a new vision of TFEB as master regulator of metabolic flexibility during physical exercise in a PGC1α-independent fashion.

Riassunto

Il muscolo scheletrico è il tessuto più abbondante dell'organismo e rappresenta più del 40% della massa corporea. Questo organo è responsabile del 30% della spesa energetica a riposo, suggerendo la sua importanza non solo a livello di locomozione ma anche nel controllo del metabolismo a livello sistemico. Infatti il muscolo scheletrico è un tessuto estremamente dinamico, capace di modulare il suo metabolismo in seguito a stimoli di diversa natura. Uno stimolo che attiva maggiori adattamenti metabolici è l'esercizio, che è noto attivare anche l'autofagia.
L'esercizio fisico stimola molti effetti benefici sul contenuto e funzionalità mitocondriale, ossidazione degli acidi grassi e assorbimento del glucosio; tuttavia, è considerato uno stimolo che danneggia la normale omeostasi delle fibre muscolari per cui necessita di essere controbilanciato dall'attivazione di meccanismi trascrizionalmente controllati che contrastano gli stress meccanici e metabolici prodotti durante la contrazione. Il ruolo dei fattori di trascrizione FoxO e TFEB nel regolare la degradazione proteica e l'autofagia è largamente conosciuto. Tuttavia, il ruolo di TFEB nel muscolo scheletrico e i suoi possibili effetti nel regolare gli adattamenti derivanti dall'esercizio in questo tessuto non sono ancora chiari.

TFEB è stato proposto come fattore chiave nel coordinare autofagia e biogenesi lisosomiale in cellule in coltura, con diverse evidenze che dimostrano la regolazione della sua attività. In particolare è noto come la fosforilazione operata da mTORC1 sia in grado di prevenire l'attivazione di TFEB sequestrandolo nel citoplasma. Tuttavia, non esistono dati riguardanti le possibili fosfatasi coinvolte nell'attivazione di TFEB.
Mediante l'utilizzo di uno High Content Screening in grado di monitorare la traslocazione di TFEB nel nucleo durante la starvation, abbiamo identificato il gene PPP3CB, codificante la subunità catalitica della calcineurina, come uno dei migliori geni coinvolti nella rilocalizzazione di TFEB. Abbiamo dimostrato che l'attività della calcineurina è necessaria e sufficiente per spingere TFEB nel nucleo, dove può espletare la sua funzione. Tuttavia, la calcineurina è noto essere attiva nel muscolo scheletrico durante la contrazione

come conseguenza dei transienti di calcio. Per questo motivo ci siamo chiesti se l'attività della calcineurina possa influenzare la traslocazione di TFEB nel nucleo anche nel muscolo scheletrico durante l'esercizio fisico. Utilizzando un reporter TFEB-GFP abbiamo dimostrato che l'attività della calcineurina è necessaria e sufficiente a promuovere la traslocazione nucleare di TFEB anche nel muscolo scheletrico durante la contrazione. Tuttavia il significato fisiologico di questo avvenimento rimane da essere spiegato.

Per rispondere a questa domanda abbiamo usato degli approcci di *gain* e *loss of function* utilizzando infezioni virali con vettori per l'overespressione di TFEB, una linea di topi con delezione muscolo specifica di TFEB e un'altra linea in cui l'overespressione di TFEB può essere attivata in muscolo grazie al tamoxifen.

Da uno studio di espressione genica in muscoli overesprimenti TFEB e TFEB deficienti, abbiamo trovato che le vie di segnale principalmente coinvolte dalle manipolazioni genetiche erano quelle correlate alla biogenesi mitocondriale, utilizzo dei lipidi e omeostasi del glucosio. Abbiamo perciò cominciato a dissezionare il ruolo di TFEB nel muscolo scheletrico provando che la sua attivazione è richiesta per la biogenesi mitocondriale, che è per l'appunto aumentata nei muscoli transgenici. Infatti, in questi abbiamo trovato un aumento nel numero e nella dimensione dei mitocondri, mentre abbiamo riportato solo una piccola percentuale di mitocondri disfunzionali nei muscoli knockout.

Questi cambiamenti sono accompagnati da un'attivazione dei geni TFEB-dipendenti responsabili per la biogenesi e funzionalità mitocondriale. Inoltre, questi cambiamenti morfometrici e di espressione genica correlano con un aumento nella respirazione mitocondriale e nell'attività dei complessi della catena respiratoria. Per questo motivo i muscoli transgenici producono più ATP dei wildtype, mentre i muscoli KO presentano una ridotta sintesi di ATP a causa di una disfunzionalità della membrana mitocondriale che dissipa il gradiente protonico. Tuttavia, per capire se questi cambiamenti dipendono direttamente da TFEB indipendentemente da PGC1α, abbiamo monitorato l'espressione di NRF1/2, TFAM e altri geni coinvolti nella biogenesi mitocondriale in un modello in cui PGC1α è deleto e TFEB overespresso. Questi dati di espressione uniti alle misure delle attività dei complessi dimostrano che TFEB è in grado di indurre autonomamente la biogenesi mitocondriale legandosi direttamente ai promotori dei geni NRF1 e NRF2.

A questo punto abbiamo sottoposto a esercizio i topi riscontrando che gli animali transgenici resistono maggiormente all'attività fisica; al contrario i topi KO presentano una marcata intolleranza all'esercizio a causa della scarsa produzione di ATP. Per spiegare meglio questo fenomeno, grazie a misurazioni di parametri metabolici abbiamo riscontrato che i topi KO fanno affidamento maggiormente nell'ossidazione del glucosio sia a riposo che durante le fasi iniziali dell'esercizio fisico, spiegando l'intolleranza con la fine delle riserve di glicogeno. Inoltre, le quantificazioni del lattato nel siero prima e dopo l'esercizio suggeriscono che i muscoli KO dipendono maggiormente dalla glicolisi anaerobia a differenza delle controparti wildtype e transgenica. A questo punto, per investigare più in dettaglio il ruolo dell'ossidazione del glucosio che sembra essere alla base dell'intolleranza all'esercizio, abbiamo misurato i livelli di glucosio intramuscolare negli animali KO, notando che a riposo questi presentano una riduzione considerevole delle riserve. Per questo motivo gli animali KO, dopo i primi momenti di esercizio, sono costretti a cambiare il loro metabolismo verso una maggiore ossidazione degli acidi grassi che comunque non riesce a supportare la domanda energetica a causa dei mitocondri disfunzionali.

Tutte queste evidenze indicano che TFEB controlla più il metabolismo rispetto all'autofagia la quale non è influenzata dalla modulazione genetica di TFEB; più in dettaglio TFEB sembra controllare direttamente il metabolismo del glucosio che è alterato negli animali TFEB-deficienti. Un ridotto assorbimento del glucosio e una ridotta sintesi del glicogeno durante gli EU-clamps spiegano perché le riserve di glicogeno sono ridotte negli animali KO mentre la controparte transgenica ne accumula in più. Questi effetti fenotipici sono accompagnati da un cambiamento nell'espressione di geni connessi all'omeostasi del glucosio, con maggiore presenza di trascritti per i trasportatori di glucosio and regolatori della sintesi del glicogeno nei muscoli transgenici, anche in assenza di PGC1α. Inoltre, l'overespressione di TFEB è in grado di modulare anche l'attività di nNOS e AMPK, influenzando l'omeostasi del glucosio non solo dal punto di visto trascrizionale, ma impattando anche sulle vie di segnale ad esso correlate.

In conclusione tutte queste scoperte sostengono fortemente una nuova visione di TFEB come un fattore chiave nella regolazione della flessibilità metabolica durante l'esercizio fisico in modo indipendente da PGC1α.

Publications

Pastore N, Vainshtein A, Klisch T, **Armani A**, Huynh T, Herz NJ, Polishchuk EV, Sandri M, Ballabio A (2016) TFE3 regulates whole body energy metabolism in cooperation with TFEB. EMBO Molecular Medicine, *submitted* *

Mansueto G, **Armani A**, Viscomi C, D'Orsi L, De Cegli R, Polishchuk E.V., Lamperti C, Di Meo I, Romanello V, Marchet S, Saha P.K., Zong H, Blaauw B, Solagna F, Tezze C, Grumati P, Bonaldo P, Pessin J.E, Zeviani M, Sandri M, Ballabio A (2016) Transcription factor EB controls metabolic flexibility during exercise. *Cell Metabolism*, in press*

Milan G*, Romanello V*, Pescatore F*, **Armani A**, Paik JH, Frasson L, Seydel A, Zhao J, Abraham R, Goldberg AL, Blaauw B, DePinho RA, Sandri M. (2015) Regulation of autophagy and the ubiquitin-proteasome system by the FoxO transcriptional network during muscle atrophy. *Nat Commun*. 10;6:6670

Vainshtein A, Desjardins EM, **Armani A**, Sandri M, Hood DA. (2015) PGC-1α modulates denervation-induced mitophagy in skeletal muscle. *Skelet Muscle*. 18;5:9.

Medina DL, Di Paola S, Peluso I, **Armani A**, De Stefani D, Venditti R, Montefusco S, Scotto-Rosato A, Prezioso C, Forrester A, Settembre C, Wang W, Gao O, Xu H, Sandri M, Rizzuto R, De Matteis MA, Ballabio A. (2015) Lysosomal calcium signalling regulates autophagy through calcineurin and TFEB. *Nat Cell Biol*. 17(3):288-99.

Conte M, Vasuri F, Bertaggia E, **Armani A**, Santoro A, Bellavista E, Degiovanni A, D'Errico-Grigioni A, Trisolino G, Capri M, Franchi MV, Narici MV, Sandri M, Franceschi C, Salvioli S. (2015) Differential expression of perilipin 2 and 5 in human skeletal muscle during aging and their association with atrophy-related genes. *Biogerontology*. 16(3):329-40.

1 Introduction

1.1 Skeletal muscle

Skeletal muscle is the most abundant tissue in the whole organism representing almost 40% of the body weight and, due to its predominant protein component, can be considered the major protein reservoir of the organism (Bonaldo & Sandri, 2013).
It is primarily know for its control of body posture and movement; nevertheless it has been demonstrated since early 80s its important role in the control of blood glycemia and metabolic homeostasis (DeFronzo, Ferrannini, Sato, Felig, & Wahren, 1981; DeFronzo, Jacot, et al., 1981).
Starting from these evidences, researchers focused their attention on this organ not only for its contractile properties but also for its pivotal role in controlling whole body metabolism.

1.1.1 Structure and function

Skeletal muscle is a highly complex organ, made up of specialized contractile cells called myofibers. Nonetheless, this organ needs the contribution of other tissues in order to maintain its homeostasis and guarantee its proper functionality.
That is the case of connective tissue that provides a robust extra-cellular matrix (ECM) able to determine a specialized organization of muscle fibers. ECM can be found not only surrounding myofibers (endomysium); indeed connective tissue is also able to create an envelope (perimysium) that groups fibers in fascicles. Furthermore, an additional layer of ECM, the epimysium, glues together all fascicles in order to form the final entire muscle.
Skeletal muscles are also connected to bones through tendons, specialized structures mainly composed by ECM proteins which couple muscle contraction to movement generation (Figure 1).
However, connective tissue is not the only tissue required; blood vessels and nerves are also principal components that can be found inside a muscle, positioned in the ECM forming the endomysium. Blood vessels are fundamental to support and ensure metabolites

exchanges; moreover, nerve terminals from motor-neurons are contacting myofibers in specialized synapses called neuromuscular junctions (NMJs) in order to provide the stimulus required for contraction.

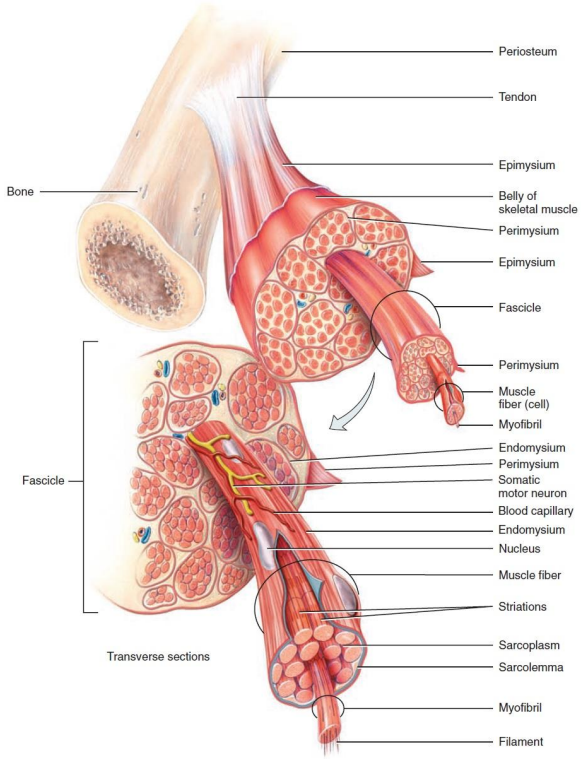

Figure 1 - Schematic representation of skeletal muscle structure

From a histological point of view, skeletal muscle is a complex post-mitotic tissue formed by a tight organisation of myofibers, long cylindrical multinucleated cells.

Due to their particular specialization in contraction, muscle cells present an extremely reduced cytosol with all the space occupied by thousand of myofibrils composed by long series of sarcomeres, the contractile units of the cell. A sarcomere is a huge protein complex composed by regularly alterned actin and myosin filaments, kept in the correct position by several important structural and regulatory proteins such as troponin, tropomyosin, titin and desmin.

Sarcomeres were described for the first time thanks to microscopy techniques that highlighted the presence of isotropic (light band) and anisotropic (dark band) zones, forming the specific striated aspect of skeletal muscle.

Later electron microscope analysis led to the identification of a precise structural pattern in which two electrondense lines observed across the extremities (Z-lines) define the sarcomeric unit. Moreover from these studies, a light band (I-band) and a dark band (A-band) can be observed. Each I-band spans between to adjacent sarcomeres, including the Z-line in its middle; in addition, within the A-band, a paler region called the H-band presents in the middle a thin M-line, the middle-line of the sarcomere.

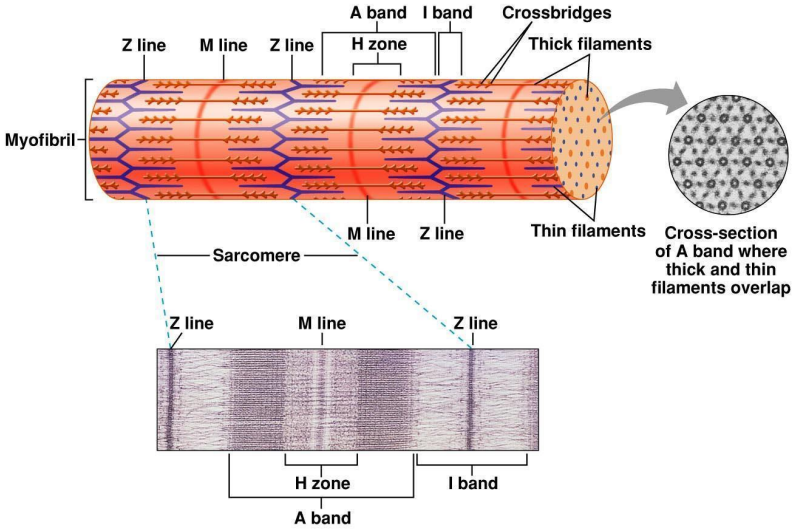

Figure 2 - Scheme of sarcomere organization

These bands are not only morphological features but also functional units since they are characterized by the presence of different contractile proteins. Actin filaments (thin filaments) are the major components of the I-band and extend into the A band where the overlapping with myosin filaments gives rise to the known shift in light conductance. Thick filaments extend throughout the entire A-band and are thought to overlap in middle of the sarcomere where they give rise to M-band. Another structural protein, called titin, extends from the Z-line of the sarcomere, where it binds the thin filament system, to the M-band, where it is thought to interact with the thick filaments. Several proteins important for the stability of the sarcomeric structure are found in the Z-line as well as in the M band of the sarcomere (Figure 2). Actin filaments and titin molecules are cross-linked in the Z-disc via the Z-line protein alpha-actinin. The M-band myosins together with the M proteins bridge the thick filament system to the M-band part of titin (the elastic filaments).

Moreover several regulatory proteins, such as tropomyosin and troponin bind myosin molecules, modulating their contraction properties.

Contraction is the typical feature of muscle fibers, which are able to convert chemical energy into mechanical force generation. In 1954, scientists published two groundbreaking papers describing the molecular basis of muscle contraction. These works described the position of myosin and actin filaments at various stages of contraction in muscle fibers and proposed how this interaction, now known as "cross-bridge", produced contractile force. Using high-resolution microscopy, A. F. Huxley and R. Niedergerke (A. F. Huxley & Niedergerke, 1954) and H. E. Huxley and J. Hanson (H. Huxley & Hanson, 1954) observed changes in the sarcomeres as muscle tissue shortened. They noticed that the A-band remained relatively constant in length during contraction suggesting that the myosin filaments remained central and constant in length while other regions of the sarcomere shortened. The investigators also observed that the I-band changed its length along with the sarcomere and H-band disappears. These observations led them to propose the sliding filament theory, which states that the sliding of actin on myosin is the source muscle tension. Thus, since actin is tethered to Z-lines, any shortening of the actin filament length would result in a shortening of the entire sarcomere with the two Z-lines defining at the boundaries getting closer one to the other.

Muscle contraction is determined by a mechanism called excitation-contraction coupling. Excitation is coming from a motor neuron that is contacting myofibers at the neuro-muscular junction; action potential is traveling from the neuron to the plasma membrane (sarcolemma) of the post-sinaptic cell (muscle cell) where the induced depolarization triggers a series of intracellular events leading to muscle contraction. Sarcolemma depolarization results in an increase in cytosolic calcium, the so-called calcium transient, which activates calcium-sensitive contractile proteins and allows myosin head to contact thin filaments and pull them towards M-line thanks to ATP hydrolysis. In this way, the electrical stimulus is converted in a signal cascade that brings chemical energy to be transformed in mechanical force.

The coordination of contraction in all the sarcomeres present in a myofiber makes it possible to modify the length of the whole muscle cell and as consequence of the entire muscle.

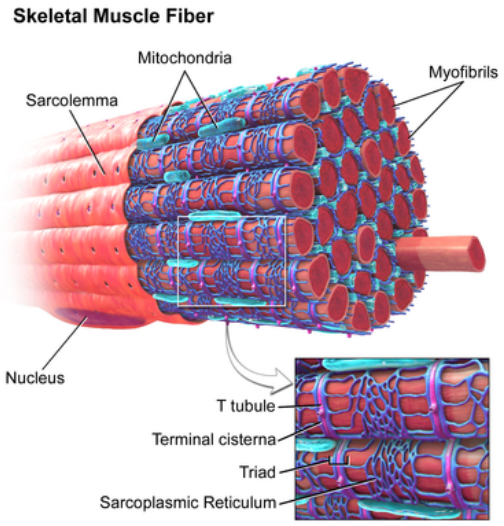

Figure 3 - T-tubuls and triad organization in a skeletal muscle fiber

To allow the simultaneous contraction of all sarcomeres, muscle fibers display a particular structure in which the sarcolemma penetrates into the cytoplasm between myofibrils, forming membranous tubules running parallel to the Z-line, the transverse tubules (T-tubules) (Figure 3). Thanks to the Ryanodine Receptor complex (RyR1), T-tubules are electrically coupled with the terminal cisternae, particular expansions of the sarcoplasmic reticulum (SR) that extend from both sides of T-tubules into the myofibrils. SR is the enlargement of smooth Endoplasmic Reticulum (ER) and contains the majority of calcium ions required for contraction. Anatomically, the structure formed by T-tubules surrounded by two smooth ER cisternae is called triad and it allows the transmission of membrane depolarization from the sarcolemma to the ER. The contraction starts when an action potential diffuses from the motor neuron to the sarcolemma and then it travels along T-tubules until it reaches the sarcoplasmic reticulum. Here the action potential, through the release of acetylcholine (ACh) from the synaptic terminal, induces changes in the permeability of the sarcoplasmic reticulum, allowing the flow of calcium ions into the cytosol between myofibrils. Here, the release of calcium ions induces the myosin heads to

interact with the actin, allowing muscle contraction, an ATP dependent process. Energy in skeletal muscle is provided by mitochondria, which, due to the particular spatial organisation, are located closed to Z-lines.

1.1.2 Muscle fiber diversity

Contractile properties of skeletal muscle depend principally on their fiber type composition. Indeed mammalian muscle fibers are divided in two distinct classes: type I, also called slow-twitch fibers, and type II, referred as fast-twitch fibers. This classification, based on the speed of tension development and relaxation, also coincides with histochemical staining for myosin ATPase activity, which is higher in fast-type II fibers. This classification mainly considers the mechanical properties of different fiber types; however, since early studies, muscles have been also classified as red and white, depending on their fresh appearance. This difference in color reflects both the amount of blood perfusion as well as the abundance of the oxygen transport protein myoglobin, which is closely related to mitochondrial density and the relative contribution of oxidative metabolism in the different fiber types.
At this point it is clear that besides mechanical properties different fiber types also display peculiar metabolic features, mitochondrial contents and resistance to fatigue (Pette & Heilmann, 1979; Schiaffino, Sandri, & Murgia, 2007).

Each muscle is composed by a combination of fiber types, whose abundance affects not only the type of contraction the muscle undergoes (fast or slow) but metabolism and physiology of the specific organ.
Different fiber types are also characterized by peculiar Myosin Heavy Chain (MHC) protein expression. Type I fibers express the slow isoform of MHC (MHCβ or MHC1), and present a great mitochondrial content, high levels of myoglobin, high capillary densities and high oxidative capacity. Conversely, type II fast fibers are divided in three different groups depending on which myosin isotype is expressed; indeed distinct genes encode for MHC IIa, IIx (also called IId) and IIb. Type IIa myofibers are faster than type I, but they are still relatively fatigue-resistant. IIa fibers are relatively slower than IIx and IIb

and have an oxidative metabolism due to the rich content of mitochondria (Schiaffino & Reggiani, 1996, 2011). Given all these characteristics, IIa fibers are also termed fast oxidative because they exhibit fast contraction, high oxidative capacity and a relative fatigue resistance. By the other hand, type IIx and IIb fibers are known as fast-glycolitic showing a prominent glycolitic metabolism, poor mitochondrial content, high myosin ATPase activity; all these features, coupled with the expression of MHC IIb and MHC IIx proteins, determine the fastest rate of contraction and the highest level of fatigability.

The fiber-type profile of different muscles is initially established during development independently of neural influences even if nerve activity has a major role in the maintenance and modulation of fiber properties in adulthood. During postnatal development and regeneration, a default nerve activity-independent pathway of muscle fiber differentiation leads to the activation of the fast gene program. On the contrary, post-natal induction and maintenance of the slow gene program is dependent on slow motor-neuron activity. Thus, nerves have an impact on fiber type determination and modulation of nerve activity can result in a switch of fiber type in adult skeletal muscles (Murgia et al., 2000).

At this point it is clear that the transcription of different fiber type-specific genes must be precisely coordinated in skeletal muscle fibers to maintain muscle function; for this reason different signaling pathways control muscle fiber type specific gene programs. Moreover fiber type transformations involve changes in all muscle cell compartments, including components of the excitation-contraction coupling, cell metabolism, and contractile machinery. Thus, fiber type composition is generally determined during development, but the possible adaptive “transformation” of muscle fibers from one type to another is still hotly debated (Booth, Laye, & Spangenburg, 2010).

1.2 Skeletal muscle plasticity: hypertrophy versus atrophy

Skeletal muscle is an extremely plastic tissue, able to adapt to a broad variety of stimuli including to only nutritional status, but also mechanical overload, nerve activity, exercise and stimulation by growth factors and hormones (Mounier, Theret, Lantier, Foretz, & Viollet, 2015).

Muscle mass is indeed highly dynamic and muscle fiber size can vary according to physiological and pathological conditions. In any case, muscle size is the outcome of a balance between protein synthesis and protein degradation (Figure 4). Thus, muscle growth is determined by excessive synthesis that leads to muscle hypertrophy; on the other hand, excessive protein degradation, loss of organelles and cytoplasm are the major causes of muscle atrophy.

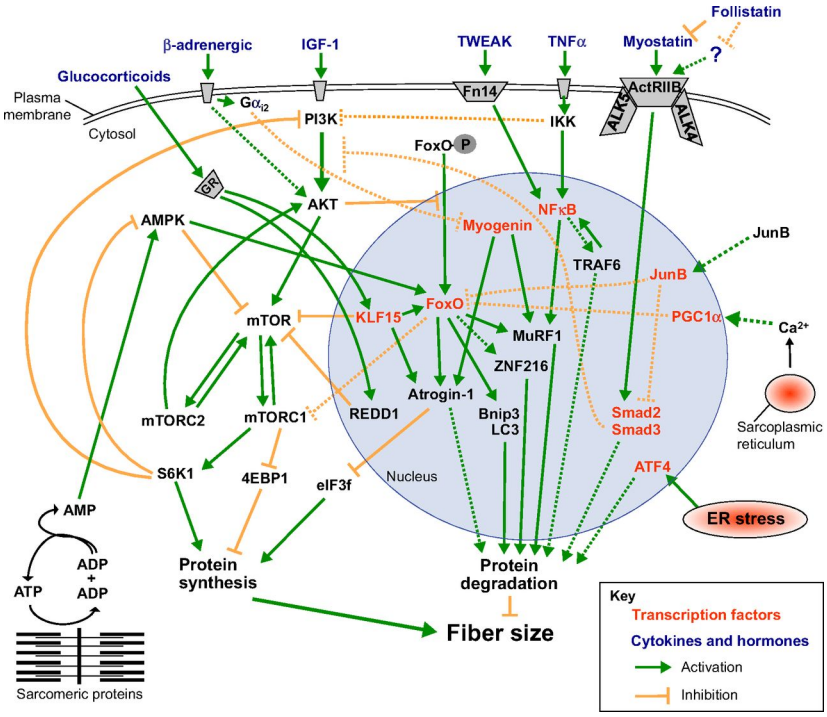

Figure 4 - Schematic view of the main pathways controlling muscle mass (Bonaldo & Sandri, 2013)

1.2.1 Muscle hypertrophy

In response to physical activity, or upon hormones stimulation, muscle mass is increased mainly as a result of prompted biosynthesis and decreased degradation of its protein constituents (McCarthy & Esser, 2007). The outcome of this anabolic state is named muscle hypertrophy, and is paralleled by an increase in the force developed by the muscle during contraction (Velloso, 2008). The IGF1-AKT signaling is the major pathway controlling muscle growth. IGF1 can be produced either by liver under growth hormone

(GH) control, or locally by skeletal muscle itself. Specific isoforms that drive load- and stretch-induced adaptations in skeletal muscle have been discovered and characterized. Binding of IGF1 to its receptor starts a signal cascade that culminates in the activation of AKT by phosphorylation. Active AKT inhibits protein degradation by phosphorylating and thus repressing the transcription factors of the FoxO family; in parallel, it stimulates protein synthesis via mammalian target of rapamycin (mTOR) activation and glycogen synthase kinase 3β (GSK3β) inhibition (Schiaffino & Mammucari, 2011). Active mTOR, a well-known regulator of cell growth, promotes the activation of S6 kinase (S6K) and blocks 4EB-P1, the eukaryotic translation factor 4E (eif4e) inhibitor; also AKT-driven inhibition of GSK3β stimulates proteins synthesis, preventing GSK3β inhibitory action on protein translation promoted by eIF2B (Glass, 2005). To better clarify the role of AKT in skeletal muscle hypertrophy, a conditional transgenic mouse was produced in which constitutively active form of AKT in expressed in skeletal muscle only after tamoxifen treatment. Upon activation of the transgene, these mice undergo a significant increase in muscle mass mainly due to newly synthesized proteins (Blaauw et al., 2009), providing strong evidence supporting the idea that AKT activation is sufficient to induce skeletal muscle growth and that IGF1-AKT axis is the major mediator of muscle hypertrophy. Nevertheless, recent findings reported that also TGF-β and BMP pathways contribute to the regulation of muscle mass in adulthood (Sartori et al., 2009; Sartori et al., 2013).
In conclusion, different pathways are now emerging, trying to clarify all the signal cascades involved in the control of muscle hypertrophy.

1.2.2 Muscle atrophy

Differently from hypertrophy, muscle atrophy is instead a decrease in myofiber size mainly determined by loss of organelles, cytoplasm and proteins. This process is physiologically induced during aging or it is due to muscle disuse, but is also important in many pathological conditions accompanied by muscle wasting such as cancer, diabetes, heart and renal failure (Lecker et al., 2006; Sandri, 2016). In 1969, Alfred Goldberg demonstrated that an increase in protein degradation contributed to the loss of muscle mass and myofibrillar proteins following denervation and glucocorticoid treatment (Goldberg, 1969). In most muscle atrophy models overall rates of protein synthesis are suppressed and

rates of protein degradation are consistently elevated, determining in turn the observed rapid loss of muscular proteins (Bonaldo & Sandri, 2013). This is paralleled by a reduction in the activity of the AKT pathway representing a permissive condition for the activation of FoxOs transcription factors. When active AKT levels are reduced, FoxOs are dephosphorylated and therefore able to translocate to the nucleus, where they can drive the expression of several atrophy-related genes. FoxO3 is the member of the family that firstly has been identified to promote the expression of two fundamental muscle specific ubitiquitin-ligases, Atrogin-1 and MuRF-1 (Bodine et al., 2001; Gomes, Lecker, Jagoe, Navon, & Goldberg, 2001; Sandri et al., 2004). Moreover FoxO3 has also been demonstrated to be necessary and sufficient for the induction of autophagy in adult skeletal muscle (Mammucari et al., 2007; Zhao et al., 2007).

In all the catabolic states, the loss of muscle mass involves a common pattern of transcriptional changes that includes the induction of genes for protein degradation, autophagy regulation and a decrease in expression of various genes involved in different cellular processes like energy production and growth. This group of coordinately regulated genes has been identified, and all the genes belonging to the atrophic program are now called “atrogenes”(Lecker et al., 2006).

These genes encode for proteins involved in different cellular processes like energy production, transcription factors, regulators of protein synthesis and enzymes belonging to different metabolic pathways. Recent findings shed new light in the role of the FoxOs family members in the regulation of all these “atrogenes”, contributing to highlighting the FoxOs signature in muscle atrophy (Milan et al., 2015).

Nevertheless, another family of transcription factors able to upregulate the expression of a reduced subset of atrogenes un skeletal muscle is NF-κB. It was shown that NF-κB signaling pathway can mediate the effects of inflammatory cytokines, in particular TNF-α during muscle wasting and cancer cachexia (Bonaldo & Sandri, 2013; Sandri, 2016).

In any case, these and likely other not yet identified signaling pathways contribute to muscle atrophy by influencing the activity of the main degradative machineries of the cell: the ubiquitin-proteasome and the autophagy-lysosome systems.

1.3 Protein and organelles breakdown in skeletal muscle

Degradation of unnecessary or damaged components in eukaryotic cells involves the ubiquitin-proteasome (UPS) or the autophagic-lysosomal (ALS) systems (Lilienbaum, 2013). The coordinated function of these two pathways is critical to maintain the delicate balance between anabolism and catabolism in cells; therefore a huge number of signaling pathways are involved in this fine regulation. In multicellular organisms these machineries are also essential to modulate the activity of hormones, to fight against pathogenic microorganisms, to recycle nutrients during starvation, to eliminate unnecessary structures and organelles during cell differentiation and to renew tissue components preventing and delaying aging (Mizushima & Levine, 2010). In skeletal muscle, protein breakdown occurs not only following disuse- or pathology-induced atrophy, but it is also necessary to remodel the tissue during development, to cope with nutrient depletion stress, or to remove damaged component (Schiaffino, Dyar, Ciciliot, Blaauw, & Sandri, 2013). A proper removal of damaged or unnecessary cellular components is thus essential to avoid accumulation of this material aggregates harmful for muscle function (Bonaldo & Sandri, 2013). This phenomenon is particularly relevant after exercise sessions; indeed during and after contraction UPS and autophagy are activated to allow the clearance of contractile proteins and mitochondria that become damaged as a consequence of energetic, oxidative and mechanical stresses produced during contraction (Vainshtein & Hood, 2016).

1.3.1 The ubiquitin-proteasome system

Ubiquitin-proteasome system (UPS) is primarily involved in the degradation of intracellular short-lived proteins, but it is also associated with different regulatory functions. A conjugation system composed of three enzymes, E1, E2, E3 activates and subsequently binds chains or single molecules of ubiquitin, an 8.5 kDa regulatory protein that target proteins and commit them to degradation (Figure 5). The reaction is highly specific and broad range of E3 ligases, differentially expressed and activated in several conditions in the cell, determine the substrate specificity of the conjugation reaction (Gomes et al., 2001). Chains of ubiquitin molecules are generated through isopeptide bonds formed between the C-terminus of one ubiquitin molecule and a specific lysine residue in the next. Ubiquitin has seven Lys residues, which are all used for

polymerization, but polyubiquitin chains formed via Lys at 48 or 63 are the best characterized. A polyubiquitin chain formed via Lys48 functions mainly as a marker for proteolysis; in contrast, Lys63-linked polyubiuqitinated proteins are involved in membrane trafficking processes (Tenno et al., 2004).

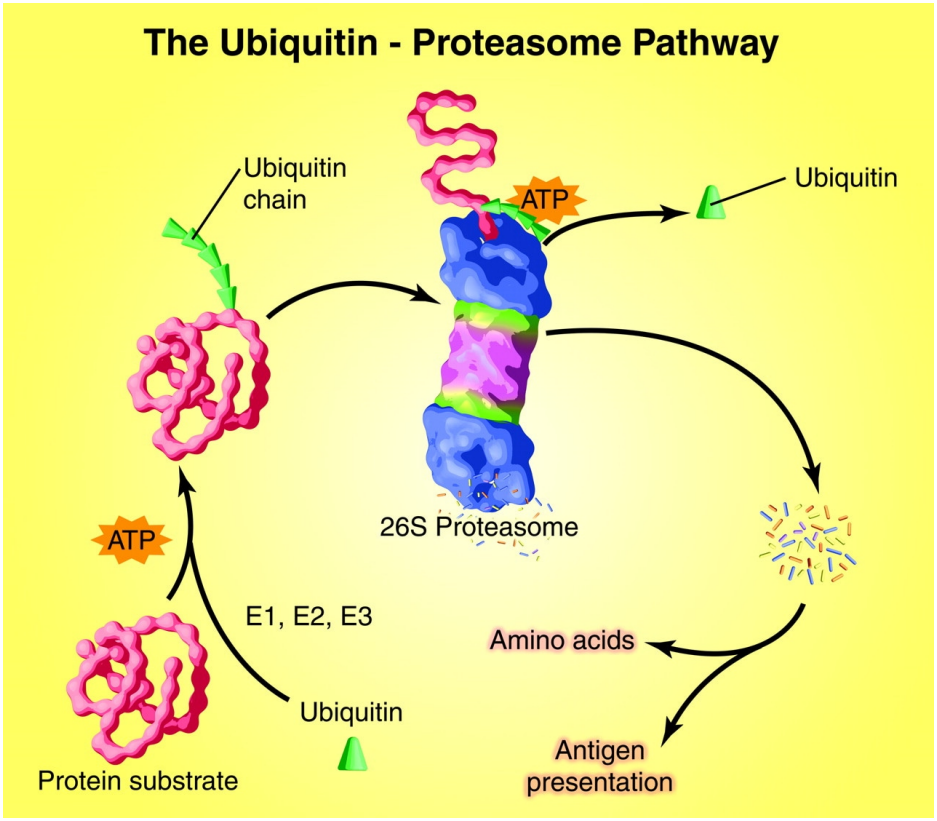

Figure 5 - Schematin view of the Ubiquitin Proteasome system for protein degradation (Lecker, Goldberg, & Mitch, 2006)

Proteins that need to be degraded, following the proper ubiquitination reaction, are addressed and recognized by the 26S proteasome, an ATP-dependent multienzyme complex with proteolytic activity. Through this system the normal turnover of intracellular proteins is maintained, and damaged or not properly folded proteins are degraded. The products of this degradation process are small peptides and free amino acids that can be reused for *de novo* biosynthesis or energy production (Hershko & Ciechanover, 1998).

The ubiquitin-proteasome system is constitutively active in skeletal muscle in order to sustain protein turnover and guarantee correct homeostasis; nevertheless, UPS is

responsible for the breakdown of most soluble and myofibrillar proteins during atrophy (Lecker et al., 2006). Indeed, the decrease in muscle mass in catabolic conditions is associated with: (a) increased muscular polyubiquitinated proteins; (b) increased proteasomal ATP-dependent activity; (c) increased protein breakdown that can be efficiently blocked by proteasome inhibitors; (4) upregulation of transcripts encoding ubiquitin, ubiquitin-conjugating enzymes (E2), ubiquitin-protein ligases (E3) and several proteasome subunits. Among the atrogenes, two E3 ubiquitin ligases, Fbxo32 (also known as Atrogin-1) and TRIM63 (also referred as Muscle Ring Finger 1, MuRF-1) (Bodine et al., 2001; Gomes et al., 2001), are the most upregulated genes in different models of muscle atrophy, being responsible for the increased protein breakdown. These two enzymes have a muscle specific gene expression pattern and are activated by FoxO3; for this reason they can be considered the main effectors of the signaling pathways activating the atrophic program.

However, since two ubiquitin ligases cannot account for the degradation of all sarcomeric and soluble proteins, additional E3s are for sure involved in muscle loss; recent studies highlighted new E3 ligases under FoxOs control whose activity is impinging in muscle mass loss during fasting or denervation (Milan et al., 2015; Sartori et al., 2013). For this reason, identification and characterization of E3 enzymes, together with their respective substrates, might be an important step to understand the mechanisms that control muscle mass loss and, thus, the first step to identify molecular targets for pharmacological intervention in muscle diseases.

1.3.2 The autophagy-lysosome system

The role of the lysosome system is to degrade large intra- or extracellular structures, such as huge protein complexes, organelles and pathogens. Extracellular material is degraded by lysosomes in a process called endocytosis in which substrates are engulfed by portions of the plasma membrane forming the so-called endocytic vesicles that are suddenly fused with lysosomes. Lysosomes are hydrolytic enzyme-containing organelles specialized in the digestion of endocytosed material and in the release of constituents to the cytosol (Pryor & Luzio, 2009). When lysosomes contribute to the breakdown of material of intracellular origin, the process is instead named autophagy (from the greek αυτοζ “self” and φαγειν

"eating") (Glick, Barth, & Macleod, 2010; van Meel & Klumperman, 2008). Autophagy is an evolutionarily conserved process that is typically induced under nutrient poor conditions to ensure cellular homeostasis thanks to protein aggregates and organelles degradation providing in this way metabolites necessary to support biosynthesis and metabolic processes.

Different types of lysosome-mediated self-digestion can be distinguished (Figure 6). In microautophagy the target of the digestion is a small portion of the cytosol that is directly engulfed by the lysosome without intervention of other vesicles (Mijaljica, Prescott, & Devenish, 2011). Although it is still unknown whether microautophagy occurs in skeletal muscle, some findings indicate that microautophagy can participate in glycogen uptake into lysosomes (Takikita et al., 2010).

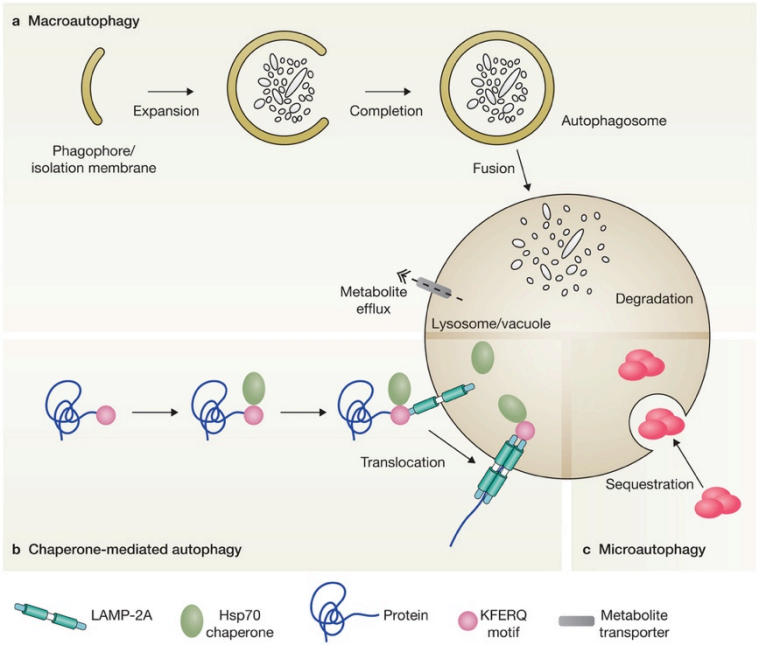

Figure 6 - Scheme of the different type of autophagy: **a.** maroautophagy, **b.** chaperone mediated autophagy and **c.** microautophagy (Cuervo, 2011)

The chaperone protein Hsc70 (Heat shock protein cognate 70) mediates instead a different kind of lysosomal self-digestion called Chaperone-Mediated-Autophagy (CMA). When this chaperone recognizes a specific aminoacidic sequence (KFERQ) exposed on the surface of a misfolded protein, it is able to help protein translocation directly into lysosomal lumen where degradation takes place (Bejarano & Cuervo, 2010). CMA has

raised interest owing to its potential role in aging, neurodegenerative disorders and lysosomal storage diseases (Kon & Cuervo, 2010); however, whether it has a role in skeletal muscle homeostasis is still largely unknown.

So far, most data on the role of autophagy in muscle are related to macroautophagy, the process that allows the degradation of superfluous or damaged organelles and supramolecular complexes.

Macroautophagy, hereafter referred to as autophagy, has been first studied in the model system *Saccharomyces cerevisiae*, leading to the identification of more than thirty genes involved in this process (Inoue & Klionsky, 2010). The importance of this process is now worldwide accepted leading to Yoshinori Ohsumi the Nobel Prize in Medicine in 2016 for his discoveries related to autophagy.

For most of the autophagy-related genes (ATG genes), mammalian counterparts have been subsequently identified, thus demonstrating that this mechanism is highly conserved during evolution (Abounit, Scarabelli, & McCauley, 2012). In this process, cytoplasmic components including protein aggregates and organelles are engulfed by double-membrane structures known as autophagosomes, which fuse with lysosomes to deliver their cargo for degradation. Generation of different mouse reporter lines for autophagic markers showed that a basal autophagy rate is present in all tissues, even if stress conditions, such as nutrient deprivation, oxidative stress and hypoxic conditions can activate autophagy at different levels in a tissue specific manner.

Thus, as for all degradative pathways, autophagy regulation is essential to specifically "switch on" the process for the limited time it is required. In different stress conditions, different signaling pathways are activated, most of them converging on the kinase mTOR, which plays a central role in the integration of cellular inputs and autophagy regulation (Tooze & Yoshimori, 2010). During nutrient deprivation or under genotoxic stress conditions, AMPK and p53 signaling pathways are activated thus inhibiting mTOR. Conversely, AKT and MAPK signaling is active under anabolic conditions or in response to extracellular signals respectively, leading to mTOR activation. One of the target of active mTOR kinase is ULK1, a crucial protein for autophagy initiation. Phosphorylation by mTOR inactivates ULK1, while its active form is able to assemble with other ATG proteins (ATG13, FIP200, ATG101 and others) in a complex that localizes at specialized

sites initiating the formation of a double membrane structure called isolation membrane or phagophore. Phagophore is the autophagosome precursor and its formation requires the class III phosphoinositide 3-kinase (PI3K) Vps34, which acts in a large macromolecular complex containing BECLIN1, ATG14, FIP200 and Vps15 (p150). The elongation of the autophagosomal membranes is a critical step that is associated with two ubiquitination-like reactions. In the first one, ATG7 and ATG10, an E1 and E2-like enzymes respectively, conjugate ATG12 to ATG5. The ATG5-ATG12 conjugates then interact non-covalently with Atg16L1 to form a large complex that facilitate the action of the LC3 conjugation system. The whole complex associates with growing phagophores but dissociates once the autophagosome formation is complete (and so the membrane is closed). In this phase, membranes are recruited especially form ER and mitochondria (Tooze & Yoshimori, 2010). In the second ubiquitin-like reaction, microtubule-associated protein 1 light chain 3 or LC3 (MAP1LC3, the mammalian homolog of yeast Atg8), after a proteolytic cleavage by ATG4 that generate the cytosolic form of the protein (LC3-I), is then conjugated to the lipid phosphatidylethanolamine (PE) with a covalent bond, through the action of ATG7 (E1-like) and ATG3 (E2- like) to form LC3-II (Rubinsztein, Marino, & Kroemer, 2011).

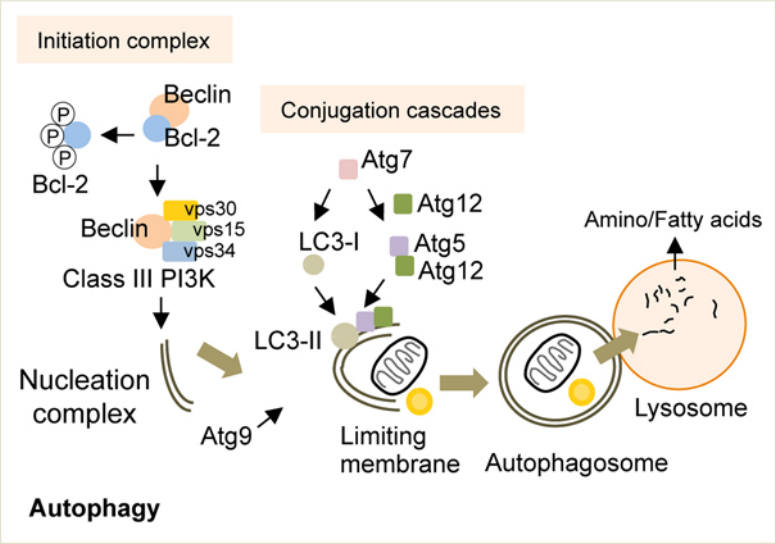

Figure 7 - Schematic view of autophagy initiation steps and mechanisms of membrane elongation

Thus, the lipidated form of LC3 is finally attached to the growing autophagosome membrane, where it is kept during the whole process. For this reason LC3 is considered a reliable marker of the entire process and the quantification of its two forms can provide important information about autophagy induction and flux. LC3-II is required both on the outer and inner membranes of the nascent autophagosome. Once the cytoplasmic cargo is completely wrapped, the double membrane structure closes to become the mature autophagosome that finally fuses with lysosomes. This fusion generates the so-called autophago-lysosome, which digest the cargo and some of the components of the vesicle itself (Abounit et al., 2012). Indeed, the fusion between the outer autophagosomal membrane with the lysosomal one determines the degradation of the inner membrane and of the proteins that are associated with it. Because of the transient nature of the autophagosomes, the lifetime of LC3 and its homologues is rather short. This feature represents the main difference between the ubiquitin-proteasome system and the autophagy-lysosome one, where the fate of the ubiquitin and ubiquitin-like proteins is different. Indeed, while the ubiquitin proteasome pathway recycles ubiquitin molecules, the autophagy-lysosome system progressively loses the ubiquitin-like proteins (LC3s), forcing the cell to replenish them in order to maintain the autophagic flux.

Autophagy is primarily considered to be a non-selective degradation pathway, but the significance of more selective forms of the process is becoming increasingly evident. Selective autophagy relies on cargo-specific autophagy receptors that facilitate cargo sequestration into autophagosomes. Autophagy receptors directly interact with the structure that needs to be specifically eliminated by autophagy, as well as with LC3 present in the internal surface of the growing autophagosomes. This interaction is mostly mediated through a specific amino acid sequence present in the autophagy receptors and commonly referred to as the LC3-interacting region. One of the most important and well-known ubiquitin-associated proteins that provide a link between autophagy and selective protein degradation is p62, also called sequestosome 1 (SQSTM1 but hereafter referred as p62). In this way p62 acts as a bridge between ubiquitinated proteins that has to be degraded and LC3-II located in the inner membrane of the autophagosome. Thus, since LC3-II in the inner autophagosomal membrane is degraded together with other cellular constituents by

lysosomal proteases, also p62 trapped by LC3 is destroyed during the normal happening of the process, accumulating only in case of the impaired autophagic flux (Ichimura & Komatsu, 2010). p62 is more linked to the autophagy-lysosome system rather than to ubiquitin-proteasome, being required in the targeting of dysfunctional mytochondria for lysosomal degradation in a specific form of the process called mitophagy. Moreover other organelles can be specifically targeted for autophagic degradation (nucleophagy, reticulophagy, ribophagy) supporting the idea that the cell presents strict criteria and high specificity for self-eating.

1.4 Transcription factor EB

The transcription factor EB (TFEB) is a member of the microphthalmia family of basic helix-loop-helix– leucine-zipper (bHLH-Zip) transcription factors (MiT family). The role of MiT family in the regulation of basic cellular processes has only recently become more clear. Recent evidences showed that TFEB has an important function in organelle biogenesis and metabolic processes; in particular an increased number of new works clarified the mechanisms leading to TFEB activation and its role in the regulation of lysosomal function and autophagy, both *in vitro* and *in vivo*.

1.4.1 MiT family of transcription factors

MiT/TFE (Microphthalmia/TFE) transcription factor family is a subfamily of basic/helix-loop-helix/leucine zipper (bHLH-LZ) transcription factors. During past years four members have been identified: microphthalmia-associated transcription factor (MiTF), TFEB, TFE3 and TFEC (Steingrimsson, Copeland, & Jenkins, 2004). All members of the MiTF/TFE family share a similar structure that incluedes three critically important regions (Figure 8). They share an identical basic motif for binding to specific areas of DNA while they present highly similar HLH and Zip regions, which are instead critical for protein-protein interactions. Homodimerization and heterodimerization within members of the MiTF/TFE family is critical for binding to DNA and transcriptional activation of target genes (Martina, Diab, Li, & Puertollano, 2014). TFEB, MITF and TFE3 also contain a conserved activation domain that is important for their transcriptional activation.

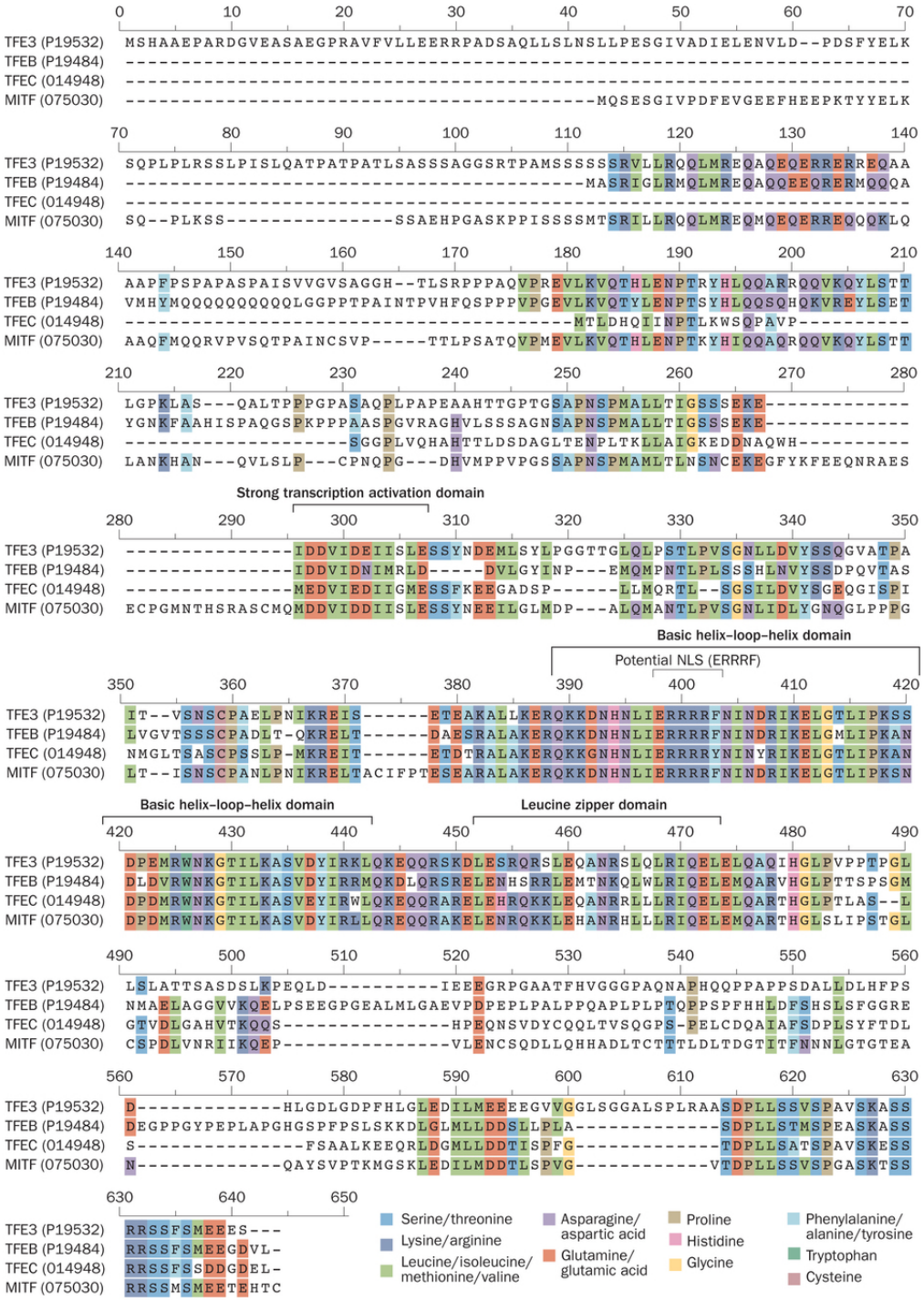

Figure 8 - Multialignement showing the different conserved region shared by all the four members of the MiT transcription factors family (Napolitano & Ballabio, 2016)

The activation domain is missing in TFEC, which is the most divergent member of the family and appears to inhibit, rather than activate, transcription (Napolitano & Ballabio, 2016).

MiT members bind the palindromic CACGTG E-box, a motif also recognized by other bHLH-Zip transcription factors, such as MYC, MAX and MAD proteins (Hemesath et al., 1994); differently from other bHLH-Zip transcription factors, MiT proteins also bind the asymmetric TCATGTG M-box sequence. Binding to DNA sequences is possible through the formation of both homodimers and heterodimers with any other family member, as already mentioned. However, MiT proteins are not able to heterodimerize with other bHLH-Zip transcription factors because they present a specific conservation of three residues in the Zip domain that generates an unusual folding allowing the specific interaction among only MiT members, while preventing the binding to other bHLH-Zip transcription factors (Pogenberg et al., 2012). All this four members are conserved among vertebrates and a single orthologous gene is found also in lower organisms such as *Drosophila melanogaster* and *Caenorhabditis elegans*.

In mammalian, each member has a typical expression pattern. MiTF is predominantly expressed in melanocytes, osteoclasts, macrophages and heart, whereas TFEC expression is restricted to of cells myeloid origins. In contrast, TFE3 and TFEB show a more ubiquitous expression and have been detected in multiple cell types (Martina et al., 2014).

Plenty of evidences supports the important role played by this family of transcription factors in many cellular and developmental processes. MITF is critical for development, survival, and differentiation of neural crest-derived melanocytes and retinal pigmented epithelium (RPE) and collaborates with TFE3 to regulate osteoclastogenesis and mast cell differentiation (Martina et al., 2014). TFE3 was first identified as a protein that binds to the mE3 motif within the immunoglobulin heavy-chain enhancer and was implicated, together with TFEB, in humoral immunity. Finally, TFEB was shown to be essential for placental vascularization.

Mutation and/or aberrant expression of several MiTF/TFE family members have been linked to different types of cancer in humans, such as renal carcinomas, alveolar sarcomas, and melanomas.

Furthermore, recent evidences suggest that some members of the family, in particular TFE3 and TFEB, function as critical factors in nutrient sensing and maintenance of cellular homeostasis. In particular, thanks to the hard work of prof. Ballabio and collaborators, it has emerged the role of TFEB in lysosomal homeostasis, autophagy regulation and energy metabolism.

1.4.2 TFEB gene network and function

As mentioned before, lysosomes are crucial components of the cellular degradation and recycling system, and their correct function is necessary to maintain proper cell homeostasis(Ballabio, 2016). These organelles are indeed involved in a number of essential cellular processes, including endocytosis, autophagy and lysosomal exocytosis (Medina et al., 2011; Settembre et al., 2013). Although lysosomes were originally described as static organelles devoted to terminal degradation of waste material and lysosomal biogenesis was considered as a housekeeping process, recent discoveries supporting the idea that lysosomal biogenesis and function are finely transcriptionally regulated changed the way of looking at these organelles. Microarray analysis revealed that genes encoding for lysosomal proteins are co-expressed in different cell types and under different conditions (Sardiello et al., 2009). Subsequent promoter analysis of lysosomal genes revealed that they share a common 10-base E-box-like palindromic sequence, the so-called coordinated lysosomal expression and regulation (CLEAR) motif. TFEB has been identified as the candidate transcription factor that directly binds to CLEAR elements, thereby promoting the expression of the entire network of genes containing the CLEAR regulatory motif in their promoter (namely the CLEAR network) (Palmieri et al., 2011). Accordingly, TFEB overexpression in cell culture results in an increased number of lysosomes and higher levels of lysosomal enzymes, thus enhancing lysosomal catabolic activity.

Altogether these findings indicate that TFEB is a master regulator of the lysosomal biogenesis program. Furthermore, through the regulation of TFEB activity, cells can monitor lysosomal function and adapt to degradation requirements and/or environmental signals.

Subsequent work has shown that TFEB is also able to orchestrate the expression of a broader number of genes, which are not only involved in lysosomal biogenesis and function, but also in autophagy and lysosomal exocytosis (Palmieri et al., 2011). In particular, TFEB has been shown to bind to the promoter regions and induce the expression of numerous autophagy genes important for autophagosome biogenesis and autophagosome-lysosome fusion (Settembre et al., 2011), supporting the transcription of these regulators that are normally degraded throughout the process. TFEB is not the only transcription factor implicated in autophagy regulation. FoxO3, HIF-1 and p53 have also been shown to regulate the expression of autophagy genes in response to different stress conditions; however, while these latter regulators promote genes involved in initial steps of autophagosome formation, TFEB appears to control a more comprehensive autophagy gene network, coordinating the two main degradative pathways of the cell.

Moreover, TFEB has also been found to induce lysosomal exocytosis (Medina et al., 2011), a process by which lysosomes fuse to the plasma membrane and secrete their content to the extracellular space.

Importantly, TFEB does not regulate the basal transcription of its targets but rather enhances their transcriptional levels in response to environmental cues. Therefore, by modulating the processes of lysosomal biogenesis, autophagy and lysosomal exocytosis, TFEB coordinates a transcriptional program able to control the main cellular degradative pathways and to promote intracellular clearance.

1.4.3 Regulation of TFEB activity

Understanding the mechanisms regulating TFEB activation has been the first necessary step in order to exploit the different functions of this transcription factor to modulate cellular clearance in pathological conditions. The activity of TFEB is strictly regulated through post-translational modifications, protein–protein interactions and subcellular relocalization. So far, TFEB activation during nutrient deprivation has been the most studied model; in resting cells, under nutrient-rich conditions, TFEB is largely cytosolic and inactive. Conversely, upon starvation or under conditions of lysosomal dysfunction or stress, TFEB rapidly translocates to the nucleus and activates the transcription of its target genes (Settembre et al., 2011). In addition, TFEB activation also promotes its own

transcription, which represents an additional feedback-loop that further sustains lysosomal signaling and function.

TFEB cellular localization and activity are mainly controlled by its phosphorylation status. Two particular serine residues, Ser142 and Ser211, in the TFEB protein play a crucial role in determining its subcellular localization. When both of these two serine residues are phosphorylated, TFEB is kept inactive in the cytosol. Accordingly, variants of TFEB carrying Ser-to-Ala mutations of either Ser142 or Ser211 are always nuclear and constitutively active (Settembre et al., 2012). Phosphorylation of Ser211, in particular, has been shown to serve as a docking site for the chaperone 14-3-3, which sequesters TFEB in the cytosol and prevents its nuclear translocation, probably by masking its nuclear localization signal (NLS) (Martina, Chen, Gucek, & Puertollano, 2012).

mTORC1 complex and ERK2, both master controllers of cellular growth, are the main protein kinases known to phosphorylate TFEB under nutrient-rich conditions in most cell types. Remarkably, mTORC1 activation occurs at the lysosomal membrane (Sancak et al., 2010). In the presence of nutrients, a mechanism involving the v-ATPase complex promotes the activation of the small Rag (Ras-related GTP-binding) GTPases, which recruit mTORC1 to the lysosomal membrane, thus promoting its activation through the small GTPase Rheb. Interestingly, active Rag GTPases also bind to TFEB and recruit it to the lysosomal membrane, thereby promoting its phosphorylation by mTORC1. This evidence suggests that mTORC1- mediated TFEB phosphorylation can occur at the lysosomal membrane (Martina et al., 2014). Upon starvation or lysosomal stress, mTORC1 is released from the lysosomal membrane and becomes inactive, reducing its inhibitory activity on TFEB and allowing potential phosphatases to act removing the inhibitory phosphorylation (Figure 9). Interestingly, starvation, through a calcium transient lysosome-dependent, activates the phosphatase calcineurin, which in turn dephosphorylates TFEB and promotes its nuclear translocation (Medina et al., 2015). Moreover, *in vivo* data demonstrate that calcineurin is also promoting TFEB activation in skeletal muscle during exercise, suggesting a potential role for TFEB in controlling contraction-dependent adaptations to physical training.

In conclusion, further studies will be needed to fully understand how different pathways communicate with each other to modulate TFEB activity in order to finely tune the final transcriptional outcome.

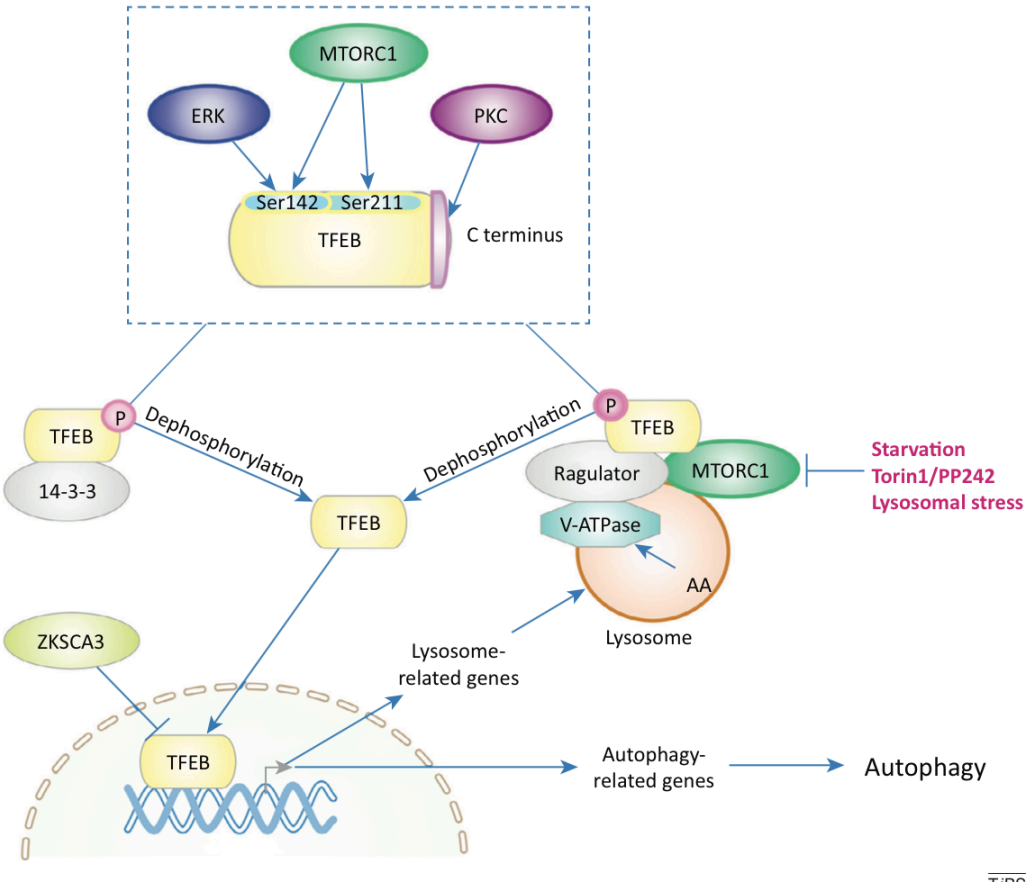

Figure 9 - Scheme representing the signaling pathways converging on TFEB activity regulation (Shen & Mizushima, 2014)

1.4.4 *In vivo* studies and potential role of TFEB as therapeutic target for disease

TFEB tissue-specific functions, as well as the modulation of its activity, have been long investigated. TFEB-null mice die at embryonic stages, suggesting important role of this transcription factor during development. This lethality has precluded a systematic characterization of TFEB function in different tissues; therefore, the generation of conditional mouse models has been the only way to circumvent this problem. The use of

such mice has revealed that TFEB surprisingly possesses specialized completely different functions in different tissues.

Liver-specific deletion and viral-mediated overexpression of TFEB in the liver has revealed a central role for this protein in regulating liver lipid metabolism. TFEB has been shown to control lipid catabolism and to directly regulate the transcription of Pgc1α, a key regulator of energy metabolism. Indeed, TFEB depletion in liver results in impaired catabolism and exacerbated metabolic imbalance in obese mice, whereas TFEB overexpression has the opposite effect and rescues obesity and associated metabolic syndrome (Settembre et al., 2013). Moreover, our evidences using gain and loss of function approaches in skeletal muscle show that TFEB control glucose homeostasis and energy balance in this tissue during exercise.

Nonetheless, due to its involvement in intracellular clearance pathways, TFEB has been studied as an appealing therapeutic target for many diseases associated with autophagic or lysosomal dysfunction and the accumulation of toxic aggregates.

Indeed, induction of TFEB activity has already been successfully used as a therapeutic strategy in several disease models. Overexpression of TFEB in cellular and mouse models of several lysosomal storage disorders (LSDs), such as Pompe disease and others, has been shown to be beneficial in reducing substrate accumulation and improving autophagy and lysosomal function with a consequent amelioration of the severity of tissue phenotype (Spampanato et al., 2013).

Moreover also neurodegenerative diseases such as Parkinson's and Alzheimer's benefit from TFEB overexpression in the tissue involved in the pathology (Decressac et al., 2013). Indeed intracellular clearance of intracellular aggregates through autophagy reactivation and lysosomal exocytosis represents an appealing therapeutic strategy that, in any case, requires further investigations in order to understand the possible effects of long-term TFEB treatments. Indeed autophagy activation via MiT genes has been associated with tumorigenesis in different tissues. Therefore, alternative strategies, such as inducing TFEB activity for only limited periods and in a tissue specific context or enhancing only a specific subset genes of the TFEB-regulated network, should be considered when using TFEB as a therapeutic tool.

1.5 Exercise metabolism and the skeletal muscle adaptation

The benefits provided by physical activity have long been known. Indeed, physical inactivity is a known, but modifiable, risk factor that contributes to lifestyle-related diseases, including many causes of ‘‘preventable death’’ (Booth, Roberts, & Laye, 2012). Regular exercise and physical activity have been proposed in the prevention, management, and treatment of numerous chronic conditions, including hypertension, coronary heart disease, obesity, type 2 diabetes mellitus (T2DM), and age-related muscle wasting (sarcopenia) (Egan & Zierath, 2013). Thus the axiomatic statement “exercise is medicine” appears to be always more convincing, placing physical activity at the top as preventive approach for metabolic syndromes. In fact, regular exercise combined with dietary intervention has been proved to be significantly more successful than pharmacological intervention in the treatment and prevention of obesity and T2DM (Knowler et al., 2002).
While the benefits and adaptations to regular exercise are long known, molecular networks, signaling pathways and regulatory molecules that coordinate adaptive responses to exercise are still matter of debate.

1.5.1 Molecular basis of skeletal muscle adaptation to exercise

Due to its ability of contracting, skeletal muscle is the main protagonist of exercise training and training derived adaptations. Over time, skeletal muscle demonstrates remarkable malleability in functional adaptation and remodeling in response to contractile activity. Training-induced adaptations are reflected by changes in contractile protein and function, mitochondrial function remodeling, metabolic and glucose homeostasis regulation, intracellular signaling and transcriptional responses (Egan & Zierath, 2013).
The widely accepted molecular mechanisms that govern adaptations to exercise training involve gradual alterations in protein content and enzyme activities. These progressive changes reflect activation and/or repression of specific signaling pathways that regulate transcription and translation of exercise-responsive gene. Transient post-exercise changes in gene transcription include genes involved in different muscle processes: myogenic regulators, genes of carbohydrate (CHO) metabolism, lipid mobilization regulators, transporters and mitochondrial biogenesis/oxidative phosphorylation modulators (Cartee, Hepple, Bamman, & Zierath, 2016). This gene expression modulation is achieved through

mainly through alteration of transcription factor binding activity, protein stability and/or regulation of subcellular localization of different transcription factors. However, although each individual bout of exercise is necessary as a stimulus for adaptation, it alone is insufficient to alter training-induced muscle phenotype; thus, adaptation is the consequence of repetition of the stimulus of individual exercise bouts (Figure 10). More specifically, an individual exercise bout elicits a rapid, but transient, increase in relative mRNA expression of a given gene after exercise, during recovery period. Alterations in mRNA expression are typically greatest at 3-12 hours after cessation of exercise session and generally return to basal levels within 24 hours; however the temporal pattern of expression is specific for any specific gene and typology of exercise, mainly relying on the different transcription factors that are activated during the contractile stimulus. Translational processing is reflected by elevated post-exercise protein synthesis rate that results in a modest change in protein content.

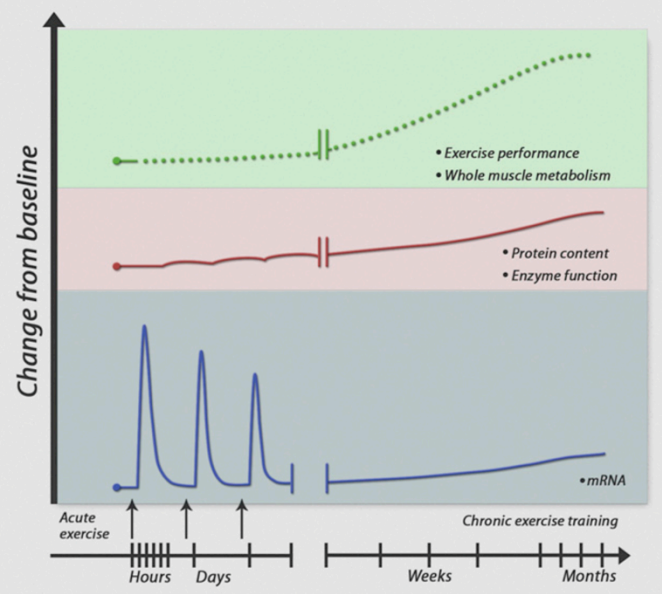

Figure 10 - Schematic representation of the molecular basis of skeletal muscle adaptation to exercise. Intracellular events gradually modify gene expression, protein expression leading to the final adaptation and increased muscle performance (Egan & Zierath, 2013)

Superimposition of repeated exercise bouts results in the gradual accumulation of protein in response to repeated, pulsed increases in relative mRNA expression. Thus, long-term

adaptation to training is due to the cumulative effects of each acute exercise bout leading to a new functional threshold. Training-induced changes in protein content or enzyme function alter metabolic responses to exercise thus resulting in improved exercise performances time by time. Summarizing, these adaptations are intrinsic to the working skeletal muscle, and collectively contribute toward maximizing substrate delivery, mitochondrial respiratory capacity, and contractile function during exercise with the net effect of promoting optimal performance during a future exercise challenge. All these features finally result in a robust defence of homeostasis against metabolic and mechanical perturbation occurring during physical activity.

1.5.2 Regulation of skeletal muscle gene expression during adaptation

An increasingly well-defined network of transcription factors and co-regulator proteins has emerged, all regulating skeletal muscle plasticity through the integration of signals from physiological stimuli and coordinated metabolic adaptations. This network exerts molecular control over contractile, metabolic, and mitochondrial adaptation altering the expression of key enzymes in CHO and lipid metabolism and coordinating this with mitochondrial biogenesis in response to exercise (Hood, 2001).

The process of mitochondrial biogenesis is complex and highly regulated, requiring the co-ordination and co-expression of genes belonging to both nuclear and mitochondrial genomes. Mechanistic studies using transgenic animals and pharmacological manipulation have explored the roles of key regulators of skeletal muscle phenotype. Many of them are sufficient to stimulate mitochondrial biogenesis, fiber-type transformation, and reprogramming of skeletal muscle metabolism, but many are not necessary for exercise-induced skeletal muscle adaptation. For example, PGC1α acts as a transcriptional co-activator through recruitment and co-regulation of multiple transcription factors that regulate skeletal muscle gene expression, including NRF-1, NRF-2, and Tfam (Lin, Handschin, & Spiegelman, 2005). Its overexpression in rodent skeletal muscle produces a phenotype remarkably similar to aerobically trained muscles, with increased mitochondrial density, respiratory capacity, ATP synthesis and improved exercise performances (Calvo et al., 2008). However, adaptive responses after exercise training are similar in WT and

PGC1α KO animals (Leick et al., 2008), suggesting that this transcriptional co-activator is not necessary for the majority of adaptive responses to exercise training.

Despite all these hunting for transcriptional regulators of mitochondrial biogenesis as consequence of exercise training, little is know about the gene expression regulation of glucose transporters and glucose homeostasis regulation. So far it is known that calcineurin phosphatase is playing a major role in the control of glucose uptake during physical training (Long & Zierath, 2008); moreover AMPK and nNOS signaling have been correlated to GLUT4-to-plasmalemma translocation during contraction (De Palma et al., 2014). Nevertheless, a sensor able to transcriptionally coordinate mitochondrial and glucose homeostasis gene expression is missing. Indeed these are only two of the major adaptation induced by physical training that have been well studied for their important role in fighting metabolic syndromes such as 2TDM and skeletal muscle aging (Cartee et al., 2016).

Thus the possibility of discovering a master coordinator of exercise-induced metabolic adaptations would be for sure the first step for pharmacological intervention in order to have "exercise in a pill".

1.5.3 Modalities of exercise

The use of the term "exercise" in the scientific community often encompasses several modifiable variables. These include the modality (e.g., aerobic versus resistance) and the frequency, intensity, and duration of exercise sessions, each of which modulating different factors impacting the metabolic and molecular responses. Aerobic (or endurance-based) and resistance (or strength-based) activities represent two extremes of the exercise continuum. Aerobic exercise imposes a high-frequency (repetition) and low-power output (load) demand on muscular contraction, whereas resistance exercise imposes a low-frequency and high-resistance demand. As a consequence, the metabolic and molecular signatures of these different modalities are distinct, specifying a peculiar molecular response coupled to a functional outcome. Although both aerobic exercise and resistance training can individually promote substantial health benefits, divergent effects are observed depending on the parameter of interest. For example, aerobic training more effectively modifies cardiovascular risk factors, whereas resistance training more effectively

maintains basal metabolic rate, muscle mass, and physical function in the elderly (Cartee et al., 2016). However, compared to either modality alone, a combination of aerobic and resistance training is more effective for reducing the insulin resistance and functional limitations in obesity and the metabolic syndrome (Davidson et al., 2009), improving even glycemic control in T2DM.

1.5.4 Metabolic response to an acute bout of exercise

During acute exercise, the contribution of various metabolic pathways to energy provision is determined by the relative intensity and absolute power output of the exercise bout. The absolute power output determines the rate of ATP demand and energy expenditure, whereas the relative exercise intensity influences the relative contributions to energy provision of carbohydrates (CHO), lipid sources and circulating/intramuscular fuel stores. The use of indirect calorimetry combined with isotope tracer methodology permitted the assessment of substrate utilization during exercise (van Loon, Greenhaff, Constantin-Teodosiu, Saris, & Wagenmakers, 2001). Fuel utilization is finely quantitatively and temporally coordinated to meet the metabolic demands of exercise.

At low-to-moderate intensities of exercise, the primary fuel sources supplying skeletal muscle energy demand are glucose, derived from hepatic glycogenolysis (or gluconeogenesis) and oral ingestion, and free fatty acids (FFAs) released by adipose tissue lipolysis. With respect to extramuscular fuel sources, as exercise intensity increases, muscle utilization of circulating FFAs declines modestly, whereas utilization of circulating glucose increases progressively up to near-maximal intensities. This is paralleled by an increase in the absolute rates of CHO oxidation and relative contribution to energy provision, with a majority of energy being provided by muscle glycogen at high intensities of exercise. When exercise at a fixed sustained intensity is prolonged (>60 minutes), an increasing energy contribution is derived from lipid oxidation. Consequently, the proportion of energy derived from muscle glycogen declines and is replaced by a progressive increase in plasma FFA oxidation. Thus, muscle glycogen is the predominant CHO source during moderate to intense exercise, and the rate of glycogenolysis is proportional to the relative exercise intensity. Conversely, intramuscular triglycerides (IMTGs) constitute only a small fraction (1-2%) of whole-body lipid stores; however they

constitute an important fuel source during prolonged (>90 minutes), moderate intensity exercise, providing 25% of total energy. As with aerobic exercise, both muscle glycogen and IMTG contribute to energy provision during resistance; however, regulation of CHO and lipid utilization during exercise is still a matter of open debates (Egan & Zierath, 2013).

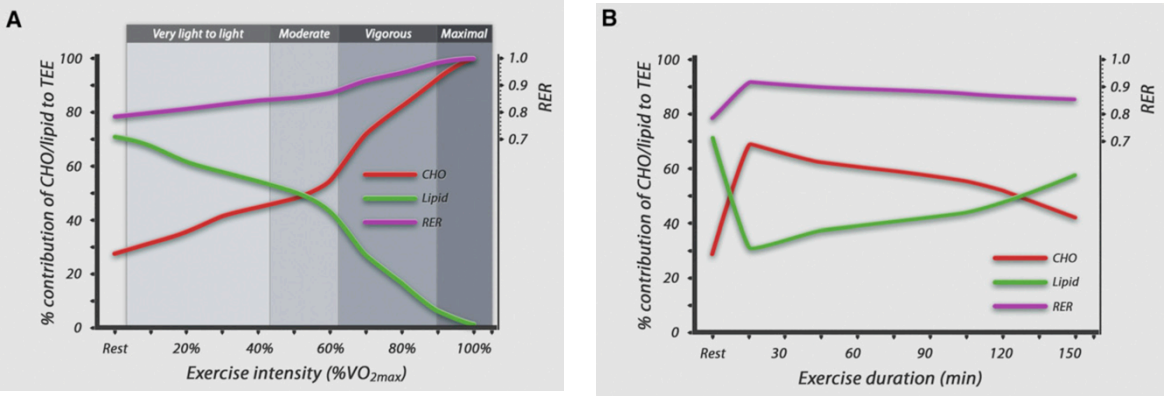

Figure 11 - Schematic tracks representing different fuel utilization in dependence of exercise intensity (A) or exercise duration at a fixed intensity (e.g. 65% VO_{2max}) (B). RER (respiratory exchange ratio) is the ratio between carbon dioxide produced and oxygen consumed; it is the index used to estimate the contribution of different fuel to energy production (Egan & Zierath, 2013)

1.5.5 Muscle metabolism during the post-exercise recovery period

After the cessation of exercise, the metabolic rate declines but remains slightly elevated (<10%) for up to 24 hr. The extent of this ‘‘excess postexercise oxygen consumption’’ (EPOC) is proportional to the metabolic stress and determined by the intensity, duration, and type of exercise bout (Borsheim & Bahr, 2003) and this feature is the basis of the beneficial effect of exercise in increasing insulin-sensitivity.

This recovery period is characterized mainly by two major phases: (1) recovery of myocellular homeostasis in the immediate hours after exercise, and (2) cellular contributions to adaptation to exercise.

In contrast to the reliance on CHO metabolism during exercise, an increase in lipid oxidation and “sparing” of CHO sources for energy provision occurs during the recovery period. This shift accommodates the high metabolic priority of resynthesizing muscle glycogen storage, whereas the oxidation of lipid from both IMTG and circulating FFA

sources is elevated to meet fuel requirements. The prolonged elevation in lipid oxidation in the post-exercise period represents a key event in exercise-mediated effects on whole-body lipid metabolism, mediating beneficial effects of exercise in obese people. Lipid oxidation rates can reach 25% of that reported during exercise, and contribute greater than 60% of oxidative metabolism during recovery. Several other biosynthetic processes contribute to homeostatic recovery at a local level, including elevated rates of mitochondrial and myofibrillar protein synthesis.

In contrast to the rapid glycogen depletion during sustained or prolonged exercise, the replenishment of muscle glycogen to pre-exercise levels requires 24-48 hours and can be heavily altered by dietary interventions. Indeed, high CHO intake in the recovery period often produces a "supercompensation" effect in which glycogen repletion markedly exceeds pre-exercise concentrations.

1.5.6 Activity dependent signaling pathways

Skeletal muscle contraction leads to a dramatic perturbation in mechanical strain, ATP turnover, calcium fluxes, redox balance and intracellular oxygen pressure; all these changes have been implicated in the activation of signal transduction cascades regulating skeletal muscle plasticity. In turn, various cellular stress sensors transduce these homeostatic perturbations in transcriptional alterations providing a framework, known as excitation-transcription coupling (Figure 12), that integrates signaling events regulated by cellular bioenergetics and stress and the expression of genes that dictate skeletal muscle phenotypic adaptation to exercise training.

One of the first perturbations of cellular homeostasis occurring during contraction involves calcium and its related signaling. Upon action potential arrival, sarcolemma undergoes a strong depolarization that in turn allows a massive calcium release from reticulum inside the myofiber. This calcium transient is essential to allow the interaction between myosin and actin and therefore to activate muscle contraction. Nevertheless, calcium oscillations during contractions lead to the activation of different signaling pathways involved in the determination of fiber type. In particular the Ca^{2+}-calmodulin complex is known to activate numerous downstream signaling kinases and phosphatases such as CaMK and calcineurin

(Cn). Calcineurin has a pivotal role in the regulation of the slow gene program. Indeed, the overexpression of an activated form of Cn leads to small increase in slow fibers, while the genetic ablation of Cn in skeletal muscle prevents a fast-to-slow fiber-type transformation during overload hypertrophy (Parsons et al., 2004). Activated Cn dephosphorylates many substrates including the nuclear factor of activated T cells (NFAT), the myocyte enhancer factor 2 (MEF2) transcription factors and TFEB. Translocation of NFAT into the nucleus induces a slow gene program inhibiting the fast program while MEF2 activation, together with various co-factors, plays an important role in the regulation of fiber type metabolism, activating the well-known transcriptional co-regulator PGC1α.
The role of Cn in dephosphorylating TFEB has been recently published (Medina et al., 2015) even if the evidences clarifying the meaning of this TFEB nuclear translocation have not yet been published and will be discussed throughout all the Results section.

Another important pathway activated during exercise is mediated by the action of the kinase AMPK. This serine/threonine kinas, activated thanks to an increase in the AMP/ATP ratio, modulates acutely cellular metabolism through phosphorylation of metabolic enzymes (Jager, Handschin, St-Pierre, & Spiegelman, 2007). Given the rate of ATP turnover during contraction, AMPK functions as a signal transducer that responds to an altered cellular energy status in order to provide metabolic adaptations (Egan & Zierath, 2013). AMPK activation acts to conserve ATP by inhibiting biosynthetic and anabolic pathways, stimulating catabolic conditions to restore energy homeostasis. In skeletal muscle acute AMPK activation stimulates an increase in insulin-indipendent glucose transport, due to the translocation of GLUT4 to the membrane (Merrill, Kurth, Hardie, & Winder, 1997). Several studies have shown that AMPK is a negative regulator of skeletal muscle protein synthesis and consequent growth; indeed, AMPK phosphorylates tuberous sclerosis complex 2 (TSC2) and also directly mTORC1, leading to an inhibition of translation initiation. Besides its role in repressing protein synthesis, AMPK activation also stimulates protein degradation through phosphorylation and activation of FoxO3 and stimulating the ubiquitin-proteasome and the autophagy-lysosome systems. Chronic AMPK activation alters metabolic gene expression and induces mitochondrial biogenesis phosphorylating the well-known co-regulator PGC1α (Jager et al., 2007).

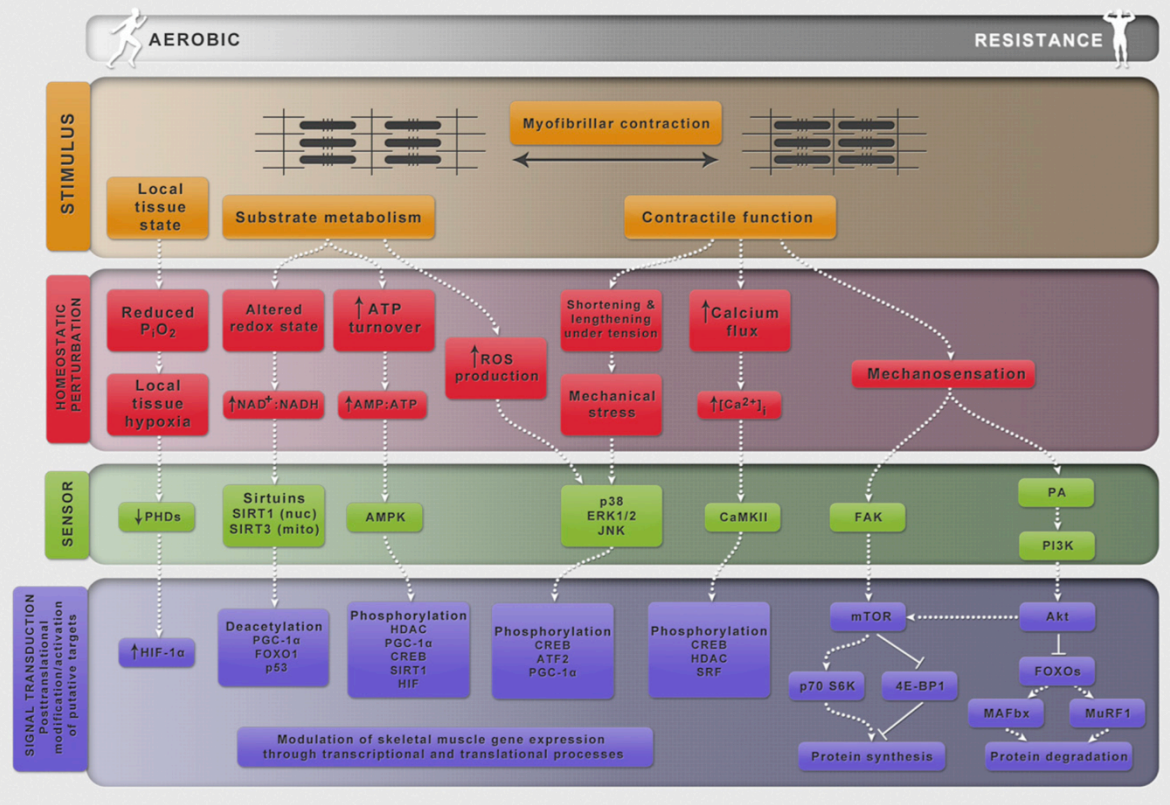

Figure 12 - Schematic of excitation-transcription coupling in skeletal muscle (Egan & Zierath, 2013)

Exercise is also a potent autophagy activator in skeletal muscle (Grumati, Coletto, Sandri, & Bonaldo, 2011; He et al., 2012). Autophagy is normally constitutively active in adult skeletal muscle even if at a low rate. In this tissue, different stimuli, such as starvation and denervation-induced atrophy can strongly induce this process, as well as muscle contraction.

Autophagy is not required to sustain physical training but it is fundamental in the recovery period to remove damaged mitochondria and structures produced during contraction (Lo Verso, Carnio, Vainshtein, & Sandri, 2014; Vainshtein & Hood, 2016). Indeed, since mitochondria produce the energy required for muscle contraction, their proper integrity is essential to maintain muscle homeostasis. The mechanical and energetic perturbations associated with exercise result in immediate increase in ROS in skeletal muscle that in turn can irreversibly damage mitochondria. Thus, in an effort to prevent cell death, damaged mitochondria are sequestered by autophagosomes and degraded before apoptosis or necrosis can be triggered.

Beside the above described mechanisms, other pathways are usually active during contraction, all of them depending on a different stimulus such as redox stress, mechanical loading and oxygen unbalance.

It is noteworthy to mention the new emerging role of skeletal muscle during exercise as a secretory organ that secretes cytokines and exosomes in the circulation system (Glund et al., 2007; Safdar, Saleem, & Tarnopolsky, 2016). The understanding of skeletal muscle endocrine function and the crosstalk among this and other organs will be for sure a fertile avenue for future research.

In conclusion, the pleiotropic effects of exercise and the complexity of responses at both metabolic and molecular level suggest that there is no singular pathway mediating exercise-training adaptations. For these reasons, all these highlights are far from the possibility to be condensed in pharmacological therapy that can be used as an "exercise mimetic". However, compounds actives on particular exercise-activated pathways could be for sure used as adjunct treatment to exercise to potentiate or ameliorate a particular adaptive response.

2 Aim of the study

Skeletal muscle is a highly dynamic tissue able to adapt to different physiopatological stimuli. However molecular mechanisms that lead to myofibers adaptations to exercise are still under debate. It is also well established the role of exercise in promoting mitochondrial biogenesis and increasing mitochondrial performances; furthermore substrate utilization and glucose uptake are deeply influenced by physical training. Nevertheless, a common regulator able to coordinate substrate absorption and mitochondrial fuel utilization was still missing.

My PhD project has been focused on the dissection of the role of the transcription factor EB in skeletal muscle. Based on our findings proving that its activity is promoted during muscle contraction, we tried to clarify the meaning of this context specific activation.
Thus, I was involved in a project aimed to dissect the role of this transcription in skeletal muscle. By mean of gain and loss of function approaches we went through the understanding of the gene network controlled by TFEB, giving a new perspective on this transcription factor, till now known mainly because of its pivotal role in autophagy regulation.

3 MATERIALS AND METHODS

3.1 High-content nuclear translocation assay

$HeLa^{TFEB\text{-}GFP}$ cells were reverse transfected in 96 or 384-well plates, incubated for 12h, starved, washed, fixed and stained with DAPI. For the acquisition of the images, at least 5 images fields were acquired per well of the 96/384-well plate by using confocal automated microscopy (Opera high-content system; Perkin-Elmer). A dedicated script was developed to perform the analysis of TFEB localization on the different images (Harmony and Acapella software; Perkin-Elmer). The script calculates the ratio value resulting from the average intensity of nuclear TFEB–GFP fluorescence divided by the average of the cytosolic intensity of TFEB–GFP fluorescence. The results were normalized using negative (RPMI medium) and positive (HBSS) control samples in the same plate. At least two independent experiments, and up to 3,000 individual cells per treatment from at least two independent wells, are routinely analysed. *P* values were calculated on the basis of mean values from independent wells. The data are represented by the percentage of nuclear translocation versus the indicated control using Excel (Microsoft) or Prism software (GraphPad software).

The TFEB–GFP nuclear translocation analyses of different populations of transfected cells (detected by immunofluorescence of tagged-plasmids) were performed by a modified script that calculates the ratio value resulting from the average intensity of nuclear TFEB–GFP fluorescence divided by the average of the cytosolic intensity of TFEB–GFP fluorescence on both positive-transfected and negative-transfected cells.

3.2 Cell culture, plasmids, siRNA transfection and drugs tratments

Stable HeLa$^{TFEB-GFP}$ cell line was previously described (Settembre et al., 2012). HeLa cells were cultured in DMEM or RPMI 1640 media supplemented with 10% fetal bovine serum, 200 μM L-glutamine, 100 μM sodium pyruvate, in 5% CO_2 at 37°C.

Cells were silenced with PPP3CB siRNA oligonucleotides (Ambion, 4390824) or non-targeting siRNAs (Thermo, D-001810-10-05), by direct or reverse transfection, using Lipofectamine RNAiMAX reagent (Invitrogen) according to the protocol from the manufacturer. siRNA-transfected cells were collected after 72 h, if not otherwise stated. The plasmid carrying a constitutively active form of the human calcineurin catalytic subunit (ΔCnA) was donated by B. Rothermel (The University of Texas Southwestern Medical Center, USA). Cells were transfected using Lipofectamine LTX – Plus reagent (Invitrogen) according to the protocol from the manufacturers. The following drugs were used: FK506 (5μM, otherwise indicated) and cyclosporine A (10 μM, otherwise indicated). Starvation medium was HBSS, 10 mM HEPES.

3.3 *In vivo* skeletal muscle electroporation, plasmids and IF

Animals were handled by specialized personnel under the control of inspectors of the Veterinary Service of the Local Sanitary Service (ASL 16— Padova), the local officers of the Ministry of Health. Mice were housed in individual cages in an environmentally controlled room (23 °C, 12-h light– dark cycle) with ad libitum access to food and water. All procedures are specified in the projects approved by the Italian Ministero Salute, Ufficio VI (authorization numbers C65) and by the Ethics Committee of the University of Padova. All experiments were performed on 3- to 4-month-old C57BL/6J male mice. *In vivo* transfection experiments were performed by i.m. injection of expression plasmids in *Tibialis Anterior* (TA) muscles followed by electroporation. Animals were anesthetized by an intraperitoneal injection of xylazine (Xilor) (20 mg/Kg) and Zoletil (10 mg/Kg). TA muscles were isolated through a small hindlimb incision, and DNA was injected along the

muscle length. Electric pulses were then applied by two stainless steel spatula electrodes placed on each side of the isolated muscle belly (50 Volts/cm, 5 pulses, 200 ms intervals). 10 days after transfection mice performed concentric exercise on a treadmill (LE 8710 Panlab Technology 2B, Biological Instruments), with a 10 incline, until they were exhausted and then were euthanized.Muscles were removed and frozen in liquid nitrogen for subsequent analyses.

TA muscles were transfected with the following different plasmids:

- full-length TFEB-GFP
- ΔCnA;
- CnB;
- myc-CAIN.

3.4 Immunofluorescence

Frozen muscle serial sections (7 μm) were fixed in 4% paraformaldehyde in PBS for 10 min, washed twice in PBS (Sigma-Aldrich) for 5 min at room temperature (RT), and incubated in 0.3% TritonX-100 in PBS for 2 min at RT. After washing in PBS, sections were incubated in blocking solution (10% normal goat serum, 5% BSA in PBS) for 1h at RT. Anti-Dystrophin (Abcam) or anti-myc (Cell Signaling) were added separately to each serial section for 16 h at 4°C. Sections were washed twice in PBS, incubated with anti-rabbit Cy3 for 1 h at RT, washed twice, incubated with DAPI and then mounted with Elvanol.

3.5 Acute exercise, mild exercise and training protocols

For acute exercise, 3-5 moths-old mice were subjected to concentric exercise consisting of one day running on a treadmill (Biological Instruments, LE 8710 Panlab Technology 2B) to exhaustion, with a 10 degree decline, at increasing velocity, according to the protocol of exercise previously described (He et al., 2012). Briefly, exercise consists in 17 cm/sec for 40 minutes, 18 cm/sec for 10 min, 20 cm/sec for 10 min, 22 cm/sec for 10 min, and then

increasing velocity of 1cm/sec and or 2 cm/sec alternatively every 5 minutes, until they were exhausted. Exhaustion was defined as the point at which mice spent more than 5 s on the electric shocker without attempting to resume running.

Mild exercise was performed letting mice running on the treadmill for 1 hour at 15 cm/sec speed for 4 days. Training was performed for a total of 7 weeks increasing the speed of 5 cm/sec every week. The starting speed was the 50% of the maximal speed (exhaustion test) that corresponded to 25cm/sec and the final speed reached at the end of the training period was 55 cm/sec.

3.6 Generation of muscle-specific TFEB Knockout and inducible muscle-specific transgenic mice and AAV infection procedures

Mice bearing *Tcfeb*-floxed alleles (Tcfeb$^{f/f}$) (Settembre et al., 2013)were crossed with transgenic mice expressing Cre either under the control of a Myosin Light Chain 1 fast promoter (*MLC1f-Cre*) (Bothe, Haspel, Smith, Wiener, & Burden, 2000). For all experiments involving *TFEB*-KO mice, control mice were mice Tcfeb$^{f/f}$ that did not carry the *MLC1f-Cre* transgene.

To generate inducible muscle-specific TFEB transgenic animals, a line carrying *Tcfeb*3XFlag cDNA inserted after a CAGCAT cassette [chicken actin promoter (CAG) followed by chloramphenicol acetyltransferase (CAT) cDNA flanked by 2 loxP sites] (Settembre et al., 2011) was crossed with transgenic mice expressing Cre-ER driven by human skeletal actin promoter (HSA) (McCarthy, Srikuea, Kirby, Peterson, & Esser, 2012). Tamoxifen- induced Cre LoxP recombination was activated by IP injection of tamoxifen-containing for 3 days. Muscles were collected 2 weeks after the tamoxifen treatment. Cre-negative littermates, also receiving tamoxifen treatment, were used as controls. Adult mice (3 to 5 months-old) of the same sex and age were used for each individual experiment.

The PGC1α Knockout mouse line was obtained from Jackson Laboratory (Bruce Spiegelman, Dana- Farber Cancer Institute) (Lin et al., 2004).

In vivo TFEB overexpression experiments were performed by i.m. injection of a total dose of 10^{11} GC of AAV2.1 vector preparation. Muscles were removed 21 days after injection and frozen in liquid nitrogen for subsequent analyses.

All mice used were males and maintained in a C57BL/6 strain background. Standard food and water were given ad libitum. Mice were maintained in a temperature - and humidity-controlled animal-care facility, with a 12 hr light/dark cycle and free access to water and food (Standard Diet, Mucedola, Italy). All experiments were performed on 3- to 5-month-old male mice; mice of the same sex and age were used for each individual experiment.
For fasting experiments, control animals were fed *ad libitum*; food pellets were removed from the cages of the fasted animals. All procedures were formerly approved by the Italian Public Health, Animal Health, Nutrition and Food Safety, Italian Ministry of Health.

3.6.1 Genotyping of muscle specific TFEB knockout and transgenic mice

Mice were identified by analyzing the presence of Cre-recombinase on genomic DNA and by the presence of floxed *Tcfeb* allele (Tcfeb$^{f/f}$) for KO animals and *Tcfeb*3xFLAG for transgenic animals. Cre recombinase was always kept heterozygous in order to avoid aspecific recombination. Tcfeb floxed allele was maintained in a homozygous background with Cre heterozygous. Transgenic mice were obtained keeping both Cre and Tcfeb3XFLAG allele heterozygous.
Caudal biopsies were lysed in the following lysis buffer containing Tris-HCL 1M pH 7.5 and Proteinase K 10mg/mL (Life Technologies). Samples were incubated for 1 hour at 57°C and then the proteinase K was inactivated at 99°C for 5 minutes. PCR protocol for Cre, Tcfeb$^{f/f}$ and Tcfeb3XFLAG have been described in (Milan et al., 2015; Settembre et al., 2013).

3.7 Microarray data processing

The data discussed in this work have been deposited in NCBIs Gene Expression Omnibus (GEO) and are accessible through GEO Series accession number GSE62975

(*TFEB*_overexpression muscle dataset) and GSE62976 (*TFEB*-KO_muscle dataset). The two muscle studies (GSE62975 and GSE62976) are part of the SuperSeries GSE62980.
The SuperSeries has been named: Expression data from mice after knockout or overexpression of *Tcfeb* in muscle. Low-level analysis to convert probe level data to gene level expression was performed using Robust Multiarray Average (RMA) implemented using the RMA function of the Bioconductor project.

3.7.1 Statistical analysis of differential gene expression

For each gene, a Bayesian t-test (Cyber-t) (Baldi & Long, 2001) was used on RMA normalized data to determine if there was a significant difference in expression between mice overexpressing TFEB (TFEB overexpression muscle mice) versus not-injected mice used as control and Tcfeb knock-down (KO) mice muscle-specific versus WT mice. P-value adjustment for multiple comparisons was done with the False Discovery Rate (FDR) of Benjamini-Hochberg. The threshold for statistical significance chosen for both muscle microarray datasets analysis was FDR<0.05; a further filtering was performed for TFEB overexpression muscle dataset (GSE62975) by selection genes with an absolute Fold Change ≥1.5 for both increased (up- regulated genes) and decreased (down-regulated genes) expression levels.

3.7.2 Microarray data analysis

Gene Ontology Enrichment Analysis (GOEA) (Dennis et al., 2003)was performed for each microarray dataset on the up-regulated and down-regulated gene lists, separately, by using the DAVID online tool (DAVID Bioinformatics Resources 6.7) restricting the output to all Biological Process terms (BP_ALL) and to all Cellular Compartments terms (CC_ALL). The threshold for statistical significance of GOEA was FDR≤10% and Enrichment Score ≥1.5.

3.8 Electron microscopy

Small pieces of muscle tissue were fixed in a mixture of 2% paraformaldehyde and 1% Glutaraldehyde prepared in 0.2 M Hepes. Samples were suddenly post-fixed in a mixture of osmium tetroxide and potassium ferrocyanide, dehydrated in ethanol and

propyleneoxide and embedded in epoxy resin as described previously(Polishchuk et al., 2014). Thin 65 nm sections were cut using a Leica EM UC7 ultramicrotome. EM images were acquired using a FEI Tecnai-12 electron microscope (FEI, Eindhoven, Netherlands) equipped with a VELETTA CCD digital camera (Soft Imaging Systems GmbH, Munster, Germany). Morphometric analysis of number and size of mitochondria was performed using iTEM software (Olympus SIS, Germany). Number of mitochondria was counted using the same magnification within 100 μm square field of view. For each experiment, between 154 and 196 individual mitochondrial diameters were measured from 3 mice per group.

3.9 Biochemical Analysis of Mitochondrial Respiratory Chain Complex

All these experiments were performed in collaboration with the laboratory of prof. Zeviani (MRC-Mitochondrial Biology Unit, Cambridge, UK).

Muscle samples stored in liquid nitrogen were homogenized in 10 mM phosphate buffer (pH 7.4), and the spectrophotometric activity of cI, cII, cIII and cIV, as well as CS, was measured as described in (Bugiani et al., 2004). More in detail, complex I activity was measured using 50 μg mitochondrial protein in a reaction containing 250 mM sucrose, 2 mM EDTA, 100 mM Tris–HCl pH 7.4, between 10 and 100 μM decyl-ubiquinone and 2 mM KCN at 30° C. Reactions were started by the addition of 50 μM NADH and oxidation was followed at 340 nm for 2 minutes. Rotenone was used to block any rotenone insensitive activity. Complex II activity was measured by incubating 40 μg of mitochondrial protein at 30° C in a reaction mix containing 50 mM KH2PO4, pH 7.4, 20 mM succinate, 2 μg/mL antimycin A, 2 μg/mL rotenone, 2 mM KCN and 50 μM 2,6-dichlorophenolindophenol (DCPIP). Reactions were initiated by adding 50μM DB to the reaction and followed measuring the change in absorbance at 600 nm for 2 min. Complex III activity is measured by incubating 20 μg mitochondrial proteins at 30° C in a reaction mix containing 250 mM sucrose, 50 mM Tris–HCl, 1 mM EDTA, 50 μM cytochrome c

and 2 mM KCN. Decylubiquinol (DBH2) was used an electron donor. The reaction was started by the addition of 50 μM DBH2 and the change in absorbance of cytochrome c at 550 nm was followed for 2 min. 5 μg of antimycin A were added to duplicate reactions to measure any antimycin A-insensitive activity. Complex IV activity was measured by adding 10 μg mitochondria to a mix containing 10 mM KH2PO4, pH 7.2 and between 5 and 50 μM ferrocytochrome c. The rate of oxidation of ferrocytochrome c was recorded for 2 min (extinction coefficient of 27.2 mM− 1 cm− 1). Citrate synthase activity was measured at 30° C by using 10 μg mitochondria to a reaction mixture containing 125 mM Tris–HCl, 100 μM DTNB (5,5′-dithiobis(2-nitrobenzoic acid) and 300 μM acetyl coenzyme A. The reaction is initiated by the addition of 500 μM oxaloacetate, and DTNB reduction at 412 nm was measured for 2 min. The mitochondrial respiratory chain activities were expressed as nmoles/min/mg of protein.

3.10 ATP quantification in skeletal muscle

For the quantitative determination of Adenosine 5'triphosphate (ATP) gastrocnemius muscle samples stored in liquid nitrogen were homogenized in sterile water and analyzed according to the manufacturer's instructions of ATP Bioluminescent Assay Kit (Sigma-Aldrich).

3.11 Isolation of skeletal myofibers and measurements of mitochondrial membrane potential

Muscle fibers were isolated from FDB muscle and mitochondrial membrane potential measured by epifluorescence microscopy on the basis of the accumulation of TMRM fluorescence, as previously described (Lo Verso et al., 2014). Fibers were considered as depolarizing when they lost more than 10% of the initial value of TMRM fluorescence. Imaging was performed with a Zeiss Axiovert 100 TV inverted microscope equipped with

a 12-bit digital cooled charge-coupled device camera (Micromax, Princeton Instruments). The results were analyzed with MetaFluor imaging software (Universal Imaging).

3.12 Mitochondrial respiration assay

Mitochondria from mouse skeletal muscle were isolated as described (Frezza, Cipolat, & Scorrano, 2007). The rate of mitochondria oxygen consumption was measured at 30°C in an incubator chamber with a Clark/type O2 electrode filled with 2ml of incubation medium (125 mM KCl, 10 mM Pi.Tris, 20 mM Tris-HCl, 0,1 mM EGTA, ph 7,2). All measured were performed using mitochondria (0,2 mg mitochondrial protein/ml) incubated either with glutamate (5 mM)/ malate (2,5 mM) or /and succinate (5 mM) as substrates, in the presence (state 3) and in absence (state 4) of 100 mM ADP (Frezza et al., 2007).

3.13 Morphological Analysis

For SDH activity, 10μm thick sections from frozen tissue were collected on coverslips. The reaction mix contained: 5 mM phosphate buffer pH 7.4, 5 mM EDTA, 1 mM KCN, 0.2 mM Phenazine methosulfate (PMS), 50 mM Succinic acid, 1.5 mM Nitro blue tetrazolium (NBT). Sections were incubated for 20 min at 37° C. PAS staining was performed in 10μm thick sections from frozen tissue. Briefly, sections were fixed in Carnoy's solution for 10 minutes at room temperature (RT), washed three times in water and incubated for 5 minutes in 0.5% periodic acid. After washes section were allowed to react with Schiff's reactive, washed again, dehydrated and mounted with the appropriate mounting medium.

For cross sectional area detection, sections were immunolabeled with dystrophin antibody as previously described. Cross-sectional area was measured using ImageJ software in at least 1000 fibers and compared with the area of age-matched control. Images were captured using a Leica DFC300-FX digital charge-coupled device camera by using Leica DC Viewer software and morphometric analyses were made using the software ImageJ 1.47 version. The total myofiber number was calculated from entire muscle section based

on assembled mosaic image (×20 magnification). Fyber typing was determined by immunofluorescence using combinations of the following monoclonal antibodies from DSHB: BA-D5 for type 1 MyHC isoform, SC-71 for type 2A MyHC isoform and BF-F3 for type 2B. 2X fybers were calculated by difference. Images were captured using a Leica DFC300-FX digital charge-coupled device camera by using Leica DC Viewer software, and morphometric analyses were made using the software ImageJ 1.47 version.

3.14 Immunohistochemistry

Frozen muscle serial sections (7 μm) were fixed in 4% paraformaldehyde in PBS for 10 min, washed twice in PBS (Sigma-Aldrich) for 5 min at room temperature (RT), and incubated in 0.03% H_2O_2 in Methanol for 10 min at RT. After washing in PBS, sections were incubated in blocking solution (10% normal goat serum, 5% BSA in PBS) for 1h at RT. Anti-TFEB mAb (Bethil Laboratories) was added separately to each serial section for 16 h at 4°C. Sections were washed twice in PBS, incubated with biotin-conjugated (goat anti-rabbit IgG1, 5 μg/ml with 1% normal goat serum and 0,5% BSA in PBS) for 2 h at 4°C, washed twice, incubated with HRP-conjugated streptavidin (*Nova*RED substrate kit for peroxidase) (Vector Laboratories), following the manufacturer instructions. Slices were then rinsed in distilled water for 5 min, and counterstained with hematoxylin.

3.15 Western Blot Analysis and Antibodies

Total homogenates were prepared in Lysis buffer (50 mM Tris HCl [pH 8], 150 mM NaCl, 1% TritonX-100, 2% SDS) with the addition of a protease and phosphatase inhibitor cocktail (Roche). Protein concentration was determined with BCA kit (Pierce). 50 μg of total protein lysate were run through a SDS-PAGE and electroblotted onto a PVDF membrane, which was then matched with different antibodies. The following antibodies were used: anti-GAPDH (cat. sc-32233) anti-nNOS (cat. sc-648) from Santa Cruz

Biotechnology; anti-Gys (cat. 3886), anti-pGys (cat. 3891) , anti-AMPK (cat.2532), anti-pAMPK (cat. 2531), anti-pACC (cat. 3661) from Cell Signaling; anti-LC3B (cat. L7543), anti-p62 (cat. P0067) from Sigma Aldrich.

3.16 Whole Body Indirect Calorimetry.

Mice were individually housed in the chamber with a 12-h light/12-h dark cycle in an ambient temperature of 22–24° C. V_{O2} and V_{CO2} rates were determined under Oxymax system settings as follows: air flow, 0.6 l/min; sample flow, 0.5 l/min; settling time, 6 min; and measuring time, 3 min. The system was calibrated against a standard gas mixture to measure O2 (V_{O2}) consumed and CO2 (V_{CO2}) generated. Energy expenditure (EE), oxygen consumption (V_{O2}) and CO2 generated (V_{CO2}) during running was determined as described by Shemesh (Shemesh et al., 2014). Briefly, mice were acclimatized to a treadmill (Columbus Instruments) by running at 10 m/min for 15 min over three consecutive days. On the fourth day, groups of mice were run at 10 m/min, progressing to 15 m/min. Energy expenditure, oxygen consumption (V_{O2}) and carbon dioxide production (V_{CO2}) were recorded during running intervals, and the total distance run to exhaustion was determined.

3.17 Plasma metabolites analysis.

Blood was collected from the orbital plexus. Plasma or serum were prepared and frozen in aliquots at −20° C or used immediately after collection. A specific enzymatic kit was used for determination lactate (Abcam). Plasma glucose was monitored by a glucometer. Insulin was measured by ELISA (Millipore) following manufacturer indications.

3.18 Tissue metabolites quantification

Muscle free fatty acids were extracted as follows: briefly, pulverized muscle was homogenized in PBS, then extracted using chloroform/methanol (2:1), dried overnight and re-suspended in a solution of 60% butanol 40% Triton X-114/methanol (2:1). Measurements were normalized to protein content in the initial homogenate by DC protein

assay (Bio-Rad). The quantitative determination of glycogen amount was performed according to the manufacture's instruction of the Glycogen Colorimetric/Fluorometric Assay Kit (BioVision).

3.19 In Vivo Assessment of Insulin Action and Glucose Metabolism

Four days before the experiment, the mice were anesthetized and an indwelling catheter was introduced in the left internal jugular vein. The mice were fully recovered from the surgery before the *in vivo* experiments, as reflected by their reaching preoperative weight. After an overnight fast, EU clamps were conducted in conscious mice as previously described (Zong, Armoni, Harel, Karnieli, & Pessin, 2012).

The 2-h EU clamp was conducted with a prime continuous infusion of human insulin (4 mill units/kg/min) and a variable infusion of 25% glucose to maintain glucose at <150 mg/dl. Insulin stimulated whole body glucose metabolism was estimated using a prime continuous infusion of [3-^{3}H] glucose (10 μCi bolus, 0.1 μCi/min; PerkinElmer Life Sciences). To determine the rate of basal glucose turnover, [3-^{3}H] glucose (0.05 μCi/min) was infused for 2 h (basal period) before starting the EU clamp, and a blood sample was taken at the end of this basal period. To assess insulin- stimulated tissue-specific glucose uptake, 2-deoxy-d-[1-^{14}C] glucose (PerkinElmer Life Sciences) was administered as a bolus (10 μCi) 75 min after the start of the clamp. Blood samples were taken at 80, 90, 100, 110, and 120 min after the start of the EU clamp. At the end of the EU clamp, different muscle groups were rapidly dissected and frozen at -80° C for analysis. For the determination of plasma [3-^{3}H] glucose and 2-deoxy-d-[1-^{14}C]glucose concentrations, plasma was deproteinized with $ZnSO_4$ and $Ba(OH)_2$, dried to remove $^{3}H_2O$, resuspended in water, and counted in scintillation fluid (Ultima Gold; Packard Instrument Co.). For the determination of tissue 2-deoxy-d-[1-^{14}C]glucose (2-DG)-6-phosphate (2-DG-6-P) content, tissue samples were homogenized, and the supernatants were subjected to an ion-exchange column to separate 2-DG-6-P from 2-DG, as described previously. The radioactivity of ^{3}H in tissue glycogen was determined by digesting tissue samples in KOH and precipitating

glycogen with ethanol as previously described. Muscle glycogen synthesis was calculated as muscle [^{3}H] glycogen content divided by the area under the plasma [^{3}H] glucose-specific activity profile.

3.20 Autophagic flux quantification

We monitored autophagic flux in fed and 24 h starving mice by using colchicine as previously described (Milan et al., 2015). Briefly muscle specific transgenic TFEB mice were treated with 0,4 mg/kg colchicine or vehicle by i.p. injection each 12 hours and starved. The treatment was repeated two times before muscle harvesting.

3.21 *In vivo* ChIP Assays

We performed ChIP assays on TFEB3XFlag overexpressing or WT muscle, by using the Chromatin Immunoprecipitation (ChIP) assay kit (Millipore) according to (Milan et al., 2015). Briefly, muscle were homogenized on ice and integer nuclei were extracted and fixed with 1% formaldehyde solution at RT for 10 min. After washing nuclei were sonicated to obtain a chromatin size centered in 700bp. Chromatin was divided in aliquots, pre-cleared and incubated overnight with the following antibodies. We used anti-FLAG antibody (F7425Sigma-Aldrich). Oligonucleotide primers for amplification of a TFEB binding site on the GLUT1, GLUT4, nNOS, NRF1, NRF2 and TFAM promoters are listed below, together with the position with respect to TSS where CLEAR site is located.

Atlas	Site	CLEAR Matrix analysis	Chrom	TSS_Position	Primer Fw	Primer Rev
nNOS	**P1**	AAGCCAGGTGACCA	chr5	-191	AGCCCTTTGGTTCTTGAGA	AGGAGAGAGAGTGGAGTGG
	P2	TGAGCAGGTGACGT	chr5	262	TCTTCCTGACCTGTTGCTTA	AGCCAAGACGACTCCCA
GLUT1	**P1**	AGAGCAGGTGAGGG	chr4	-3465	GTCATGTCAGGTGGGAAGG	CTCCCAAGTGTCCCAAAGG
	P2	CCTTCAGGTGAACC	chr4	-831	TGATCAGGAGAGAGGAGAAGG	GGTGAGTAGGACAGTCAATAGC
GLUT4	**P1**	CCACCACCTGACTT	chr11	-4642	GTGCTGGAACTCTCTCTGTA	CATAGCCAGTTTCAAGCCAAC
TFAM	**P1+P2**	AGTCCACGTGATCT	chr10	-932	AGTGGTTTGGCTGGCTA	ACCCAAACAACTAGCCCTCA
		AGATCAAGTGAAGA	chr10	-825		
NRF1	**P1**	TCCTCATCTGACTC	chr6	65	TGAGCAACTGGTAAGGAACAG	AGGGTGTTTGCTGCTGA
NRF2	**P1**	AGGGCACTTGATCT	chr2	-2053	GTAAGATGTCAGATAACCCAGGA	CCCAAGGTCATACAGTAATCTCTG
	P2	GTCTCATGTGATGG		-3677	CCTCTCAATGTTCTAACCCACAG	CTCCTCAGCAATCTCAGCAA

3.22 Statistical analysis.

Data are expressed as mean values ±SE. Results were evaluated by repeated-measures ANOVA, multivariate analysis of variance (MANOVA), or Student's two-tail t test. A p value < 0.05 was considered statistically significant. In all figures, *p<0.05, **p<0.01, and ***p<0.001.

3.23 Real-time PCR

For mtDNA content analysis, SYBR Green real-time PCR was performed using primers specific to a mouse mtDNA region in the ND1 gene and primers specific to RNaseP, a single copy gene taken as a nuclear gene reference, as described (Viscomi et al., 2009). For the analysis of transcripts, total RNA was extracted from liquid nitrogen snap frozen muscle by Trizol, according to the manufacturer's instructions (Invitrogen, Carlsbad, CA, USA). Of total RNA, 2 μg was treated with RNase free-DNase and retrotranscribed using the ''cDNA cycle'' kit (QuantiTect Reverse Transcription Kit - QIAGEN). Approximately 2–5 ng of cDNA was used for real-time PCR assay (SYBR®Green PCR Master Mix Applied Biosystem) using primers specific for amplification of several genes. Autophagic, Lipid Metabolism and Glucose Metabolism gene-specific primers are listed below. Fold change values were calculated using the ΔΔCt method. An unpaired *t*-test was used to calculate statistical significance.

List of murine primers for RT-PCR

Gene Name	Primer Sequence
TCFEB F	GCAGAAGAAAGACAATCACAA
TCFEB R	GCCTTGGGGATCAGCATT
GLUT1 F	AGCAGCAAGAAGGTGACG
GLUT1 R	CACGGAGAGAGACCAAAGC
GLUT4 F	CCGCGGCCTCCTATGAGATACT
GLUT4 R	AGGCACCCCGAAGATGAGT
NOS1 F	CCAAAGCAGAGATGAAAGACACA
NOS1 R	TCTTGGTAGGAGACTGTTTGC
PGC1alpha F	AGCCGTGACCAGTGACAACGAG
PGC1alpha R	GCTGCATGGTTCTGAGTGCTAAG
GAPDH F	TGCACCACCAACTGCTTAGC
GAPDH R	TCTTCTGGGTGGCAGTGATC
TBC1D1 F	GTCCCGGGGTAATAAAGCCA
TBC1D1 R	TTGTCACCCATGGACAGCTC
PGC1-beta F	ACTGAAAGAGGCCCAGCAGA
PGC1-beta R	ATTGGAAGGGCCTTGTCTGA
PPAR-alpha F	CCTACGCTTGGGGATGAAGA
PPAR-alpha R	CCCCATTTCGGTAGCAGGTA
DLAT F	TGTTTCATCGGTGTTGAGTCTG
DLAT R	TGCTAATGATGTGCCCTTGTG
CRAT F	GGAGAAGAGAGCCAGTCCAG
CRAT R	AGATAATCCTCCCACCGCTG

CPT1b F	GACAGTACCCTCCTTCCACC
CPT1b R	ACCAGCAAGAACAGGGTAAGA
CS F	GACCCTCGCTATTCCTGTCA
CS R	AGTTCATCTCCGTCATGCCA
COX8B F	CGAAGTTCACAGTGGTTCCC
COX8B R	GCTGGAACCATGAAGCCAAC
MDH2 F	TGAACGGGAAGGAAGGAGTC
MDH2 R	AATGCCCAGGTTCTTCTCCA
CYC1 F	GGCTCCTCCCATCTACACAG
CYC1 R	CTGACCACTTATGCCGCTTC
ATP5A1 F	GACAGTACCCTCCTTCCACC
ATP5A1 R	ACCAGCAAGAACAGGGTAAGA
SDHA F	TTACCTGCGTTTCCCCTCAT
SDHA R	AAGTCTGGCGCAACTCAATC
NRF1 F	CAGACACGTTTGCTTCGGAAA
NRF1 R	CCCACTCGCGTCGTGTACT
NRF2 F	GATCAGGCGACATGTTAACGTT
NRF2 R	AGAGCCCAGTCAAACCCTTTC
HK2 F	TGGGTTTCACCTTCTCGTTC
HK2 R	TGGACTTGAACCCCTTAGTCC
HK1 F	TGGTGGAAAAGATCCGAGAG
HK1 R	TTTGGTGCATGATTCTGGAG
COX1 F	TGCTAGCCGCAGGCATTACT
COX1 R	CGGGATCAAAGAAAGTTGTGTTT
COX2 F	CAGGCCGACTAAATCAAGCAA
COX2 R	GAGCATTGGCCATAGAATAATCCT
COX4 F	TCACTGCGCTCGTTCTGAT
COX4 R	CGATCGAAAGTATGAGGGATG
COX5a F	TCATCCAGGAACTTAGACCAACT
COX5a R	AGTCCTTAGGAAGCCCATCG
TFAM F	AGATATGGGTGTGGCCCTTG
TFAM R	AAAGCCTGGCAGCTTCTTTG
CD36 F	CCAAATGAAGATGAGCATAGGACAT
CD36 R	GTTGACCTGCAGTCGTTTTGC
ND1 F	CATAAGCCTGCGTCAGATCA
ND1 R	CCTGTGTTGGGTTGACAGTG
RNasiP F	GCCTACACTGGAGTCCGTGCTACT
RNasiP R	CTGACCACACACGAGCTGGTAGAA
PPAR gamma F	CGTGCAGCTACTGCATGTGA
PPAR gamma R	GGGTGGGACTTTCCTGCTAA
PPAR delta F	ATGGGGGACCAGAACACAC
PPAR delta R	GGAGGAATTCTGGGAGAGGT
GYS F	TTGGAAGACTGGGAGGATGA
GYS R	CATTCATCCCCTGTCACCTT
PYGM F	CTACGAAAAGGACCCCAG
PYGM R	CATGGTGTTCTGCAGTGTC
Atrogin F	GCAAACACTGCCACATTCTCTC
Atrogin R	CTTGAGGGGAAAGTGAGACG
Murf1 F	ACCTGCTGGTGGAAAACATC
Murf1 R	ACCTGCTGGTGGAAAACATC

Fbxo31 F	GTATGGCGTTTGTGAGAACC
Fbxo31 R	AGCCCCAAAATGTGTCTGTA
Fbxo21 F	TCAATAACCTCAAGGCGTTC
Fbxo21 R	GTTTTGCACACAAGCTCCA
ITCH F	CCACCCACCCCACGAAGACC
ITCH R	CTAGGGCCCGAGCCTCCAGA
p62 F	CCCAGTGTCTTGGCATTCTT
p62 R	AGGGAAAGCAGAGGAAGCTC
LC3 F	CACTGCTCTGTCTTGTGTAGGTTG
LC3 R	TCGTTGTGCCTTTATTAGTGCATC
PINK F	TGGAATATCTCGGCAGGTTC
PINK R	CGGATGATGTTAGGGTGTGG
Parkin F	CCATCTTGCTGGGACGA
Parkin R	GCCTGTTGCTGGTGATCA
BNIP3 F	TTCCACTAGCACCTTCTGATGA
BNIP3 R	GAACACCGCATTTACAGAACAA
GabarapL F	CATCGTGGAGAAGGCTCCTA
GabarapL R	ATACAGCTGGCCCATGGTAG
mTOR F	GAGAAGGGTATGAATCGAGATGA
mTOR R	CCCATGAGGTCTTTGCAGTA
S6 F	AGCCCAGGACCAAAGCACCCAA
S6 R	TCCTGGCGCTTTTCTTTGGCTTCC
MUSA1 F	TCGTGGAATGGTAATCTTGC
MUSA1 R	CCTCCCGTTTCTCTATCACG

4 Results

4.1 Calcineurin is the phosphatase driving TFEB nuclear translocation

Previous studies demonstrated that the mTOR-mediated phosphorylation of TFEB in serine residue Ser 211 is responsible for its interaction with the 14-3-3 protein, resulting in TFEB cytoplasmic localization (Settembre et al., 2012). Conversely, conditions that lead to mTOR inhibition, such as starvation, promote TFEB nuclear translocation and transcriptional activation of its target genes (Sancak et al., 2010; Zoncu et al., 2011).

Although the role of the kinases mediating TFEB phosphorylation has been defined, the phosphatases involved in its dephosphorylation have remained elusive.

For this reason(Known that), in the HCS Facility at TIGEM we performed a high-content screening of a phosphatase siRNA library in order to identify the enzymes responsible for TFEB dephosphorilation.

The screening was based on a cellular assay in which TFEB cytoplasm-to-nucleus shuttling during starvation was monitored. We tested the effects of the specific inhibition of each of 231 phosphatases of the library on TFEB subcellular localization in a TFEB-GFP cell line. If the silenced phosphatase was critical for TFEB shuttling to the nucleus, this would result in TFEB cytoplasmic localization during starvation (Figure 1a).

The most significant hit identified by the primary screening is the calcineurin catalytic subunit isoform beta (PPP3CB; Figure 1b); indeed, inhibition of PPP3CB is able to suppress starvation-induced TFEB nuclear translocation as shown in Figure 1c.

For this reason we focused subsequent studies exclusively on this phosphatase.

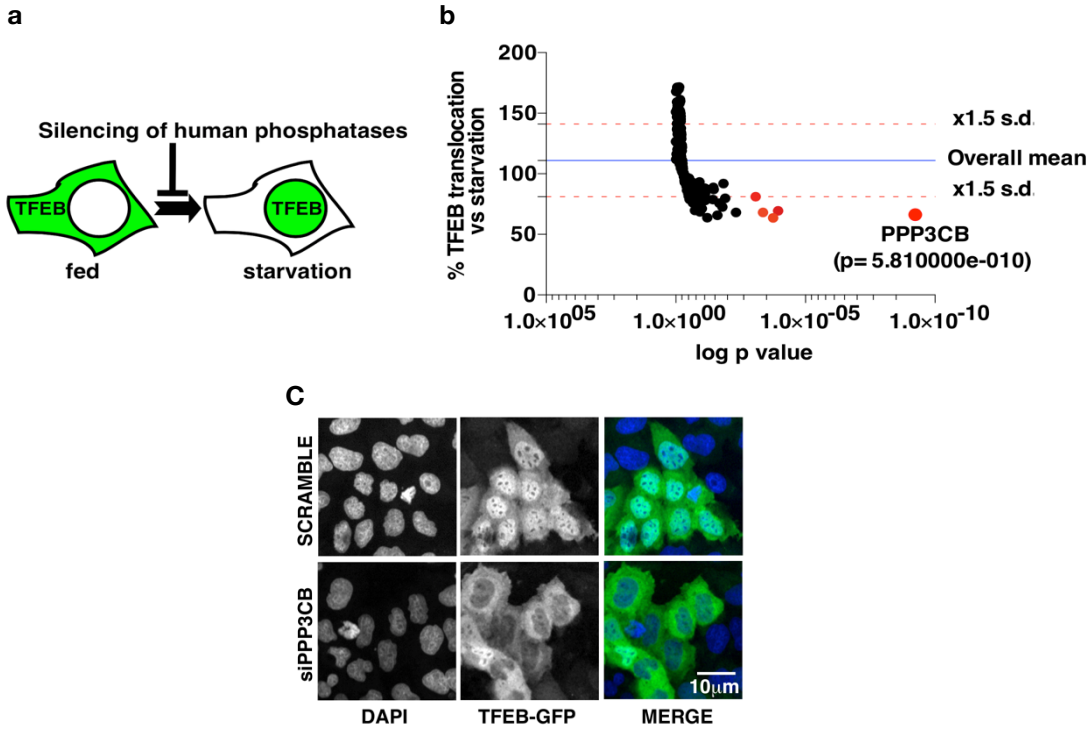

Figure 13 – High Content Screening identifies calcineurin as promoter of TFEB translocation. **a.** Assay design: HeLa TFEB-GFP cells were reverse transfected with siRNAs against each of 231 phosphatease of a human library and tested for TFEB nuclear localization during starvation. If the phosphatase silenced was critical for TFEB relocalization, this would result in cytosolic TFEB in absence of nutrients. **b.** Statistical analysis of the results. The graph scores the significance (log p-value) of the ability of individual siRNAs to inhibit starvation-mediated TFEB nuclear translocation. The top 5 best-scored siRNAs (p value<0.01), corresponding to 5 different phosphatases, are indicated with red dots. The siRNA against PPP3CB, the catalytic subunit of the calcineurin gene isoform beta, had the most significant score score. **c.** Representative images from the HCS using PPP3CB siRNA (siPPP3CB).

The ability of calcineurin to promote TFEB nuclear translocation was further confirmed 3 in the HeLa$^{TFEB\text{-}GFP}$ cell line by using a set of 3 different PPP3CB siRNAs, as well as the pool of 3 (Figure 2a). Once more, inhibition of the catalytic subunit of calcineurin results in TFEB cytoplasmic localization during starvation.

In addition, calcineurin inhibitors cyclosporin A and tacrolimus (FK506), both jointly and individually, reduced TFEB nuclear translocation during starvation (Figure 2b).

Finally, overexpression of ΔCnA, a constitutively active form of the subunit, induced TFEB nuclear translocation in normally fed cells, suggesting that calcineurin activity is not only necessary but is sufficient to induce TFEB nuclear relocalization (Figure 2c).

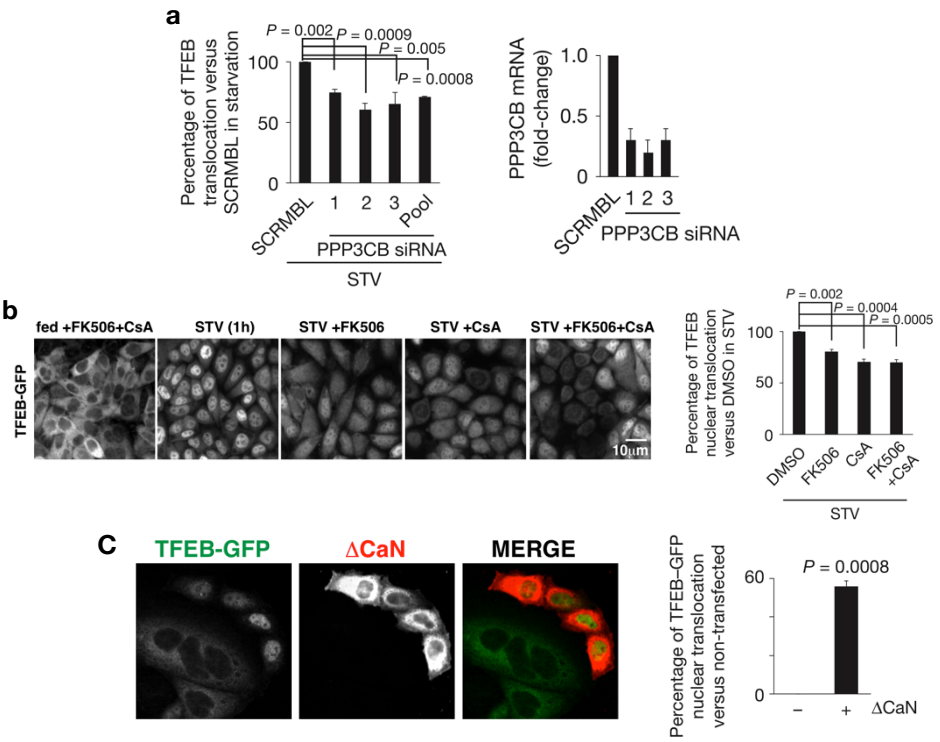

Figure 14 – Calcineurin regulates TFEB nuclear translocation. a. The left plot represents the percentage of nuclear TFEB in starved (STV) cells (3h) silenced with each single PPP3CB oligonucleotide or the pool of the 3 oligonucleotides compared with starved control cells transfected with scramble (SCRMBL) siRNA oligonucleotides. qRT-PCR analysis of PPP3CB mRNA levels confirms the efficacy of siRNA-mediated silencing (right plot). Bar graphs show mean ± s.d. for n = 3 independent experiments. **b.** Pharmacological inhibition of calcineurin reduces starvation-mediated TFEB nuclear localization. Images from normally fed or 1 h starved HeLa$^{TFEB\text{-}GFP}$ cells treated with FK506 (5 μM) and/or CsA (10 μM). Plot represents the percentage of nuclear TFEB translocation compared with DMSO-treated fed and starved cells. Bar graphs show mean ± s.d. for n = 3 independent experiments. Scale bar, 10 μm. **c.** HeLa$^{TFEB\text{-}GFP}$ cells were transfected with a constitutively active form of calcineurin (HA-tagged-1CaN). The plot represents the percentage of TFEB nuclear translocation. Data show the mean ± s.d. of n = 3 independent experiments. Scale bar, 10μm.

4.2 Calcineurin modulates TFEB subcellular localization during exercise

In order to deeper investigate the role of calcineurin in promoting TFEB nuclear translocation, we moved *in vivo* focusing our attention on skeletal muscle, a tissue in which calcineurin activity has long been studied.

Transfection by electroporation of both calcineurin subunit ΔCnA and its essential regulatory subunit CnB (PP3CR1) in *Tibialis Anterior* muscles (TA) of adult wild-type mice significantly induced the nuclear translocation of TFEB-GFP reporter (Figure 3), confirming that calcineurin activity is sufficient to promote TFEB relocalization also *in vivo*.

Moreover, a single bout of acute exhaustive exercise, a physiological stimulus that strongly activates calcineurin in response to calcium transients during contraction, is able to promote TFEB-GFP nuclear translocation in muscle fibers (Figure 3). Nevertheless, this effect was almost completely blunted if the endogenous calcineurin inhibitor, CAIN, was overexpressed into myofibers (Figure 3).

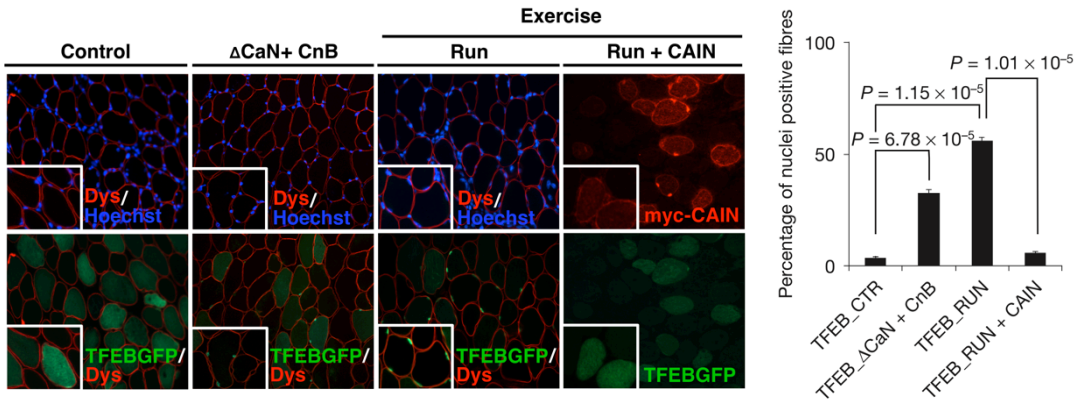

Figure 15 - Exercise induces TFEB nuclear translocation through calcineurin. Muscles were transfected by electroporation with TFEB–GFP (green), ΔCnA, its regulatory subunit (CnB) and the calcineurin inhibitor Myc–CAIN. Dystrophin antibody (Dys, red) was used to visualize myofibers. The plot shows the percentages of TFEB-positive nuclei in muscles under the following conditions: sedentary (control), sedentary with calcineurin (ΔCnA +CnB), exercised (run), exercised with CAIN (run + CAIN). The graph represents mean ± s.d. of $n = 3$ mice. Scale bar, 50 μm

In conclusion, these gain and loss-of-function data demonstrate that calcineurin plays a crucial role in the regulation of TFEB subcellular localization in skeletal muscle during an energy-demanding condition such as physical exercise.

4.3 Generation of muscle specific TFEB overexpressing and KO animals

Previous evidences showed that TFEB nuclear shuttling is a phenomenon triggered in skeletal muscle by energy demanding conditions, such as physical exercise.

Skeletal muscle, an important insulin and autophagy-dependent tissue (Grumati & Bonaldo, 2012; Mammucari et al., 2007; Masiero et al., 2009), is the principal organ involved in contraction; for this reason we started to investigate the role of TFEB in this tissue, trying to explain the physiological meaning of TFEB nuclear translocation during physical training.

For this purpose we took advantage of 3 different genetic models in which we could activate or down-regulate the expression of our transcription factor specifically in skeletal muscle.

Overexpression of Tcfeb, the murine homologue of human TFEB, was achieved in skeletal muscle by means of viral mediated gene transfer using the Adeno Associated Virus (AAV) system. Adult mice were injected intramuscularly (TA or GNM muscles) with either AAV2.1-CMV-TFEB or AAV2.1-CMV-GFP control vector; mice were sacrificed after 21 days, time required for an efficient TFEB expression (Figure 4a).

In addition, we generated a tamoxifen inducible muscle-specific TFEB transgenic mouse line; this was possible by crossing a line in which Tcfeb3XFlag cDNA was inserted after a CAGCAT cassette and another line expressing Cre-ER under the control of human skeletal actin (HSA) promoter (McCarthy et al., 2012). 3 days of intraperitoneal (IP) tamoxifen treatment in both Cre-positive and Cre-negative adult mice were sufficient to activate Cre-LoxP recombination and the overexpression of TFEB only in skeletal muscle (Figure 4b), recapitulating the induction obtained with AAV2.1-TFEB delivery.

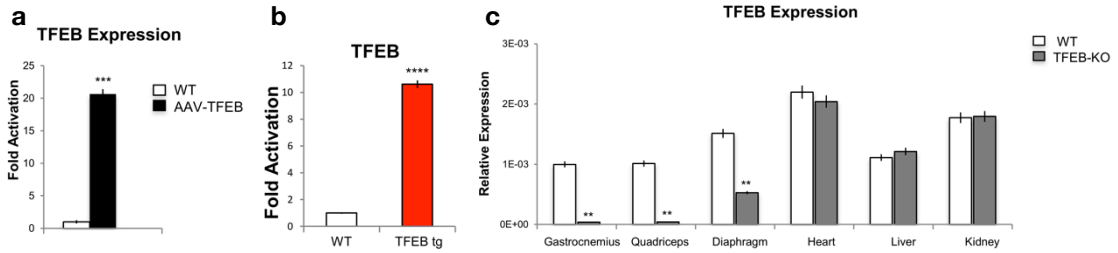

Figure 16 – Expression analysis of TFEB transcript. a. The TFEB transcript from AAV2.1-*TFEB* transfected muscle was quantified by qRT-PCR as well as from transgenic animals (**b**). Expression levels of endogenous *Tcfeb* mRNA in different tissues isolated from *TFEB*-KO and WT mice. Bar represent mean ± SE for $n = 5$; **p<0.01,***p<0.001.

For the loss of function approach, we generated a conditional muscle-specific TFEB-KO mouse line by crossing Tcfeb floxed (Settembre et al., 2013) with MLC1f-Cre transgenic mice (Bothe et al., 2000). Efficiency and specificity of the gene deletion were confirmed by quantitative real time-PCR (qRT-PCR) analysis on multiple tissues (Figure 4c).

4.4 Genome-wide analyses identified glucose-related and mitochondrial genes as downstream targets of TFEB

We started our study performing a transcriptomic analysis in skeletal muscles from both TFEB overexpressing and TFEB knock-out (KO) mice by means of whole-genome gene expression profiling experiments (SuperSeries-GSE62980).

In infected muscles, overexpression of TFEB results in the up-regulation of 1514 genes and the down-regulation of 1109 genes (GSE62975), while genetic ablation of the transcription factor increases 496 genes and suppresses 458 genes (GSE62976).

In order to identify the main cellular compartments (CCs) and the principal biological processes (BPs) related to TFEB-dependent genes, we next carried out a Gene Ontology Enrichment Analysis (GOEA). The GOEA was made on the lists of genes whose expression was either increased or decreased in transfected or knock-out muscles. Interestingly, several gene categories related to cellular metabolism, including lipid and

glucose homeostasis, are up-regulated in TFEB overexpressing muscle and down-regulated in TFEB-KO (Figure 5). Strikingly, genes involved in mitochondrial biogenesis are oppositely regulated by gain and loss of function approaches. Indeed 38 genes involved in mitochondrial function are induced in AAV2.1-TFEB infected muscles, while 73 genes are inhibited in TFEB-KO muscles.

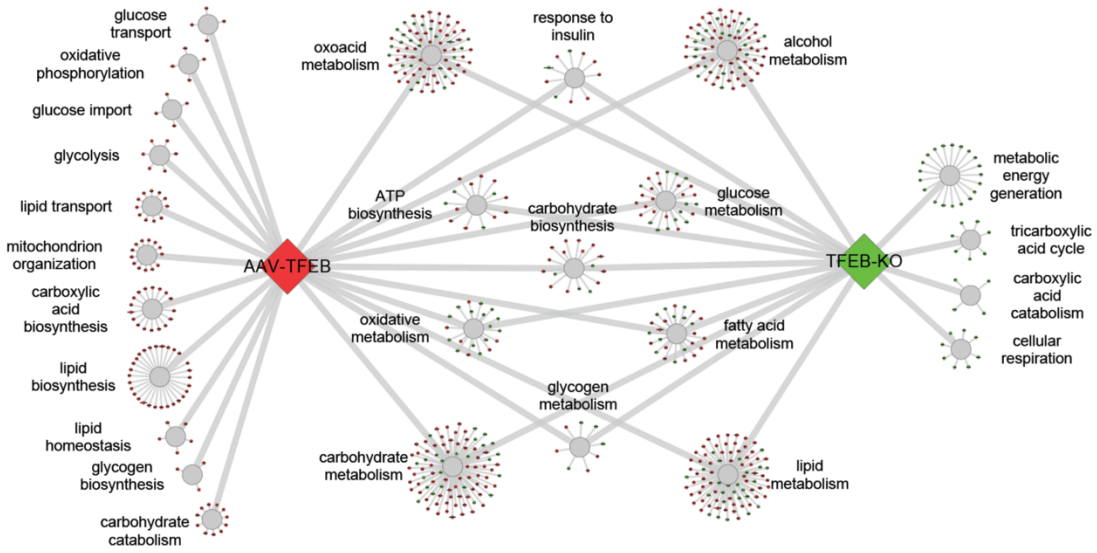

Figure 17 - TFEB gene network. Genes affected by TFEB expression are shown in colored circles. Red circles represent genes upregulated in TFEB-AAV overexpression; genes downregulated in KO animals are shown as green circles. Genes are divided in functional sub-categories; genes related to lipid and carbohydrate metabolism are strongly induced upon TFEB overexpression and blocked by TFEB deletion.

4.5 TFEB regulates mitochondrial biogenesis in skeletal muscle

Based on these gene expression evidences, we started to dissect the potential effects of TFEB on mitochondrial function analyzing mitochondrial morphology in muscles overexpressing or lacking *TFEB*. Electron microscopy (EM) analyses show a remarkable increase in mitochondrial density and volume in *TFEB*-overexpressing muscles, both from infected and transgenic animals (Figure 6b, 6d, 6e, 6f). Interestingly, mitochondrial density and size are normal in the *TFEB*-KO muscles, even if there is an increased number of damaged organelles (Figure 6c, 6e, 6f, 6h). Consistent with these EM data, infected

muscles also display an increase in mitochondrial DNA content (mtDNA), while no differences are observed in the knock-out counterpart (Figure 6g).

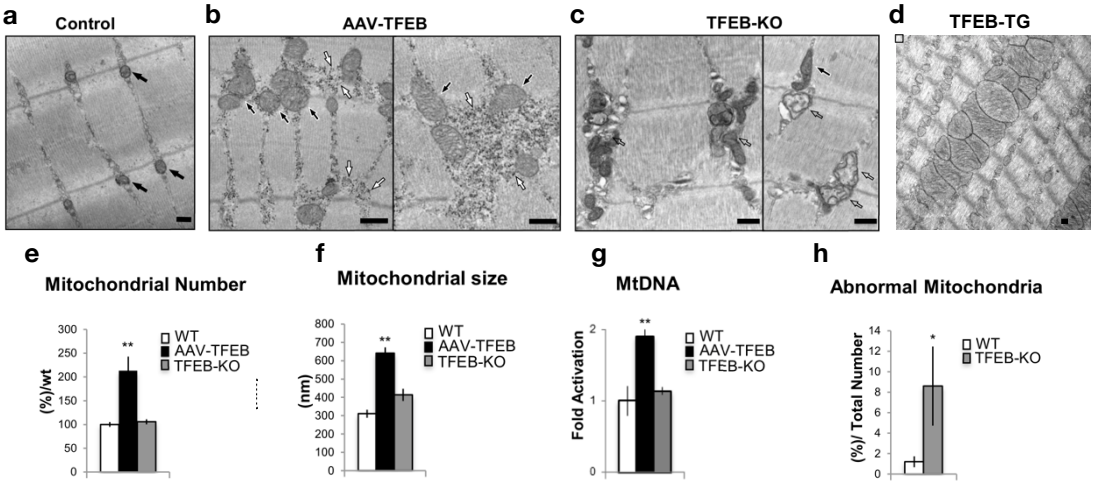

Figure 18 - TFEB induces mithocondrial biogenesis. a-d. Electron microscopy analysis of skeletal muscles from WT mice transfected with AAV2.1-*GFP* (**a**), AAV2.1-TFEB (**b**), TFEB-KO (**c**) and TFEB-TG mice (**d**). Normal mitochondria are indicated by black arrows (**a, b**), while abnormal mitochondria in TFEB-KO muscle are pointed by empty arrows (**c**). Increased mitochondrial size can be easily appreciated in TFEB-TG muscles (**d**). Scale bar represents 500 nm. **e-f**. Morphometrical analyses of mitochondria in TFEB overexpressing, TFEB-KO and control muscles. Bars represent mean±SE, n=3; **p<0.01. **g.** mtDNA copy number detection in muscles infected with AAV2.1-TFEB and from TFEB-KO and control mice. Data are shown as mean±SE, n=3; **p<0.01. **h.** Quantification of abnormal mitochondria in TFEB-KO gastrocnemius (GNM) muscles versus controls. Data are expressed as percentage of abnormal mitochondria on total mitochondria of 16. Bars represent mean±SE; *p<0.05.

Through qRT-PCR analysis we revealed that *TFEB* overexpression in muscle induces the expression of many genes involved in mitochondrial biogenesis and function (Figure 7a), including the master gene of mitochondrial biogenesis PGC1α, already known to be direct target of TFEB (Settembre et al., 2013). Moreover, another PGC-1 family member, PGC1β, was also up-regulated by *TFEB* overexpression. Consistently with these gene expression data, we found a significant induction of peroxisome proliferator activated receptor α (PPARα), PPARβ/δ and PPARγ in TFEB-overexpressing muscles. Nevertheless, *TFEB* deletion is not affecting the expression of PGC1α/β and PPAR genes with the exception of PPARα that is down-regulated.

For this reason, in order to elucidate the possible mechanisms underlying the induction of mitochondrial biogenesis gene program in *TFEB* transfected muscles, we examined the

expression of nuclear respiratory factors 1 and 2 (NRF1and NRF2), two well-known candidates regulating nuclear expression of mitochondrial genes (Scarpulla, 2006). The mRNA level of NRF2 is increased, as well as that of NRF downstream genes including mitochondrial transcription factor A (TFAM). *In vivo* chromatin immune-precipitation experiments confirm the direct recruitment of TFEB on NRF2 and NRF1 promoter (Figure 7c) but not on TFAM one (data no show), suggesting a possible mechanism TFEB-dependent and PGC1α/β-independent regulating mitochondrial biogenesis.

Finally, overexpression of *TFEB* in skeletal muscle increased the expression of different mitochondrial enzymes. Indeed, subunits of the four respiratory chain complexes and the ATP synthase, as well as genes encoding electron transport and TCAproteins were induced by *TFEB* overexpression and were reduced by *TFEB* deletion (Figure 7b).

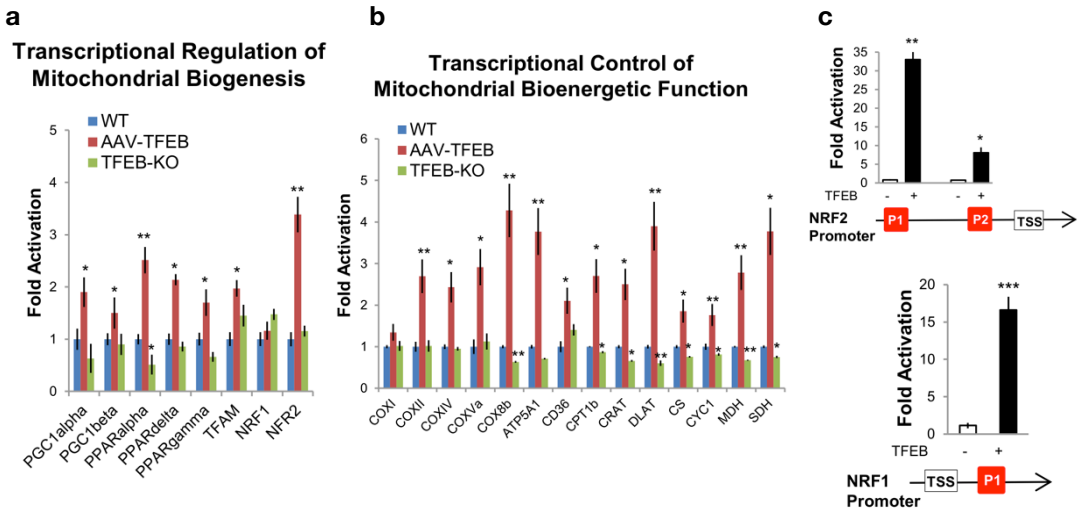

Figure 19 - TFEB regulates mitochondrial biogenesis and function gene expression. a. mRNA levels of genes related to mitochondrial biogenesis and **b.** mitochondrial function in WT (blue bar), infected (red bar) and TFEB-KO (green bar) muscles. Data were normalized for GAPDH and expressed as fold induction relative to the WT. Bars represent mean±SE, n=3; *p<0.05, **p<0.01. **c.** Chromatin immunoprecipitation analysis in muscles from TFEB transgenic and WT mice. CLEAR elements in NRF1 and NRF2 promoters are depicted as red boxes. TSS (Transcriptional Start Site) indicates the starting point of the first exon. The histograms show the amount of immunoprecipitated DNA as detected by qRT-PCR normalized to input. Bars represent mean±SE of three independent experiments; *p<0.05, **p<0.01, ***p<0.001.

4.6 TFEB regulates mitochondrial function and energy production in skeletal muscle

Data showed before clearly demonstrate a TFEB-dependent gene expression program for mitochondrial biogenesis and respiratory chain genes. For this reason, to better characterize the involvement of TFEB in mitochondrial respiration, in collaboration with the group of prof. Zeviani we analyzed the specific activities of enzymes involved in oxidative phosphorylation. Biochemical analysis of muscle samples infected with both AAV2.1-TFEB or control vector show an increase in the activities of citrate synthase, mitochondrial respiratory chain complex I (CI), CII, CIII and CIV (Figure 8a). Conversely, TFEB deletion lead to a slight decrease only in CII activity, the complex containing the SDHA flavoprotein, keeping unaltered all the other respiratory chain complexes activities (Figure 8a).

To further corroborate the role of TFEB in mitochondrial function we also took advantage of the inducible muscle-specific transgenic mouse line. Acute activation of TFEB by tamoxifen treatment in adult mice recapitulates the phenotype of AAV2.1-TFEB overexpression on mitochondria biogenesis and complex II activity, as shown by SDH staining in Figure 8b. Consistent with these data, even mitochondrial respiration is significantly enhanced in TFEB over-expressing muscles (Figure 8c).

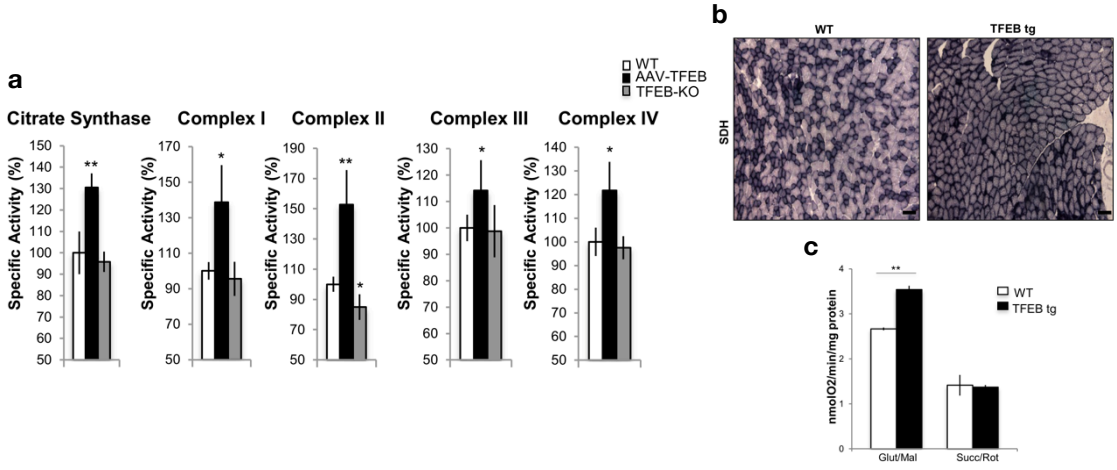

Figure 20 – TFEB regulates mitochondrial complex activity and respiration. a. Mitochondrial respiratory chain activity in muscles of WT, AAV2.1-TFEB infected and TFEB-KO mice. Data are expressed as percentage of specific activity respect to the WT. Data are expressed as mean ±SE, n=4; *p<0.05, **p<0.01. **b.** SDH staining of sections from TFEB transgenic and WT mice. Scale bar represents 100 µm. **c.** Mitochondrial respiration measurements in muscles from TFEB transgenic and control mice. TFEB induction significantly increases oxygen consumption rate when glutamate/malate are used as substrates. Data are presented as mean ± SE; n=3; **p < 0.01.

Based on these findings, we decided to assess whether these TFEB-mediated changes in mitochondrial morphology and function had any impact on energy production. Therefore we measured ATP levels that are higher in TFEB transfected muscles and lower in TFEB deficient muscles compared to controls (Figure 9a). For this reason, to understand the mechanisms underlying this significant decrease in ATP production in *TFEB*-KO muscles we checked mitochondrial function in these animals. To do that, we exploited TMRM, a fluorescent dye able to monitor mitochondrial membrane potential (Δψm), the critical parameter driving ATP production.

Therefore, we checked Δψm in isolated adult fibers from WT and TFEB-KO muscles. As expected in control mice, oligomycin-dependent inhibition of ATP synthase does not alter Δψm over time (Figure 9b) and mitochondrial depolarization is achieved only after membrane permeabilization with the protonophore carbonylcyanide-p-trifluoromethoxy phenylhydrazone (FCCP). Conversely, mitochondria of TFEB-null fibers undergo a significant depolarization after oligomycin treatment (Figure 9b), suggesting that these fibers are at least in part relying on reverse activity of ATP synthase to preserve their membrane potential. Thus, these findings elucidate that the lower ATP production in knock-out muscles is due to a mitochondrial membrane proton leak.

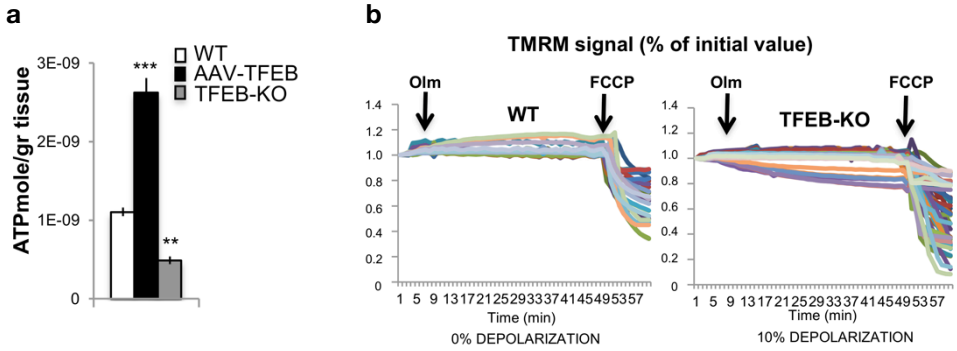

Figure 21 – TFEB regulates ATP production and mitochondrial membrane potential. a. ATP production per gr of tissue from TFEB infected and TFEB-KO mice respect to controls. Data are shown as means ± SE (n=5); **p<0.01, ***p<0.001. **b.** Mitochondrial membrane potential measurements in myofibers from FDB WT and KO muscles. Where indicated, 6 μM oligomycin or 4 μM FCCP were added. Each trace represents TMRM fluorescence of a single fiber. The fraction of myofibers with depolarizing mitochondria is indicated for each condition.

4.7 TFEB regulates mitochondrial biogenesis in skeletal muscle through a PGC1α-independent mechanism

Both PGC1α and PGC1β are master regulators of mitochondrial biogenesis and oxidative metabolism. Anyway, recent evidences suggest the presence of an independent pathway able to regulate mitochondrial biogenesis during exercise (Rowe, El-Khoury, Patten, Rustin, & Arany, 2012). Therefore, we tried to define whether TFEB is the missing sensor of physical activity that coordinates metabolic responses independently from PGC1α. To do that, we first checked the expression and localization of endogenous TFEB in PGC1α knockout (PGC1α-KO) mice before and after exercise. TFEB was expressed at lower levels and it was more cytosolic in *PGC1*α-KO mice when compared to controls (Figure 10a). Importantly, exercise restored a normal TFEB expression (Figure 10a), induced TFEB nuclear translocation (Figure 10b) and triggered up-regulation of genes related to mitochondrial biogenesis (data not shown).

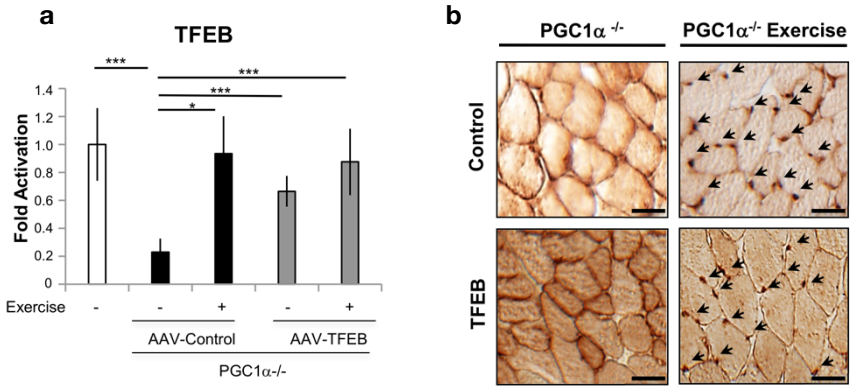

Figure 22 - Exercise induces TFEB expression and nuclear localization in PGC1α$^{-/-}$ muscle. a. TFEB mRNA levels in PGC1α$^{-/-}$ muscles infected with AAV2.1 control or AAV2.1-TFEB. Data are compared with TFEB expression in WT mice. Measurements were performed in sedentary and runner animals. Bars represent mean±SE for n=3; *p<0.05, ***p<0.001. **b.** Immunohistochemical analysis of TFEB in PGC1α$^{-/-}$ muscles from sedentary and exercised mice. Control means endogenous TFEB in muscles infected with AAV2.1 control virus. TFEB means total amounts of TFEB in muscles infected with AAV2.1-TFEB. Arrows indicate exercise-induced TFEB nuclear localization. The scale bars represent 50 μm

Electron microscopy analysis of *PGC1*α-KO muscles infected with AAV2.1-CMV-TFEB reveals an increase in mitochondrial volume and density (Figure 11a) that correlates with an augmented activity of CI, II, III and IV (Figure 11c). Moreover, the levels mitochondrial biogenesis regulator such as TFAM, NRF1 and NRF2 are significantly up-regulated by TFEB over-expression even in the absence of PGC1α (Figure 11b).
Altogether, these findings strongly suggest that the induction of mitochondrial biogenesis in *TFEB* overexpressing muscles does not depend on the presence of PGC1α.

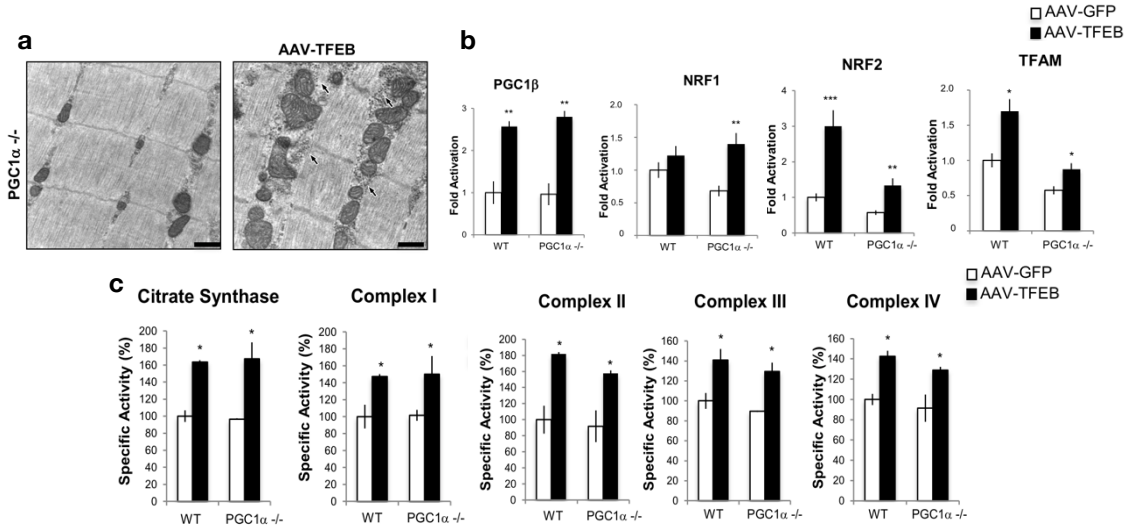

Figure 23 – TFEB controls mitochondrial biogenesis and function independently from PGC1α. a. EM images of PGC1α-/- muscles infected with AAV2.1-TFEB or AAV2.1-GFP. The electron micrographs reveal an accumulation of mitochondria in TFEB-overexpressing muscle and a granular staining consistent with glycogen particles. The scale bars represent 500 nm. **c.** The mitochondrial respiratory chain activity in WT and PGC1α-/- muscle infected with control or TFEB vector. Data are expressed as percentage respect to the WT muscles infected with control vector. Bars represent mean ± SE for n=3; *p<0.05.

4.8 TFEB controls energy balance in skeletal muscle during exercise

It is well established that physical activity has a major impact on glucose homeostasis and mitochondrial biogenesis and function (Cartee et al., 2016). For this reason, we wondered whether acute exhausting versus mild and chronic exercise trainings are equally able to activate TFEB. As readout of TFEB activation we monitored its nuclear localization. We previously proved that acute exhausting contractions lead to TFEB nuclear translocation (Figure 3) even if mild exercise is not able to promote this massive subcellular relocalization (Figure 12a). Anyway, 7 weeks of training with progressive increase of intensity without reaching exhaustion are inducing a massive TFEB nuclear translocation with concomitant cytosolic depletion comparable to the effect of one acute exhausting bout (Figure 11a). Therefore, intensity and duration of training are critical factors that affect TFEB nuclear translocation and its ability to promote transcription of genes related to mitochondrial biogenesis and function (Figure 12b).

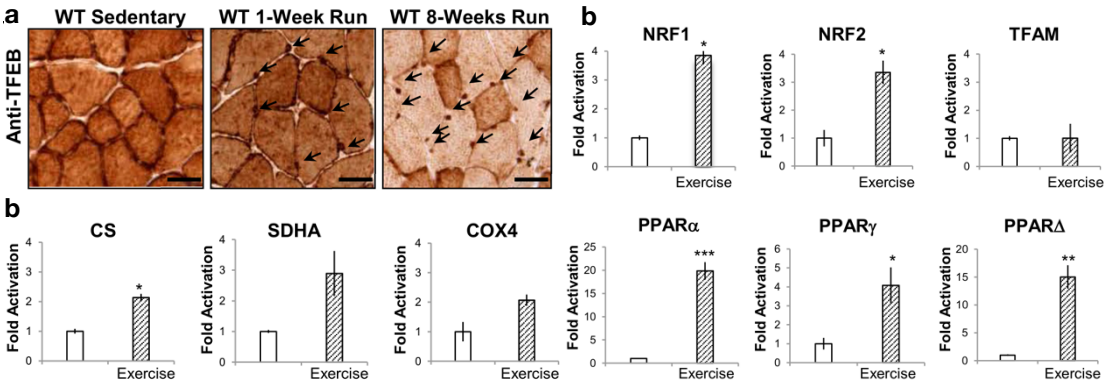

Figure 24 - TFEB nuclear translocation is induced depending on exercise intensity. a. Endogenous TFEB was immunostained in muscles of sedentary, 4 days mild exercised and 7 weeks intense trained WT mice. Arrows indicate TFEB nuclear localization, which is related to exercise intensity. **b.** Expression analysis of genes related to mitochondrial biogenesis and mitochondrial respiratory chain in WT skeletal muscle before and after acute exhastive exercise. Data are shown as mean ±SE, n=3; *p<0.05, **p<0.01.

At this point, to unravel the physiological consequences of TFEB translocation during physical activity we decided to examin exercise performance in both *TFEB*-KO and inducible muscle-specific TFEB transgenic mice. During high intensity training, *TFEB*-KO mice appear to be significantly exercise-intolerant compared to controls (Figure 13a) while the acute activation of TFEB in skeletal muscle enhances physical performances, consistently with the measured increased mitochondrial respiration.

To better understand the exercise intolerance of the *TFEB*-KO mice, in collaboration with prof. Pessin laboratory in New York, we performed calorimetric recordings during treadmill running. While WT mice maintain a constant level of energy expenditure during physical activity, the knock-out mice display a drop after 15 minutes of physical exercise (Figure 13b). Moreover, metabolic analyses reveal that in basal condition *TFEB*-KO mice have a higher respiratory exchange rate (RER) than controls (Figure 13c) suggesting that TFEB-KO mice depend more on glucose oxidation with respect to controls. In addition, while WT mice maintain a relatively constant RER during the running period, *TFEB*-KO mice show a drop of RER after 20 min (Figure 13c), indicating a shift in substrate usage from glucose to fatty acid metabolism.

Finally, we measured glucose and fatty acids levels in muscle and blood from *TFEB*-KO and TFEB transgenic mice before and after exercise. TFEB-KO mice show lower blood glucose levels compared to WT mice in basal condition (Figure 13d). However, exercise causes a 50% reduction of blood glucose in TFEB-KO, transgenic and control mice (Figure 13d). Insulin levels mirrored the changes of blood glucose, as they were reduced in basal condition in *TFEB*-KO mice and dropped after exercise in the different genotypes (Figure 13e).

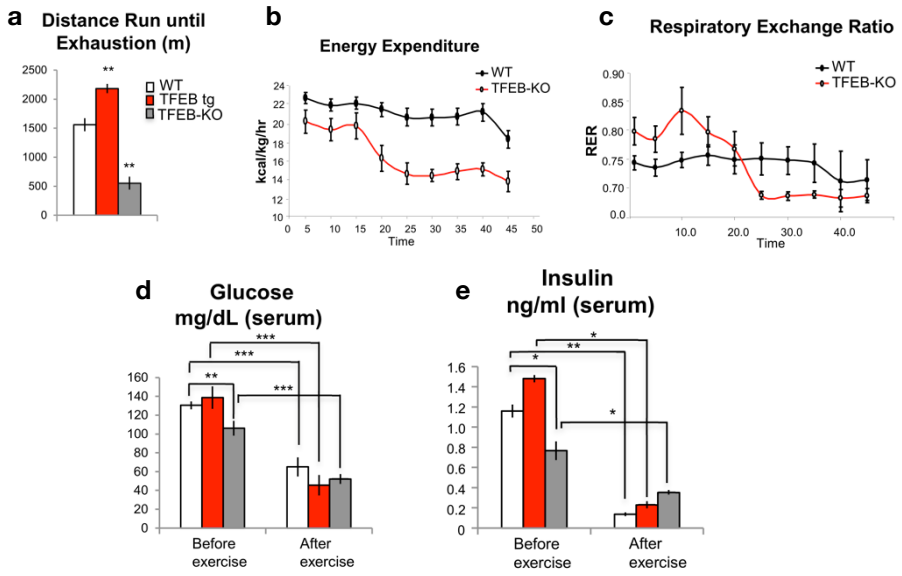

Figure 25 - TFEB controls energy balance in skeletal muscle. a. To determine exercise capacity mice were run on a treadmill; during high-intensity exercise, transgenic mice ran more than WT mice while KO animals displayed a marked exercise intolerance. Data are shown as mean±SE, n=10; **p<0.01. **b.** Energy expenditure and **c.** RER were determined during exercise in TFEB-KO and WT mice. The figure shows the mean RER measured at peak oxygen consumption, n=8. **d-e.** Serum metabolites quantification before and after high intensity exercise in WT, TFEB transgenic and TFEB-KO mice. Data are shown as mean +/-SE, n=8; *p<0.05, **p<0.01, ***p<0.001.

At this point we had enough evidences showing that *TFEB*-KO mice are hypoglycemic, contain dysfunctional mitochondria and produce less ATP.

Thus, we reasoned whether they use the anaerobic glycolysis to produce energy. Consistent with this hypothesis, we found higher levels of lactate in blood of TFEB-KO mice before and after exercise compared to controls (Figure 14a). On the contrary, lactate of transgenic mice is already lower than controls in resting condition and is not increasing after exercise, indicating that TFEB transgenic mice better oxidize glucose for energy production.

To further confirm these findings we measured glycogen content in skeletal muscle. In basal conditions, glycogen levels are remarkably lower in *TFEB*-KO mice and higher in transgenic TFEB muscles compared to WT. Enzymatic quantification shows that glycogen content is 3 fold less after TFEB ablation and 10-fold higher after TFEB overexpression

compared to controls (Figure 14b). Periodic Acid Schiff (PAS) staining (Figure 14c) confirms this glycogen accumulation in transgenic animals.

Anyway, exercise leads to glycogen consumption in transgenic, TFEB-KO and control muscles (Figure 14b) even if the lower glycogen content detected in sedentary *TFEB*-KO muscles explains the drop of RER observed after a 15 min exercise. Since glycogen is rapidly consumed in TFEB-KO mice, the additional need for energy during exhausting exercise requires a switch from glycolysis to fatty acid oxidation as detected in RER recordings. Thus, while blood free fatty acids (FFAs) concentrations are reduced after exercise in both TFEB-KO mice and controls (Figure 14d), their muscle content dramatically drops after exercise only in TFEB-KO mice (Figure 14e).

Altogether these finding indicate that TFEB is supporting metabolic flexibility of skeletal muscle during exercise, highlighting a new role for this transcription factor always referred as a master regulator of autophagy.

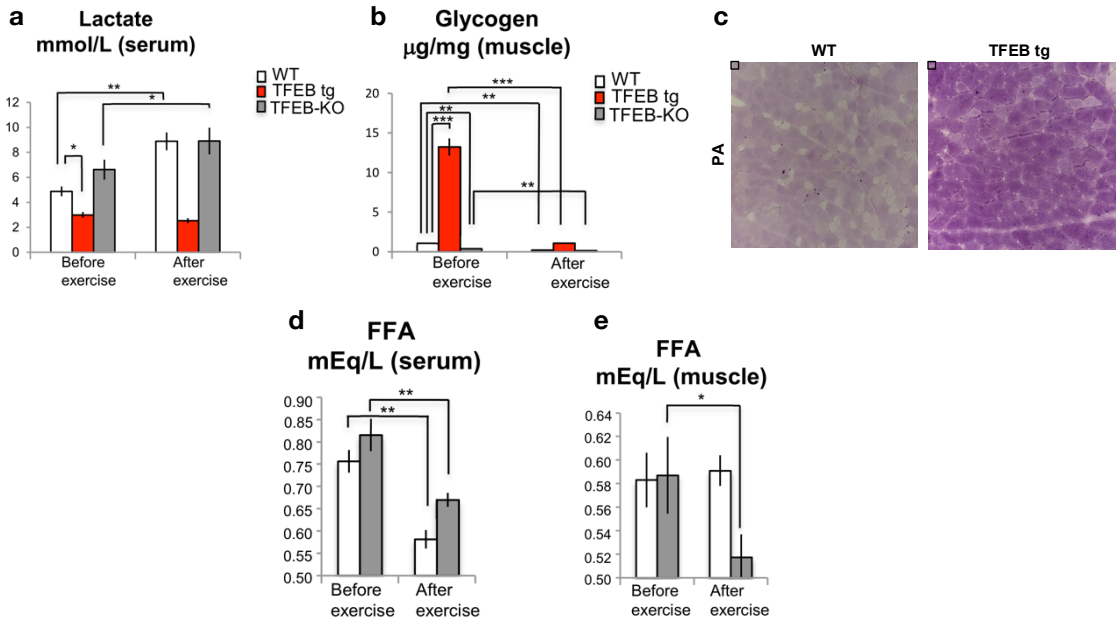

Figure 26 - Blood and muscle metabolites before and after high intensity exercise. **a.** Lactate quantification after exhaustive contraction in WT, TFEB transgenic and TFEB-KO mice. Data are shown as mean +/-SE, n=8; *p<0.05, **p<0.01, ***p<0.001. **b.** Enzymatic quantification of muscle glycogen before and after high intensity exercise in WT, TFEB transgenic and TFEB-KO mice. Data are shown as mean ±SE, n=8; **p<0.01. **c.** Periodic acid Schiff (PAS) staining of cryosections from TFEB transgenic and WT mice. **d-e.** Quantitative analysis of serum and muscle FFA before and after high intensity exercise in TFEB-KO and WT mice. Data are shown as mean +/-SE, n=8; *p<0.05, **p<0.01.

4.9 TFEB controls metabolic flexibility and energy balance independently of autophagy and proteostasis

Different evidences agree with the role of exercise as a potent activator in skeletal muscle of autophagy (Grumati, Coletto, Sandri, et al., 2011; He et al., 2012) and ubiquitin-proteasome systems (Cunha et al., 2012). In particular, in our and other laboratories it has been proved that autophagy is not required to sustain physical exercise, but is fundamental for clearance of dysfunctional mitochondria during and after training (Lo Verso et al., 2014). For this reason, we checked whether TFEB, known to be a master regulator of autophagy (Settembre et al., 2011) and from now on also an exercise-activated regulator of muscular metabolic flexibility, is mediating this new function in adult skeletal muscle through the control of this catabolic mechanism. Surprisingly, TFEB activation was not sufficient to enhance autophagy flux in presence or absence of nutrients (Figure 15a). Moreover, activation of TFEB did not induce protein breakdown and muscle loss. Indeed, most of the atrophy-related genes belonging to the ubiquitin- proteasome and autophagy-lysosome systems are not induced by TFEB over-expression (Figure 15b). Similarly, also mitophagy genes are not affected. However, when we measured cross-sectional area of transgenic muscles, we found a shift towards smaller size suggesting that also protein synthesis is not induced (Figure 15c). Thus, this decrease in fiber size is merely due to a metabolic shift and the reason for this phenomenon relies on the fact that oxidative fibers are smaller than glycolytic skeletal muscle fibers (Schiaffino & Reggiani, 2011). Furthermore, we did not find any significant difference in myosin distribution between transgenic and control muscles (Figure 15d). Therefore, TFEB controls myofibers metabolism but not myosin content/type independently from autophagy or proteostasis.

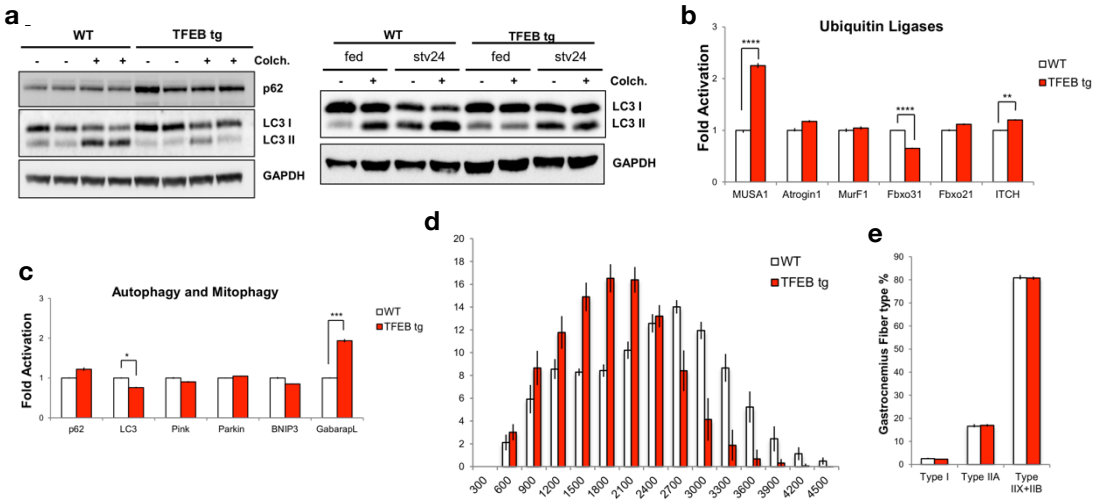

Figure 27 - TFEB controls metabolic flexibility independently from autophagy and protein breakdown. **a.** Left panel: representative blots of p62 and LC3 from muscle lysates of WT and TFEB transgenic animals in fed conditions. Mice were treated with colchicine (Colch.) or vehicle for autophagy flux measurements. Lower panel: immunoblot analysis of LC3 from muscle lysate from fed or 24 h fasted TFEB tg or control mice. GAPDH was used as loading control. **b.** Quantitative RT-PCR atrophy-related ubiquitin ligases (*MusA1, Atrogin1, MuRF1, Fbxo31, Fbxo21 and Itch*) **c.** gene expression measurements of autophagy/mitophagy genes (*p62/SQSTM1*, *LC3, Pink, Parkin, Bnip3* and *Gabarapl*). Data are normalized to GAPDH and expressed as fold increase compared to control animals. *n*=4 muscles in each group Values are mean ± SE *p<0.05, ***p<0.001, ****p<0.0001. **d.** Frequency histograms showing the distribution of myofibers cross-sectional areas (μm^2) from transgenic muscles. Values are shown as means ± SE *p<0.05, from 4 muscles in each group. **e.** Percentage of type I and different type II fibers in WT and TFEB tg muscles. Values are shown as means ± SE *p<0.05, from 4 muscles in each group.

4.10 TFEB controls glucose homeostasis and insulin sensitivity independently of PGC1α

We previously demonstrated that TFEB-KO muscles contain lower glycogen levels than controls; therefore, we reasoned that this feature could probably depend on an abnormal regulation of glucose homeostasis. Thus, always in collaboration with Pessin's lab, we performed euglycemic-hyperinsulinic (EU)-clamps observing that the glucose infusion rate (GIR) required to maintain a constant glycemia during insulin treatment is significantly reduced in *TFEB*-KO mice compared to control (Figure 16a). This reduction is consequent to a decrease in skeletal muscle glucose uptake (Figure 16b), which causes as consequence a decrease of glycogen synthesis (Figure 16c). Altogether these data demonstrate that

TFEB deficiency in skeletal muscle results in peripheral insulin resistance, reduced glucose uptake and decreased glycogen content.

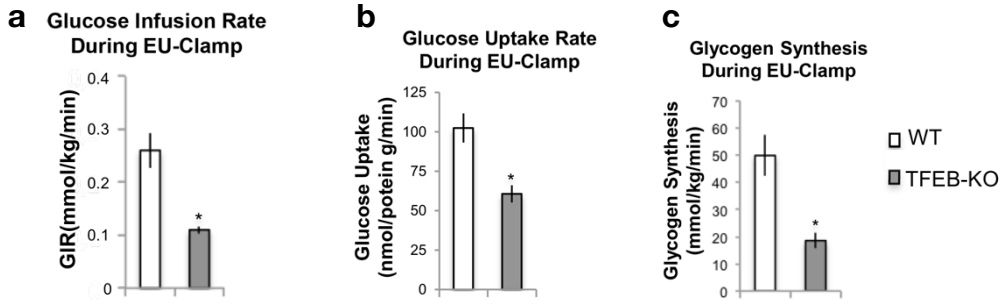

Figure 28 - TFEB ablation results in a decreased rate of insulin-stimulated glucose uptake. a. EU clamps were used to assess whole body insulin sensitivity by determining the glucose infusion rate required to maintain euglycemia in WT and TFEB-KO mice. Data represent the means ±SE from 5-6 individual mice per group; *p<0.05. **b.** TFEB deletion results in a reduction of insulin-stimulated glucose uptake in muscle. Glucose uptake into muscle tissues was determined by 2-deoxy-d-[1-^{14}C]glucose injection during the last 35 min of insulin infusion during the EU clamp. These data represent the means ±SE of 5-6 mice per group; *p<0.05. **c.** The amount of glucose conversion to glycogen in muscles from WT and TFEB-KO mice was determined during the EU clamp by infusion of [3-^{3}H]glucose. Data represent the means ± SE from 5-6 mice per group; *p<0.05.

These findings are mirroring the transcriptomic signature of TFEB-overexpressing and TFEB-KO muscles. Thus, to further confirm these evidences, we monitored the expression levels of glucose homeostasis-related genes in both muscles injected with AAV-TFEB and from transgenic mice; we found a significant increase in the expression of GLUT1 and GLUT4, the GTPase involved in GLUT4 translocation (TBC1D1) and the rate limiting enzymes of glycolysis (Hexokinase 1 and 2) (Figure 17a). The induction of genes involved in glucose uptake is also coupled with an increase of transcript and protein of GYS (Figure 17b, 17c), explaining the accumulation of glycogen in transgenic muscles. GYS activity is negatively regulated by phosphorylation of the C-terminal region by glycogen synthase kinases (GSK3s) (Jensen & Lai, 2009); anyway, the phospho-GYS levels are unchanged in AAV-*TFEB* muscles and, therefore, the pGYS/GYS ratio is dramatically decreased in *TFEB*-overexpressing muscles when compared to controls (Figure 17c).

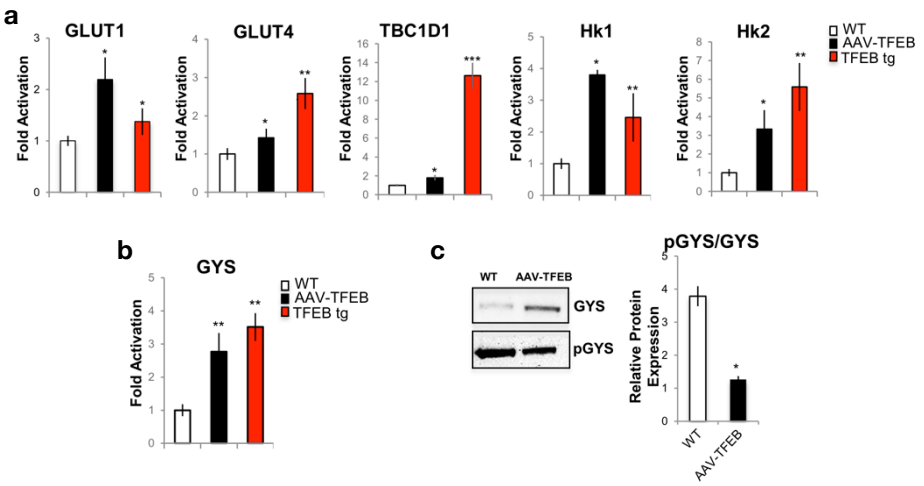

Figure 29 - TFEB controls genes related to glucose metabolism. a. qRT-PCR of glucose uptake and glycogen biosynthesis related genes in muscles both infected with AAV2.1-TFEB and form TFEB transgenic animals. Data were normalized for GAPDH and expressed as fold induction relative to WT. Data are shown as mean±SE, n=3; *p<0.05, **p<0.01. **b.** mRNA levels of glycogen synthase and **c.** western blot analysis of total and phosphorylated GYS from muscle extracts. Representative blot images are shown (left panel). Densitometric quantification is depicted on the right panel. Data are shown as mean±SE, n=3; *p<0.05.

Moreover, expression analysis of genes related to glucose metabolism does not reveal any significant difference between PGC1α-KO and controls after viral *TFEB* overexpression (Figure 18). Altogether these data strongly indicate that TFEB is able to control also muscle glucose uptake and glycogen synthesis in a PGC1α-independent manner.

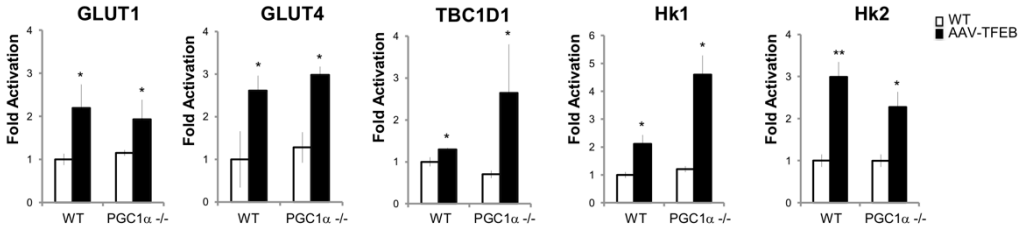

Figure 30 - TFEB regulates glycogen synthesis independently of PGC1α. qRT-PCR analysis of genes related to glucose uptake and glycogen biosynthesis in PGC1α$^{-/-}$ and WT mice infected with AAV2.1-GFP or AAV2.1-TFEB. Data are shown as mean±SE, n=3; *p<0.05, **p<0.01.

4.11 Glucose-related signaling pathways are affected by TFEB

GLUT transporters activity is known to be tightly controlled form several pathways. For this reason, we checked whether TFEB impinges not only on GLUT1-4 expression but also on glucose-related signaling. Previous studies showed that Nitric Oxide (NO) controls several metabolic aspects of skeletal muscle including mitochondrial biogenesis and glucose uptake (De Palma et al., 2014; Stamler & Meissner, 2001). NO is formed by nitric oxide synthase (NOS), via the conversion of L-arginine to L-citrulline. Skeletal muscle express neuronal (nNOS), endothelial (eNOS) and inducibile (iNOS) isoforms (Andrew & Mayer, 1999); however, nNOS is the major isoform involved in AMPK-dependent regulation of GLUT4 (Lira et al., 2007). We found that the nNOS transcription and protein expression are increased in *TFEB*-over expressing muscle and decreased in muscle from *TFEB*-KO mice (Figure 19a, 19b).

To test whether nNOS and glucose transporter genes are direct target of TFEB we further analyzed their promoters and identified CLEAR sites. Chromatin immunoprecipitation experiments showed that TFEB is recruited on nNOS, GLUT1 and GLUT4 promoters (Figure 19c), thus directly controlling their expression.

Moreover, since AMPK is a downstream target of nNOS (Lira et al., 2010), we also monitored its activation. TFEB overexpression in muscle shows a significant induction of AMPK phosphorylation and of its downstream target Acetyl-CoA carboxylase (ACC) even if no changes are found in *TFEB*-KO muscles (Figure 19d).

To conclude, all these findings highlight the role of TFEB in controlling not only glucose related genes expression, but also a part of the signaling pathways involved in glucose homeostasis.

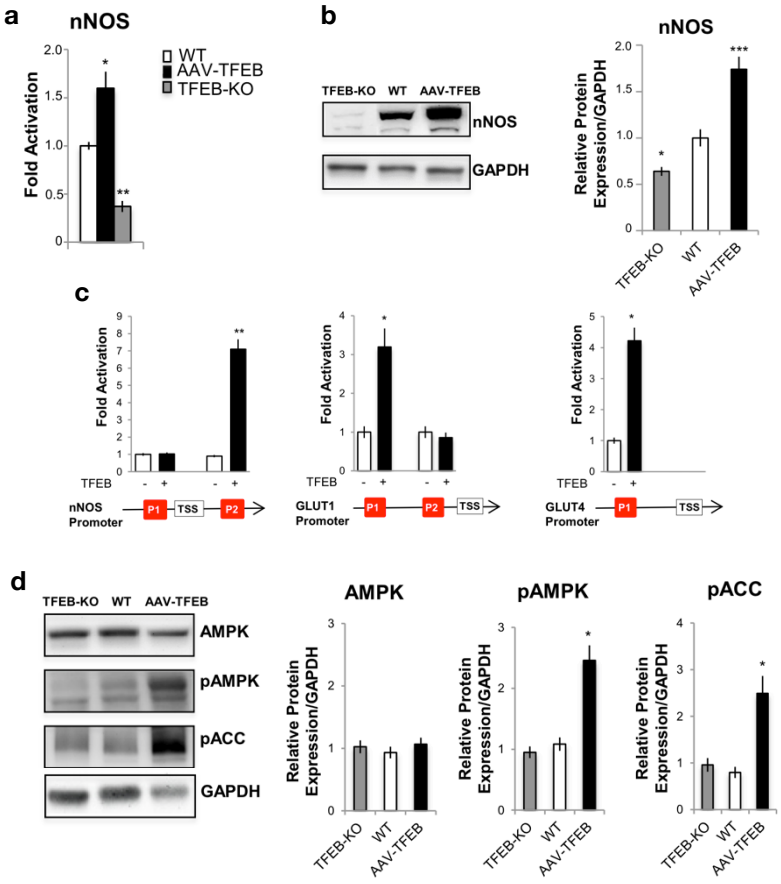

Figure 31 - TFEB controls glucose uptake via regulation of AMPK signaling pathways. a. qRT-PCR analysis of nNOS transcript in WT, TFEB-infected and TFEB-KO muscles. Value are expressed as fold induction compared to controls. Data are shown as mean±SE, n=8; *p<0.05, **p<0.01 **b.** Western Blot detection of nNOS and densitometric quantification. Values are normalized for GAPDH (*p<0.05; ***p<0.001). **c.** ChIP analyses in muscles from TFEB transgenic and WT mice on nNOS, GLUT1 and GLUT4 promoters. The histograms show the amount of immunoprecipitated DNA as detected by qRT-PCR normalized to input. Bars represent mean±SE of three independent experiments; *p<0.05, **p<0.01, ***p<0.001. **d.** Western blot analysis of AMPK, pAMPK and pACC on protein extracts from muscles infected with AAV2.1-TFEB, TFEB-KO or WT mice. Representative images (left) and densitometric quantification (right) are shown (*p<0.05).

5 Discussion

The beneficial effects of physical activity on mitochondrial content/function, fatty acid oxidation and glucose homeostasis are well known (Hawley, 2002; Holloszy & Coyle, 1984; Holloszy, Kohrt, & Hansen, 1998). All these features appear to be critical factors altered in a vast series of metabolic disorders. Moreover, dysfunctional mitochondria and insulin resistance are alarming indexes that negatively influence the process of skeletal muscle aging (Egan & Zierath, 2013). Indeed muscle activity is important to counteract disease progression in diabetes, obesity and metabolic syndrome and physical training together with dietary intervention have been reported to actively counteract ageing sarcopenia (Borst, 2004).

Calcium signalling is greatly affected by exercise and the calcium-dependent phosphatase calcineurin is one of the most important players for muscle adaptation to physical activity. We recently reported that exercise triggers TFEB nuclear localization in a calcineurin-dependent fashion(Medina et al., 2015) (Medina et al., 2015). Calcineurin dephosphorylates TFEB serine residues that play a critical role in determining TFEB subcellular localization and promotes its nuclear translocation (Medina et al., 2015). Importantly, calcium-dependent signaling also modulates exercise-dependent glucose-related pathways. Indeed, muscle-specific transgenic mice that overexpress an activated form of calcineurin show increased glycogen accumulation and lipid oxidation (Long, Glund, Garcia-Roves, & Zierath, 2007); moreover they are characterized by up-regulation of PGC1α, several glycolytic enzymes, mitochondrial genes, genes related to lipid metabolism and GLUT4 (Long & Zierath, 2008). Conversely, muscle-specific calcineurin KO mice show exercise intolerance when subjected to exhausting physical activity (Pfluger et al., 2015). Finally, immunosuppression therapy by high-dose treatment with calcineurin inhibitors cylosporin A or tacrolimus (FK-506) has been associated with higher risk for developing obesity and diabetes in patients (MI, Rego, & Lima, 2003). Altogether these data suggest that calcineurin plays a major role in glucose and lipid metabolism even if the mechanistic insights these beneficial effects of calcineurin were unknown. Our data

suggest that TFEB is a critical calcineurin downstream target that coordinates metabolic adaptations such as glucose uptake and mitochondrial function in order to optimize energy production to sustain muscle contraction.

In this work we found that TFEB is a major regulator of glucose homeostasis and mitochondrial biogenesis providing energetic support to maintain muscle contraction.
Our *in vivo* data show that the absence of TFEB causes accumulation of morphologically abnormal and dysfunctional mitochondria that display impairment in respiratory chain complex II activity and proton leakage leading to a defect in ATP production and exercise intolerance. Conversely, over expression of TFEB induces mitochondrial biogenesis, improves respiratory chain complex activities and increases ATP production. These findings are surprising since the documented effects of TFEB are mainly related to lysosomal biogenesis and autophagy regulation.
The positive effects of TFEB on the mitochondrial network in skeletal muscle appear to be independent from the transcriptional co-regulator PGC1α. We found that TFEB is sufficient to directly bind and induce the expression of NRF2 and Tfam, two major master regulators of mitochondrial biogenesis in muscle, even in the absence of PGC1α; moreover TFEB is both sufficient and required for PPARa expression. Therefore, TFEB acts independently from PGC1α to promote oxidation of glucose and lipids, which are critical substrates during the early and late phase of strenuous contraction (Egan & Zierath, 2013). Therefore, TFEB is at least one missing factor that explains why PGC1α is dispensable for exercise and mitochondrial biogenesis (Rowe et al., 2012) and not required for exercise-induced adaptations. Moreover, TFEB directly controls glucose homeostasis via GLUT1/4 expression and insulin sensitivity via nNOS. Indeed, muscle from TFEB-KO mice showed a decreased glucose uptake during (EU)-clamps and near complete absent glycogen stores under resting conditions. The insulin resistance of the TFEB deficient fibers prevents glucose oxidation and therefore drives the exercising muscle to use fatty acid oxidation (FAO) that consequently blocked Pyruvate Dehydrogenase (PDH) enzyme resulting in lactate accumulation.
Altogether these findings strongly suggest that TFEB is a critical player of metabolic flexibility during physical activity.

In a previous study TFEB was reported to regulate lipid metabolism in liver in a way that is mediated, at least in part, by PGC1α (Settembre et al., 2013). Conversely, our findings in muscle show that TFEB is directly involved in mitochondrial function and glucose homeostasis independently from PGC1α. Thus, these observations indicate that the networks of genes regulated by TFEB are context-specific as the gene expression profiles have significant tissue-specific changes, supporting distinct tissue-specific metabolic functions.

Nevertheless, TFEB not only regulates expression of glucose transporters and critical glycolytic enzymes but also factors that impinge on AMPK regulation such as neuronal nitric oxide synthase (nNOS). It was shown that nNOS controls GLUT4 expression in skeletal muscle cells through AMPK activation and endogenous nNOS is required for the up-regulation of AMPK activity by the AMP mimetic, AICAR (Higaki, Hirshman, Fujii, & Goodyear, 2001; Lira et al., 2010; McConell et al., 2010).

In summary, our results position TFEB as a central coordinator of insulin sensitivity, glucose homeostasis, lipid oxidation and mitochondrial function, further emphasizing the importance of this regulatory pathway in the metabolic response to energy demanding conditions such as physical exercise.

Thus the unknown master regulator able to coordinate at the same time fuel disposal and fuel utilization has been found.

These advances in understanding the transcriptional regulation of exercise-induced muscle adaptation obviously open new interesting perspectives for fighting metabolic diseases and age related muscle problems. A factor that modulates coordinately mitochondria functionality and blood glucose clearance in a insulin-independent manner is for sure a potential therapeutic target. It would be visionary thinking of substituting physical exercise with a pill; indeed the huge amount of pleiotropic effects cannot be modulated with a pharmacological intervention. However, the possible development of drugs mimicking TFEB action in skeletal muscle would be for sure a potential intervention to potentiate the effects of moderate exercise that also obese and old people can undergo.

Of course TFEB activation should be carefully modulated, and further studies in understanding the duration of TFEB effects and the kinetic of TFEB mediated adaptation to physical exercise should be addressed in advance.

In conclusion, these findings spread for sure new possibilities and farsighted perspectives in the fight of metabolic syndromes and aging.

6 References

Abounit, K., Scarabelli, T. M., & McCauley, R. B. (2012). Autophagy in mammalian cells. *World J Biol Chem, 3*(1), 1-6. doi:10.4331/wjbc.v3.i1.1

Andrew, P. J., & Mayer, B. (1999). Enzymatic function of nitric oxide synthases. *Cardiovasc Res, 43*(3), 521-531.

Baldi, P., & Long, A. D. (2001). A Bayesian framework for the analysis of microarray expression data: regularized t -test and statistical inferences of gene changes. *Bioinformatics, 17*(6), 509-519.

Ballabio, A. (2016). The awesome lysosome. *EMBO Mol Med, 8*(2), 73-76. doi:10.15252/emmm.201505966

Bejarano, E., & Cuervo, A. M. (2010). Chaperone-mediated autophagy. *Proc Am Thorac Soc, 7*(1), 29-39. doi:10.1513/pats.200909-102JS

Blaauw, B., Canato, M., Agatea, L., Toniolo, L., Mammucari, C., Masiero, E., . . . Reggiani, C. (2009). Inducible activation of Akt increases skeletal muscle mass and force without satellite cell activation. *FASEB J, 23*(11), 3896-3905. doi:10.1096/fj.09-131870

Bodine, S. C., Latres, E., Baumhueter, S., Lai, V. K., Nunez, L., Clarke, B. A., . . . Glass, D. J. (2001). Identification of ubiquitin ligases required for skeletal muscle atrophy. *Science, 294*(5547), 1704-1708. doi:10.1126/science.1065874

Bonaldo, P., & Sandri, M. (2013). Cellular and molecular mechanisms of muscle atrophy. *Dis Model Mech, 6*(1), 25-39. doi:10.1242/dmm.010389

Booth, F. W., Laye, M. J., & Spangenburg, E. E. (2010). Gold standards for scientists who are conducting animal-based exercise studies. *J Appl Physiol (1985), 108*(1), 219-221. doi:10.1152/japplphysiol.00125.2009

Booth, F. W., Roberts, C. K., & Laye, M. J. (2012). Lack of exercise is a major cause of chronic diseases. *Compr Physiol, 2*(2), 1143-1211. doi:10.1002/cphy.c110025

Borsheim, E., & Bahr, R. (2003). Effect of exercise intensity, duration and mode on post-exercise oxygen consumption. *Sports Med, 33*(14), 1037-1060.

Borst, S. E. (2004). Interventions for sarcopenia and muscle weakness in older people. *Age Ageing, 33*(6), 548-555. doi:10.1093/ageing/afh201

Bothe, G. W., Haspel, J. A., Smith, C. L., Wiener, H. H., & Burden, S. J. (2000). Selective expression of Cre recombinase in skeletal muscle fibers. *Genesis, 26*(2), 165-166.

Bugiani, M., Invernizzi, F., Alberio, S., Briem, E., Lamantea, E., Carrara, F., . . . Zeviani, M. (2004). Clinical and molecular findings in children with complex I deficiency. *Biochim Biophys Acta, 1659*(2-3), 136-147. doi:10.1016/j.bbabio.2004.09.006

Calvo, J. A., Daniels, T. G., Wang, X., Paul, A., Lin, J., Spiegelman, B. M., . . . Rangwala, S. M. (2008). Muscle-specific expression of PPARgamma coactivator-1alpha improves exercise performance and increases peak oxygen uptake. *J Appl Physiol (1985), 104*(5), 1304-1312. doi:10.1152/japplphysiol.01231.2007

Cartee, G. D., Hepple, R. T., Bamman, M. M., & Zierath, J. R. (2016). Exercise Promotes Healthy Aging of Skeletal Muscle. *Cell Metab, 23*(6), 1034-1047. doi:10.1016/j.cmet.2016.05.007

Cuervo, A. M. (2011). Chaperone-mediated autophagy: Dice's 'wild' idea about lysosomal selectivity. *Nat Rev Mol Cell Biol, 12*(8), 535-541. doi:10.1038/nrm3150

Cunha, T. F., Bacurau, A. V., Moreira, J. B., Paixao, N. A., Campos, J. C., Ferreira, J. C., . . . Brum, P. C. (2012). Exercise training prevents oxidative stress and ubiquitin-proteasome system overactivity and reverse skeletal muscle atrophy in heart failure. *PLoS One, 7*(8), e41701. doi:10.1371/journal.pone.0041701

Davidson, L. E., Hudson, R., Kilpatrick, K., Kuk, J. L., McMillan, K., Janiszewski, P. M., . . . Ross, R. (2009). Effects of exercise modality on insulin resistance and functional limitation in older adults: a randomized controlled trial. *Arch Intern Med, 169*(2), 122-131. doi:10.1001/archinternmed.2008.558

De Palma, C., Morisi, F., Pambianco, S., Assi, E., Touvier, T., Russo, S., . . . Clementi, E. (2014). Deficient nitric oxide signalling impairs skeletal muscle growth and performance: involvement of mitochondrial dysregulation. *Skelet Muscle, 4*(1), 22. doi:10.1186/s13395-014-0022-6

Decressac, M., Mattsson, B., Weikop, P., Lundblad, M., Jakobsson, J., & Bjorklund, A. (2013). TFEB-mediated autophagy rescues midbrain dopamine neurons from

alpha-synuclein toxicity. *Proc Natl Acad Sci U S A, 110*(19), E1817-1826. doi:10.1073/pnas.1305623110

DeFronzo, R. A., Ferrannini, E., Sato, Y., Felig, P., & Wahren, J. (1981). Synergistic interaction between exercise and insulin on peripheral glucose uptake. *J Clin Invest, 68*(6), 1468-1474.

DeFronzo, R. A., Jacot, E., Jequier, E., Maeder, E., Wahren, J., & Felber, J. P. (1981). The effect of insulin on the disposal of intravenous glucose. Results from indirect calorimetry and hepatic and femoral venous catheterization. *Diabetes, 30*(12), 1000-1007.

Dennis, G., Jr., Sherman, B. T., Hosack, D. A., Yang, J., Gao, W., Lane, H. C., & Lempicki, R. A. (2003). DAVID: Database for Annotation, Visualization, and Integrated Discovery. *Genome Biol, 4*(5), P3.

Egan, B., & Zierath, J. R. (2013). Exercise metabolism and the molecular regulation of skeletal muscle adaptation. *Cell Metab, 17*(2), 162-184. doi:10.1016/j.cmet.2012.12.012

Frezza, C., Cipolat, S., & Scorrano, L. (2007). Organelle isolation: functional mitochondria from mouse liver, muscle and cultured fibroblasts. *Nat Protoc, 2*(2), 287-295. doi:10.1038/nprot.2006.478

Glass, D. J. (2005). Skeletal muscle hypertrophy and atrophy signaling pathways. *Int J Biochem Cell Biol, 37*(10), 1974-1984. doi:10.1016/j.biocel.2005.04.018

Glick, D., Barth, S., & Macleod, K. F. (2010). Autophagy: cellular and molecular mechanisms. *J Pathol, 221*(1), 3-12. doi:10.1002/path.2697

Glund, S., Deshmukh, A., Long, Y. C., Moller, T., Koistinen, H. A., Caidahl, K., . . . Krook, A. (2007). Interleukin-6 directly increases glucose metabolism in resting human skeletal muscle. *Diabetes, 56*(6), 1630-1637. doi:10.2337/db06-1733

Goldberg, A. L. (1969). Protein turnover in skeletal muscle. II. Effects of denervation and cortisone on protein catabolism in skeletal muscle. *J Biol Chem, 244*(12), 3223-3229.

Gomes, M. D., Lecker, S. H., Jagoe, R. T., Navon, A., & Goldberg, A. L. (2001). Atrogin-1, a muscle-specific F-box protein highly expressed during muscle atrophy. *Proc Natl Acad Sci U S A, 98*(25), 14440-14445. doi:10.1073/pnas.251541198

Grumati, P., & Bonaldo, P. (2012). Autophagy in skeletal muscle homeostasis and in muscular dystrophies. *Cells, 1*(3), 325-345. doi:10.3390/cells1030325

Grumati, P., Coletto, L., Sandri, M., & Bonaldo, P. (2011). Autophagy induction rescues muscular dystrophy. *Autophagy, 7*(4), 426-428. doi:10.4161/auto.7.4.14392

Grumati, P., Coletto, L., Schiavinato, A., Castagnaro, S., Bertaggia, E., Sandri, M., & Bonaldo, P. (2011). Physical exercise stimulates autophagy in normal skeletal muscles but is detrimental for collagen VI-deficient muscles. *Autophagy, 7*(12), 1415-1423.

Hawley, J. A. (2002). Adaptations of skeletal muscle to prolonged, intense endurance training. *Clin Exp Pharmacol Physiol, 29*(3), 218-222.

He, C., Bassik, M. C., Moresi, V., Sun, K., Wei, Y., Zou, Z., . . . Levine, B. (2012). Exercise-induced BCL2-regulated autophagy is required for muscle glucose homeostasis. *Nature, 481*(7382), 511-515. doi:10.1038/nature10758

Hemesath, T. J., Steingrimsson, E., McGill, G., Hansen, M. J., Vaught, J., Hodgkinson, C. A., . . . Fisher, D. E. (1994). microphthalmia, a critical factor in melanocyte development, defines a discrete transcription factor family. *Genes Dev, 8*(22), 2770-2780.

Hershko, A., & Ciechanover, A. (1998). The ubiquitin system. *Annu Rev Biochem, 67*, 425-479. doi:10.1146/annurev.biochem.67.1.425

Higaki, Y., Hirshman, M. F., Fujii, N., & Goodyear, L. J. (2001). Nitric oxide increases glucose uptake through a mechanism that is distinct from the insulin and contraction pathways in rat skeletal muscle. *Diabetes, 50*(2), 241-247.

Holloszy, J. O., & Coyle, E. F. (1984). Adaptations of skeletal muscle to endurance exercise and their metabolic consequences. *J Appl Physiol Respir Environ Exerc Physiol, 56*(4), 831-838.

Holloszy, J. O., Kohrt, W. M., & Hansen, P. A. (1998). The regulation of carbohydrate and fat metabolism during and after exercise. *Front Biosci, 3*, D1011-1027.

Hood, D. A. (2001). Invited Review: contractile activity-induced mitochondrial biogenesis in skeletal muscle. *J Appl Physiol (1985), 90*(3), 1137-1157.

Huxley, A. F., & Niedergerke, R. (1954). Structural changes in muscle during contraction; interference microscopy of living muscle fibres. *Nature, 173*(4412), 971-973.

Huxley, H., & Hanson, J. (1954). Changes in the cross-striations of muscle during contraction and stretch and their structural interpretation. *Nature, 173*(4412), 973-976.

Ichimura, Y., & Komatsu, M. (2010). Selective degradation of p62 by autophagy. *Semin Immunopathol, 32*(4), 431-436. doi:10.1007/s00281-010-0220-1

Inoue, Y., & Klionsky, D. J. (2010). Regulation of macroautophagy in Saccharomyces cerevisiae. *Semin Cell Dev Biol, 21*(7), 664-670. doi:10.1016/j.semcdb.2010.03.009

Jager, S., Handschin, C., St-Pierre, J., & Spiegelman, B. M. (2007). AMP-activated protein kinase (AMPK) action in skeletal muscle via direct phosphorylation of PGC-1alpha. *Proc Natl Acad Sci U S A, 104*(29), 12017-12022. doi:10.1073/pnas.0705070104

Jensen, J., & Lai, Y. C. (2009). Regulation of muscle glycogen synthase phosphorylation and kinetic properties by insulin, exercise, adrenaline and role in insulin resistance. *Arch Physiol Biochem, 115*(1), 13-21. doi:10.1080/13813450902778171

Knowler, W. C., Barrett-Connor, E., Fowler, S. E., Hamman, R. F., Lachin, J. M., Walker, E. A., . . . Diabetes Prevention Program Research, G. (2002). Reduction in the incidence of type 2 diabetes with lifestyle intervention or metformin. *N Engl J Med, 346*(6), 393-403. doi:10.1056/NEJMoa012512

Kon, M., & Cuervo, A. M. (2010). Chaperone-mediated autophagy in health and disease. *FEBS Lett, 584*(7), 1399-1404. doi:10.1016/j.febslet.2009.12.025

Lecker, S. H., Goldberg, A. L., & Mitch, W. E. (2006). Protein degradation by the ubiquitin-proteasome pathway in normal and disease states. *J Am Soc Nephrol, 17*(7), 1807-1819. doi:10.1681/ASN.2006010083

Leick, L., Wojtaszewski, J. F., Johansen, S. T., Kiilerich, K., Comes, G., Hellsten, Y., . . . Pilegaard, H. (2008). PGC-1alpha is not mandatory for exercise- and training-induced adaptive gene responses in mouse skeletal muscle. *Am J Physiol Endocrinol Metab, 294*(2), E463-474. doi:10.1152/ajpendo.00666.2007

Lilienbaum, A. (2013). Relationship between the proteasomal system and autophagy. *Int J Biochem Mol Biol, 4*(1), 1-26.

Lin, J., Handschin, C., & Spiegelman, B. M. (2005). Metabolic control through the PGC-1 family of transcription coactivators. *Cell Metab, 1*(6), 361-370. doi:10.1016/j.cmet.2005.05.004

Lin, J., Wu, P. H., Tarr, P. T., Lindenberg, K. S., St-Pierre, J., Zhang, C. Y., . . . Spiegelman, B. M. (2004). Defects in adaptive energy metabolism with CNS-linked hyperactivity in PGC-1alpha null mice. *Cell, 119*(1), 121-135. doi:10.1016/j.cell.2004.09.013

Lira, V. A., Brown, D. L., Lira, A. K., Kavazis, A. N., Soltow, Q. A., Zeanah, E. H., & Criswell, D. S. (2010). Nitric oxide and AMPK cooperatively regulate PGC-1 in skeletal muscle cells. *J Physiol, 588*(Pt 18), 3551-3566. doi:10.1113/jphysiol.2010.194035

Lira, V. A., Soltow, Q. A., Long, J. H., Betters, J. L., Sellman, J. E., & Criswell, D. S. (2007). Nitric oxide increases GLUT4 expression and regulates AMPK signaling in skeletal muscle. *Am J Physiol Endocrinol Metab, 293*(4), E1062-1068. doi:10.1152/ajpendo.00045.2007

Lo Verso, F., Carnio, S., Vainshtein, A., & Sandri, M. (2014). Autophagy is not required to sustain exercise and PRKAA1/AMPK activity but is important to prevent mitochondrial damage during physical activity. *Autophagy, 10*(11), 1883-1894. doi:10.4161/auto.32154

Long, Y. C., Glund, S., Garcia-Roves, P. M., & Zierath, J. R. (2007). Calcineurin regulates skeletal muscle metabolism via coordinated changes in gene expression. *J Biol Chem, 282*(3), 1607-1614. doi:10.1074/jbc.M609208200

Long, Y. C., & Zierath, J. R. (2008). Influence of AMP-activated protein kinase and calcineurin on metabolic networks in skeletal muscle. *Am J Physiol Endocrinol Metab, 295*(3), E545-552. doi:10.1152/ajpendo.90259.2008

Mammucari, C., Milan, G., Romanello, V., Masiero, E., Rudolf, R., Del Piccolo, P., . . . Sandri, M. (2007). FoxO3 controls autophagy in skeletal muscle in vivo. *Cell Metab, 6*(6), 458-471. doi:10.1016/j.cmet.2007.11.001

Martina, J. A., Chen, Y., Gucek, M., & Puertollano, R. (2012). MTORC1 functions as a transcriptional regulator of autophagy by preventing nuclear transport of TFEB. *Autophagy, 8*(6), 903-914. doi:10.4161/auto.19653

Martina, J. A., Diab, H. I., Li, H., & Puertollano, R. (2014). Novel roles for the MiTF/TFE family of transcription factors in organelle biogenesis, nutrient sensing, and energy homeostasis. *Cell Mol Life Sci, 71*(13), 2483-2497. doi:10.1007/s00018-014-1565-8

Masiero, E., Agatea, L., Mammucari, C., Blaauw, B., Loro, E., Komatsu, M., . . . Sandri, M. (2009). Autophagy is required to maintain muscle mass. *Cell Metab, 10*(6), 507-515. doi:10.1016/j.cmet.2009.10.008

McCarthy, J. J., & Esser, K. A. (2007). Counterpoint: Satellite cell addition is not obligatory for skeletal muscle hypertrophy. *J Appl Physiol (1985), 103*(3), 1100-1102; discussion 1102-1103. doi:10.1152/japplphysiol.00101.2007a

McCarthy, J. J., Srikuea, R., Kirby, T. J., Peterson, C. A., & Esser, K. A. (2012). Inducible Cre transgenic mouse strain for skeletal muscle-specific gene targeting. *Skelet Muscle, 2*(1), 8. doi:10.1186/2044-5040-2-8

McConell, G. K., Ng, G. P., Phillips, M., Ruan, Z., Macaulay, S. L., & Wadley, G. D. (2010). Central role of nitric oxide synthase in AICAR and caffeine-induced mitochondrial biogenesis in L6 myocytes. *J Appl Physiol (1985), 108*(3), 589-595. doi:10.1152/japplphysiol.00377.2009

Medina, D. L., Di Paola, S., Peluso, I., Armani, A., De Stefani, D., Venditti, R., . . . Ballabio, A. (2015). Lysosomal calcium signalling regulates autophagy through calcineurin and TFEB. *Nat Cell Biol, 17*(3), 288-299. doi:10.1038/ncb3114

Medina, D. L., Fraldi, A., Bouche, V., Annunziata, F., Mansueto, G., Spampanato, C., . . . Ballabio, A. (2011). Transcriptional activation of lysosomal exocytosis promotes cellular clearance. *Dev Cell, 21*(3), 421-430. doi:10.1016/j.devcel.2011.07.016

Merrill, G. F., Kurth, E. J., Hardie, D. G., & Winder, W. W. (1997). AICA riboside increases AMP-activated protein kinase, fatty acid oxidation, and glucose uptake in rat muscle. *Am J Physiol, 273*(6 Pt 1), E1107-1112.

MI, T. D. C., Rego, L. O., & Lima, A. S. (2003). Post-liver transplant obesity and diabetes. *Curr Opin Clin Nutr Metab Care, 6*(4), 457-460. doi:10.1097/01.mco.0000078994.96795.d8

Mijaljica, D., Prescott, M., & Devenish, R. J. (2011). Microautophagy in mammalian cells: revisiting a 40-year-old conundrum. *Autophagy, 7*(7), 673-682.

Milan, G., Romanello, V., Pescatore, F., Armani, A., Paik, J. H., Frasson, L., . . . Sandri, M. (2015). Regulation of autophagy and the ubiquitin-proteasome system by the FoxO transcriptional network during muscle atrophy. *Nat Commun, 6*, 6670. doi:10.1038/ncomms7670

Mizushima, N., & Levine, B. (2010). Autophagy in mammalian development and differentiation. *Nat Cell Biol, 12*(9), 823-830. doi:10.1038/ncb0910-823

Mounier, R., Theret, M., Lantier, L., Foretz, M., & Viollet, B. (2015). Expanding roles for AMPK in skeletal muscle plasticity. *Trends Endocrinol Metab, 26*(6), 275-286. doi:10.1016/j.tem.2015.02.009

Murgia, M., Serrano, A. L., Calabria, E., Pallafacchina, G., Lomo, T., & Schiaffino, S. (2000). Ras is involved in nerve-activity-dependent regulation of muscle genes. *Nat Cell Biol, 2*(3), 142-147. doi:10.1038/35004013

Napolitano, G., & Ballabio, A. (2016). TFEB at a glance. *J Cell Sci, 129*(13), 2475-2481. doi:10.1242/jcs.146365

Palmieri, M., Impey, S., Kang, H., di Ronza, A., Pelz, C., Sardiello, M., & Ballabio, A. (2011). Characterization of the CLEAR network reveals an integrated control of cellular clearance pathways. *Hum Mol Genet, 20*(19), 3852-3866. doi:10.1093/hmg/ddr306

Parsons, S. A., Millay, D. P., Wilkins, B. J., Bueno, O. F., Tsika, G. L., Neilson, J. R., . . . Molkentin, J. D. (2004). Genetic loss of calcineurin blocks mechanical overload-induced skeletal muscle fiber type switching but not hypertrophy. *J Biol Chem, 279*(25), 26192-26200. doi:10.1074/jbc.M313800200

Pette, D., & Heilmann, C. (1979). Some characteristics of sarcoplasmic reticulum in fast- and slow-twitch muscles. *Biochem Soc Trans, 7*(4), 765-767.

Pfluger, P. T., Kabra, D. G., Aichler, M., Schriever, S. C., Pfuhlmann, K., Garcia, V. C., . . . Tschop, M. H. (2015). Calcineurin Links Mitochondrial Elongation with Energy Metabolism. *Cell Metab*. doi:10.1016/j.cmet.2015.08.022

Pogenberg, V., Ogmundsdottir, M. H., Bergsteinsdottir, K., Schepsky, A., Phung, B., Deineko, V., . . . Wilmanns, M. (2012). Restricted leucine zipper dimerization and specificity of DNA recognition of the melanocyte master regulator MITF. *Genes Dev, 26*(23), 2647-2658. doi:10.1101/gad.198192.112

Polishchuk, E. V., Concilli, M., Iacobacci, S., Chesi, G., Pastore, N., Piccolo, P., . . . Polishchuk, R. S. (2014). Wilson disease protein ATP7B utilizes lysosomal exocytosis to maintain copper homeostasis. *Dev Cell, 29*(6), 686-700. doi:10.1016/j.devcel.2014.04.033

Pryor, P. R., & Luzio, J. P. (2009). Delivery of endocytosed membrane proteins to the lysosome. *Biochim Biophys Acta, 1793*(4), 615-624. doi:10.1016/j.bbamcr.2008.12.022

Rowe, G. C., El-Khoury, R., Patten, I. S., Rustin, P., & Arany, Z. (2012). PGC-1alpha is dispensable for exercise-induced mitochondrial biogenesis in skeletal muscle. *PLoS One, 7*(7), e41817. doi:10.1371/journal.pone.0041817

Rubinsztein, D. C., Marino, G., & Kroemer, G. (2011). Autophagy and aging. *Cell, 146*(5), 682-695. doi:10.1016/j.cell.2011.07.030

Safdar, A., Saleem, A., & Tarnopolsky, M. A. (2016). The potential of endurance exercise-derived exosomes to treat metabolic diseases. *Nat Rev Endocrinol, 12*(9), 504-517. doi:10.1038/nrendo.2016.76

Sancak, Y., Bar-Peled, L., Zoncu, R., Markhard, A. L., Nada, S., & Sabatini, D. M. (2010). Ragulator-Rag complex targets mTORC1 to the lysosomal surface and is necessary for its activation by amino acids. *Cell, 141*(2), 290-303. doi:10.1016/j.cell.2010.02.024

Sandri, M. (2016). Protein breakdown in cancer cachexia. *Semin Cell Dev Biol, 54*, 11-19. doi:10.1016/j.semcdb.2015.11.002

Sandri, M., Sandri, C., Gilbert, A., Skurk, C., Calabria, E., Picard, A., . . . Goldberg, A. L. (2004). Foxo transcription factors induce the atrophy-related ubiquitin ligase atrogin-1 and cause skeletal muscle atrophy. *Cell, 117*(3), 399-412.

Sardiello, M., Palmieri, M., di Ronza, A., Medina, D. L., Valenza, M., Gennarino, V. A., . . . Ballabio, A. (2009). A gene network regulating lysosomal biogenesis and function. *Science, 325*(5939), 473-477. doi:10.1126/science.1174447

Sartori, R., Milan, G., Patron, M., Mammucari, C., Blaauw, B., Abraham, R., & Sandri, M. (2009). Smad2 and 3 transcription factors control muscle mass in adulthood. *Am J Physiol Cell Physiol, 296*(6), C1248-1257. doi:10.1152/ajpcell.00104.2009

Sartori, R., Schirwis, E., Blaauw, B., Bortolanza, S., Zhao, J., Enzo, E., . . . Sandri, M. (2013). BMP signaling controls muscle mass. *Nat Genet, 45*(11), 1309-1318. doi:10.1038/ng.2772

Scarpulla, R. C. (2006). Nuclear control of respiratory gene expression in mammalian cells. *J Cell Biochem, 97*(4), 673-683. doi:10.1002/jcb.20743

Schiaffino, S., Dyar, K. A., Ciciliot, S., Blaauw, B., & Sandri, M. (2013). Mechanisms regulating skeletal muscle growth and atrophy. *FEBS J, 280*(17), 4294-4314. doi:10.1111/febs.12253

Schiaffino, S., & Mammucari, C. (2011). Regulation of skeletal muscle growth by the IGF1-Akt/PKB pathway: insights from genetic models. *Skelet Muscle, 1*(1), 4. doi:10.1186/2044-5040-1-4

Schiaffino, S., & Reggiani, C. (1996). Molecular diversity of myofibrillar proteins: gene regulation and functional significance. *Physiol Rev, 76*(2), 371-423.

Schiaffino, S., & Reggiani, C. (2011). Fiber types in mammalian skeletal muscles. *Physiol Rev, 91*(4), 1447-1531. doi:10.1152/physrev.00031.2010

Schiaffino, S., Sandri, M., & Murgia, M. (2007). Activity-dependent signaling pathways controlling muscle diversity and plasticity. *Physiology (Bethesda), 22*, 269-278. doi:10.1152/physiol.00009.2007

Settembre, C., De Cegli, R., Mansueto, G., Saha, P. K., Vetrini, F., Visvikis, O., . . . Ballabio, A. (2013). TFEB controls cellular lipid metabolism through a starvation-induced autoregulatory loop. *Nat Cell Biol, 15*(6), 647-658. doi:10.1038/ncb2718

Settembre, C., Di Malta, C., Polito, V. A., Garcia Arencibia, M., Vetrini, F., Erdin, S., . . . Ballabio, A. (2011). TFEB links autophagy to lysosomal biogenesis. *Science, 332*(6036), 1429-1433. doi:10.1126/science.1204592

Settembre, C., Zoncu, R., Medina, D. L., Vetrini, F., Erdin, S., Erdin, S., . . . Ballabio, A. (2012). A lysosome-to-nucleus signalling mechanism senses and regulates the lysosome via mTOR and TFEB. *EMBO J, 31*(5), 1095-1108. doi:10.1038/emboj.2012.32

Shemesh, A., Wang, Y., Yang, Y., Yang, G. S., Johnson, D. E., Backer, J. M., . . . Zong, H. (2014). Suppression of mTORC1 activation in acid-alpha-glucosidase-deficient

cells and mice is ameliorated by leucine supplementation. *Am J Physiol Regul Integr Comp Physiol, 307*(10), R1251-1259. doi:10.1152/ajpregu.00212.2014

Shen, H. M., & Mizushima, N. (2014). At the end of the autophagic road: an emerging understanding of lysosomal functions in autophagy. *Trends Biochem Sci, 39*(2), 61-71. doi:10.1016/j.tibs.2013.12.001

Spampanato, C., Feeney, E., Li, L., Cardone, M., Lim, J. A., Annunziata, F., . . . Raben, N. (2013). Transcription factor EB (TFEB) is a new therapeutic target for Pompe disease. *EMBO Mol Med, 5*(5), 691-706. doi:10.1002/emmm.201202176

Stamler, J. S., & Meissner, G. (2001). Physiology of nitric oxide in skeletal muscle. *Physiol Rev, 81*(1), 209-237.

Steingrimsson, E., Copeland, N. G., & Jenkins, N. A. (2004). Melanocytes and the microphthalmia transcription factor network. *Annu Rev Genet, 38*, 365-411. doi:10.1146/annurev.genet.38.072902.092717

Takikita, S., Schreiner, C., Baum, R., Xie, T., Ralston, E., Plotz, P. H., & Raben, N. (2010). Fiber type conversion by PGC-1alpha activates lysosomal and autophagosomal biogenesis in both unaffected and Pompe skeletal muscle. *PLoS One, 5*(12), e15239. doi:10.1371/journal.pone.0015239

Tenno, T., Fujiwara, K., Tochio, H., Iwai, K., Morita, E. H., Hayashi, H., . . . Shirakawa, M. (2004). Structural basis for distinct roles of Lys63- and Lys48-linked polyubiquitin chains. *Genes Cells, 9*(10), 865-875. doi:10.1111/j.1365-2443.2004.00780.x

Tooze, S. A., & Yoshimori, T. (2010). The origin of the autophagosomal membrane. *Nat Cell Biol, 12*(9), 831-835. doi:10.1038/ncb0910-831

Vainshtein, A., & Hood, D. A. (2016). The regulation of autophagy during exercise in skeletal muscle. *J Appl Physiol (1985), 120*(6), 664-673. doi:10.1152/japplphysiol.00550.2015

van Loon, L. J., Greenhaff, P. L., Constantin-Teodosiu, D., Saris, W. H., & Wagenmakers, A. J. (2001). The effects of increasing exercise intensity on muscle fuel utilisation in humans. *J Physiol, 536*(Pt 1), 295-304.

van Meel, E., & Klumperman, J. (2008). Imaging and imagination: understanding the endo-lysosomal system. *Histochem Cell Biol, 129*(3), 253-266. doi:10.1007/s00418-008-0384-0

Velloso, C. P. (2008). Regulation of muscle mass by growth hormone and IGF-I. *Br J Pharmacol, 154*(3), 557-568. doi:10.1038/bjp.2008.153

Viscomi, C., Spinazzola, A., Maggioni, M., Fernandez-Vizarra, E., Massa, V., Pagano, C., . . . Zeviani, M. (2009). Early-onset liver mtDNA depletion and late-onset proteinuric nephropathy in Mpv17 knockout mice. *Hum Mol Genet, 18*(1), 12-26. doi:10.1093/hmg/ddn309

Zhao, J., Brault, J. J., Schild, A., Cao, P., Sandri, M., Schiaffino, S., . . . Goldberg, A. L. (2007). FoxO3 coordinately activates protein degradation by the autophagic/lysosomal and proteasomal pathways in atrophying muscle cells. *Cell Metab, 6*(6), 472-483. doi:10.1016/j.cmet.2007.11.004

Zoncu, R., Bar-Peled, L., Efeyan, A., Wang, S., Sancak, Y., & Sabatini, D. M. (2011). mTORC1 senses lysosomal amino acids through an inside-out mechanism that requires the vacuolar H(+)-ATPase. *Science, 334*(6056), 678-683. doi:10.1126/science.1207056

Zong, H., Armoni, M., Harel, C., Karnieli, E., & Pessin, J. E. (2012). Cytochrome P-450 CYP2E1 knockout mice are protected against high-fat diet-induced obesity and insulin resistance. *Am J Physiol Endocrinol Metab, 302*(5), E532-539. doi:10.1152/ajpendo.00258.2011